Restricted **NEA/CSNI/R(2004)16**

Organisation de Coopération et de Développement Economiques
Organisation for Economic Co-operation and Development **November 2004**

NUCLEAR ENERGY AGENCY **English – Or. English**
COMMITTEE ON THE SAFETY OF NUCLEAR INSTALLATIONS

AECL International Standard Problem ISP-41
Follow-up exercise (Phase II):
Iodine Code Comparison Exercise against CAIMAN and RTF Experiments

NUCLEAR ENERGY AGENCY
COMMITTEE ON THE SAFETY OF NUCLEAR INSTALLATIONS

AECL - IRSN
INTERNATIONAL STANDARD PROBLEM (ISP) NO. 41
FOLLOW UP EXERCISE: PHASE 2

Iodine Code Comparison Exercise against CAIMAN and RTF Experiments

Prepared by :
J. Ball[1], C. Marchand[2], H. Allelein[3], L. Cantrel[2] , R. Cripps[4], G. Glowa[1], L. Herranz[5], A. Rincon[5], J. Royen[7], A. Rydl[6], P. Schindler[8], G. Weber[3] and J. Wren[1]

Authors : J. Ball (AECL), C. Marchand (IRSN)

[1] AECL (Canada)
[2] IRSN (France)
[3] GRS (Germany)
[4] PSI (Switzerland)
[5] CIEMAT (Spain)
[6] OECD/NEA
[7] NRIR (Czech Republic)
[8] CEA (France)

Table of Contents

List of Figures

List of Tables

EXECUTIVE SUMMARY

Iodine is the major contribution in the short term to the radiological consequences of a nuclear reactor severe accident. Then, it is needed to estimate as reliable as possible the quantity of iodine and the chemical species able to be released in the environment. This evaluation should be based on consolidate evaluation with uncertainty analysis. In this context, it is necessary that iodine behaviour codes be able to provide accurate estimates of iodine volatility for experimental data obtained under a wide range of conditions relevant to reactor accident scenarios. ISP exercises are an opportunity to test the ability of the codes to do this.

The main objective of ISP exercises is to increase confidence in the validity and accuracy of the tools that are used in assessing the safety of nuclear installations. The secondary objective is to enable code users to gain experience and demonstrate their competence. The ISP 41 exercise on iodine codes has required three steps to achieve these objectives. These are:

(1) ISP 41: Computer code exercise based on a simple Radioiodine Test Facility (RTF) experiment,
(2) ISP 41 Follow-up Step 1: Parametric calculations,
(3) ISP 41 Follow-up Step 2: Computer code exercise based on complex experiments performed at the RTF and Caiman facilities.

In the final step of the exercise, the participants were: AECL(Canada), CIEMAT(Spain), NRIR (Czech Republic), PSI (Switzerland), GRS (Germany), IRSN (France).

Results of the first two steps have been documented elsewhere [1,2]. Briefly however, they showed that, although most iodine behaviour codes predicted similar qualitative trends, there were many quantitative discrepancies between code predictions. These discrepancies were identified as arising from the choice of kinetic input parameters and differences in the organic iodide sub-models within each of the codes. There was a strong "user effect" due to the participants choices for various parameters such adsorption-desorption rate constants.

The final step of the ISP 41 exercise was to perform code comparison exercises against experimental data obtained over as large a range of experimental conditions as possible. This comparison was to allow each of the code users to realistically evaluate and improve the kinetic parameters and organic iodide behaviour sub-models within their codes. Results of this final step are reported in this document.

Four intermediate scale studies were chosen for the exercise. Two experiments, CAIMAN 97/02, and Radioiodine Test Facility PHEBUS/RTF1, were chosen on the basis that they were representative of selected severe accident conditions (pH 5, 90ºC sump, dose-rate of 1kGy·h^{-1}, and the presence of painted surfaces in both the gas and aqueous phases). Two additional experiments were chosen for validation of organic iodide formation sub-models on the basis that they demonstrated that organic iodides contributed significantly to the volatile iodine fraction. In RTF Phase 10 Test 1, the effect of painted surfaces on pH, iodine volatility and organic iodide formation at

60ºC were examined. In this experiment, the pH was initially fixed at 10, uncontrolled between 75 and 200 h, and set at 10 again for the remainder of the experiment (see pH profile in Appendix C, Section 6). CAIMAN 2001/01 used only a painted surface in the gas phase, a higher dose-rate in the liquid phase (3 $kGy \cdot h^{-1}$), higher initial iodide concentration, pH=5 and a sump temperature of 110ºC.

Calculations on the four experiments were first performed "blind" to test the predictive capabilities of the codes. Subsequently, the experimental results were made available to each of the participants, and a second set of calculations was performed in which user-defined kinetic parameters (such as those for the radiolytic oxidation of I^- to I_2, and parameters for organic iodide sub-models) were optimized to provide a best fit to all of the experimental data. All the modifications proposed had to be justified and further validated.

In agreement with previous ISP-41 exercises, this code comparison exercise demonstrated that all of the iodine behaviour codes predicted the correct trends regarding iodine volatility. However, in the blind calculations, there was a very large discrepancy between quantitative code results (between 3 and 5 orders of magnitude for gas phase iodine concentrations). Open calculations improved the quantitative agreement between calculations and experimental data, but there were still significant discrepancies between model predictions and experimental results. None of the codes predicted all of the important parameters for all four of the tests to within the criteria determined for this exercise and there were some modifications that were not mechanistically sound.

This exercise demonstrated that many of the codes differed in their prediction of the overall rate of production of I_2(aq). Most codes overestimated the overall rate at pH 5, and 90 and 110º C, but underestimated it at higher pH and 60ºC. Because the codes predicted the overall I_2 production rate differently, there were difficulties assessing the performance of the organic iodide sub-models in each of the codes. Nonetheless, some general observations of organic iodide production rates were made. It appears that COCOSYS slightly underestimates organic iodide production rates, whereas IMPAIR and IODE NRIR overestimate. IODE 4.2 appears to overestimate organic iodide production rates at high pH values, but predicts well at lower pH values. LIRIC, IMOD and IODE 5.1 appear to produce the appropriate amount of organic iodide for a given predicted I_2 concentration.

One of the problems in predicting organic iodide concentrations is that, for homogeneous aqueous phase processes, the organic iodide formation depends on the quantity of organic impurities in the liquid phase, a parameter that is difficult to predict. For ISP calculations, it was possible for participants to estimate the concentration, because there was information available on measured total carbon (CAIMAN) or organic impurity concentrations (RTF). However, for reactor applications it is uncertain whether the default values for organic impurities in each of the iodine codes are adequate for the prediction of organic iodide production. Moreover there is a need for improvement in knowledge of initial conditions mainly release from the primary circuit - or reactor applications.

From the simulations of PHEBUS RTF1, and CAIMAN 97/02, the experiments identified by the participants as being most representative of reactor accident

conditions, it is evident that there is still some work to be done to improve the iodine behaviour codes so that they can be used confidently as predictive tools for reactor applications. As an example, only 2 of the 8 codes correctly simulated the gas phase iodine concentration at the end of the CAIMAN 97/02 experiment. Conclusion of analysis is made in term of codes and not models because it is not possible to perform an analysis without taking into account the strong link between the different elementary models. A few of the participants have provided information regarding further code improvements that have been investigated since the optimization exercises were performed. These improvements demonstrate that better agreement between code calculations and experimental data can be achieved by making adjustments to the existing codes, and using consistent modeling approaches. It is imperative, however, that these modifications be validated over a wide range of experimental conditions.

Depending upon the application, additional information may be required in order that the iodine behaviour codes can be used as predictive tools for reactor accident scenarios. This additional information could include such things as:

- Reactor and accident specific information regarding thermalhydraulic parameters for the determination of mass transfer and the adsorption-desorption rate constants (these parameters were fixed in this exercise),
- Information regarding the presence of other fission products, and control rod materials,
- the qualification of the source of iodine released into containment.

Further code improvements are expected to be an on-going process for each organization as a result of this ISP-41 exercise, and as new experimental data becomes available. The participants in this ISP are encouraged to apply their optimized models to calculations of RTF tests (e.g. ACE RTF, and Phebus RTF) and other experiments available in the literature.

1. INTRODUCTION

International Standard Problem (ISP) exercises are comparative exercises in which predictions of different computer codes for a given physical problem are compared with each other, or with the results of a carefully controlled experimental study. The main goal of ISP exercises is to increase confidence in the validity and accuracy of the tools that are used in assessing the safety of nuclear installations.

The ISP 41 exercise, a comparison of iodine behaviour models, was first proposed at the Fourth Iodine Chemistry Workshop held at Paul Scherrer Institute (PSI), Switzerland in June 1996. In the first phase of the ISP, results of a Radioiodine Test Facility (RTF) experiment performed under controlled and limited conditions, were chosen as a starting point for evaluation of the various iodine behaviour codes in the hope that the basic components of each code could be compared [1]. The experiment was ideal for demonstrating the ability of all of the codes to model the influence of pH on iodine volatility, one of the most important aspects of iodine behaviour. Participants were given details of the experimental set-up, conditions and procedures of the RTF test, and were asked to calculate experimentally observed parameters such as the total concentration and speciation of iodine in the gas and aqueous phases, and the distribution of iodine at the end of the test between the gas phase, the aqueous phase and surfaces exposed to each of these phases.

Results from the first step of ISP 41 are detailed elsewhere [1]. The objective of the exercise, which was to evaluate the basic components of each code, and to demonstrate their ability to simulate experimental results under controlled conditions was achieved. The exercise established that the pH dependence of iodine volatility at 25º C can be well reproduced by all codes used in the study.

Additional conclusions arising from the first phase of ISP 41 were that:

1) the performance of the iodine behavior codes is extremely reliant upon the judicious choice of user-defined kinetic parameters,

2) in order to use code calculations as predictive or interpretive tools, it must be demonstrated that the kinetic parameters used in the codes are applicable to the entire range of conditions anticipated in post-accident containment.

These conclusions led to the recommendation that two follow-up exercises be performed as part of ISP 41. The first phase of these follow-up exercises, consisting of a set of parametric studies, was described in detail elsewhere [2], and concluded that there were some areas of discrepancy between the various codes. Most of the discrepancies appeared to be quantitative in nature, that is, the codes agreed regarding the trends, but the actual amount of volatile iodine predicted by each of the codes varies considerably.
The parametric ISP exercise identified the organic iodide sub-model as contributing significantly to the discrepancy between the code predictions, parametric calculations could not identify which (if any) of the sub-models are correct, and what the range of user-defined input parameters for each of the sub-models could be. It was therefore recommended that the final step of ISP 41 be a code comparison against four

intermediate scale studies: two Caiman facility experiments, and two RTF experiments, which examine iodine volatility over a very large range of experimental conditions (dose-rate, painted surface area, temperature, pH, etc.). Two of the experiments (Phebus RTF1 and CAIMAN 97/02) were chosen because they were viewed to be representative of severe accident scenarios. RTF Phase 10 Test 1 examined the effect of painted surfaces on pH, iodine volatility and organic iodide formation at 60ºC. CAIMAN 01/01 used only a painted surface in the gas phase (to limit the source of organics), a higher dose-rate (3 $kGy \cdot h^{-1}$) in the liquid phase than CAIMAN 97/02 and RTF, higher initial iodide concentration, and a sump temperature of 110ºC. In both of the latter experiments, organic iodides contributed significantly to the volatile iodine fraction, and these were chosen for validation of organic iodide formation modelling.

The calculations were first performed as blind calculations to evaluate the predictive capability of the codes. Subsequently, the results were made available to each of the participants, and a second set of calculations were performed, with the models in each code optimized (i.e., user-defined parameters tuned to give a best fit to all of the experiments), or modified (i.e., mechanisms, or relative contributions of individual mechanisms changed). In order for a consistent comparison to be performed, some of the parameters, such as adsorption/desorption rate constants and mass transfer coefficients were fixed (See Appendix D). Modifications to the codes were to be consistent (e.g., the same for all calculations), explained, and justified. This comparison was to allow each of the code users to realistically evaluate, and improve their kinetic parameters and organic iodide behaviour sub-models. This document describes the outcome of the final set of calculations.

2. THE IODINE BEHAVIOUR CODES

The iodine behaviour codes used in this comparison exercise were IODE 5.0 and 5.1, (IRSN), LIRIC 3.3 (AECL), IMOD 2.0, IMOD 2.1 (AECL), IMPAIR (PSI), COCOSYS/AIM-F1(GRS) and modified IODE (NRIR), and IODE 4.2 (CIEMAT). The purpose of each of these codes is to describe chemical and physical processes that influence iodine behaviour under conditions relevant to post-accident containment. COCOSYS is a containment code system in which the iodine model AIM-F1 is integrated and tightly coupled with the thermal hydraulic and aerosol modules. Therefore, the fundamental components of each of these codes are similar. Each code contains sub-models for key processes such as:

1) the interconversion between non-volatile iodine species (e.g., I^-, IO_3^-) and volatile iodine species (I_2) in the aqueous and gas phases,
2) the formation and destruction of organic iodides,
3) the transport of volatile species (e.g., I_2, RI) across a liquid-gas interface,
4) the transport of iodine species to (adsorption) and from (desorption) surfaces, and
5) the transport of iodine species to condensing films and to the bulk aqueous phase by condensation flows.

Reactions between iodine and silver are not mentioned here because silver is not present is none of the four modelled experiments.

A brief description of how the codes model each of these processes is provided below.

2.1 Interconversion between Iodine Species

The iodine behaviour codes used in the current exercise model the hydrolysis of molecular iodine in essentially the same way [1,2]:

$$I_2 + H_2O = HOI + I^- + H^+ \quad (1)$$
$$HOI = OI^- + H^+ \quad (2)$$
$$3HOI = IO_3^- + 2I^- + 3H^+ \quad (3)$$

therefore, it is only in the radiolytic reaction subset that the interconversion of iodine species is modelled differently[2]. Although only important for the Phase 10 Test 1, due to the high pH, reaction (2) was omitted in the IMPAIR calculations presented in this document.

In LIRIC, a mechanistic model is used for calculating the concentrations of the water radiolysis species that subsequently react with various iodine and organic species to produce volatile iodine species, and reduce these volatile species back to non-volatile iodide. The key radiolytic reactions are:

Primary water radiolysis, i.e.,

$$4.1\ H_2O \xrightarrow{h\nu} 2.6\ e_{aq}^- + 0.6\ \bullet H + 2.7\ \bullet OH + 0.7\ H_2O_2 + 2.6\ H^+ + 0.45\ H_2 \quad (4a)$$

where the coefficients in Reaction (4a) are the G-values for the primary production from γ-radiolysis of water in units of molecules per 100 eV absorbed dose.

Secondary reactions of the primary water radiolysis products with each other and with organic and inorganic impurities and, (4b)

Oxidation and reduction of iodine species[3],

$$2I^- + 2\bullet OH \rightarrow I_2(aq) \quad (5)$$
$$I_2(aq) + 2O_2^- \rightarrow 2I^- + 2O_2 \quad (6)$$
$$I_2(aq) + H_2O_2 \rightarrow 2I^- + 2H^+ + O_2 \quad (7)$$

Reactions (5) through (7) in LIRIC is dependent upon dose-rate. Reactions (1) – (3) and (6) and (7) are extremely dependent upon the aqueous pH, and Reactions (1) and (7) have strong temperature dependences.

IODE 5.0, IODE 4.2, IMPAIR, and COCOSYS use two equations to model radiolysis of iodine species in the aqueous phase. In IODE, the equations are:

---

[2] IMOD does not explicitly contain the I_2 hydrolysis reactions. However, IMOD was constructed from LIRIC and the overall rates for volatile iodine production and decomposition used in IMOD reflect the hydrolysis processes.

[3] Note that Reactions (5) through (7) are written as overall reactions, consisting of more than one step. The codes model the individual steps separately.

$$2I^- \xleftrightarrow{h\nu} I_2 \quad (8)$$

$$I_2 + 3\,O_2 \xleftrightarrow{h\nu} 2\,IO_3^- \quad (9a)$$

The pH and dose-rate dependence of molecular iodine formation in IODE 5.0 is incorporated into the rate equations in the following manner:

Rate of I_2 production by (8) $= d[I_2]/dt = k_8\,[I^-]\cdot[H^+]^n\cdot D - k_{-8}[I_2]$, (10a)

Rate of I_2 production by (9a) $= d[I_2]/dt = k_{-9a}[IO_3^-]\cdot[H^+]^n\cdot D - k_{9a}[I_2]$ (11a)

where D is the dose-rate in $Gy\cdot s^{-1}$, and the n is a user-defined exponential term.

In IODE 5.1, there is a different formulation for the rate of production of I_2 from I^-

Rate of I_2 production by (8) $= d[I_2]/dt = k_8 D - k_{-8}\,[I_2] / ([I^-]\,[H^+]^{0.5})$ (10b)

Although of small contribution, the thermal oxidation of iodide by dissolved oxygen to produce I_2 is modelled in IMPAIR. IMPAIR and COCOSYS also contains Reaction (8) with a rate expression similar to that for IODE, but with different values for the rate constants and the exponent, and with D expressed in units of $kGy\cdot h^{-1}$. Both of these codes also contain oxidation of I_2 by O_2 in the aqueous phase, (Reaction 9b), but instead of I_2 being reversibly converted to IO_3^-, the iodine oxidation reaction is an irreversible process represented by:

$$I_2 + 3\,O_2 \rightarrow 2\,IO_3^- \quad (9b)$$

with the rate equation:

$$d[I_2]/dt = -k_9[I_2] \quad (11b)$$

Iodate is then irreversibly converted to iodide.

$$2IO_3^- \xrightarrow{h\nu} I^- + 3O_2 \quad (12)$$

with its rate defined as:

$$d[IO_3^-]\,/\,dt = -k_{12}[IO_3^-]^n\cdot D \quad (13)$$

IMOD uses Reaction (8) to represent overall (both thermal and radiolytic) interconversion of iodine species in the aqueous phase, with the rate expression formulated so as to reproduce as closely as possible the overall pH, temperature and dose-rate dependence of overall volatile iodine production predicted by LIRIC over a wide range of conditions. Reactions (1) through (7) and any iodate formation and reduction in LIRIC are represented by the equivalent of Reaction (8) in IMOD.

$$\text{NONVOLI} \longleftrightarrow \text{VOLI} \quad 8a)$$

NONVOLI represents all non-volatile iodine species, whereas VOLI represents I_2. IMOD does not distinguish between iodate and I^-, so Reaction (8a) in IMOD covers the production of I_2 from I^- and IO_3^-, and its conversion back to these species. In IMOD 2.0, the rate equation is further simplified such that the rate of production of volatile iodine species (i.e. the forward rate of Reaction (8a)) is dependent only on dose-rate and independent of pH and temperature, whereas the backward rate (reduction of I_2 to I^-) is pH, temperature and dose-rate dependent.

2.2 Organic Iodide Formation and Decomposition

The sub-models for radiolysis of organic species and formation and decomposition of organic iodides are treated quite differently in each of the various iodine behaviour codes. LIRIC and IMOD contain essentially the same sub-model to describe these processes. These codes, along with IODE(NRIR) assume that organic iodide formation is primarily an aqueous-phase process, initiated by the radiolytic decomposition of organic solvents in the aqueous phase (Reactions (14) to (16)). Decomposition of organic iodides by hydrolysis, Reaction (17), and radiolysis Reaction (18), is also incorporated into these codes.

The model for organic iodide formation and decomposition in LIRIC and IMOD is[4]:

$$RH + {\bullet}OH \rightarrow R{\bullet} + H_2O \quad (14)$$

$$R{\bullet} + O_2 \rightarrow RO_2{\bullet} \rightarrow\rightarrow CO_2 \quad (15)$$

$$R{\bullet} + I_2/HOI \rightarrow RI + I{\bullet} \quad (16)$$

$$RI + H_2O/OH^- \rightarrow I^- + H^+ + ROH \quad (17)$$

$$RI + e^-_{aq} \rightarrow I^- + R{\bullet} \quad (18)$$

In these models, the formation of organic iodides is dose-rate dependent, because both the rate of production of R• and I_2 are dependent upon the dose-rate (•OH radical concentration affects both). However, because RH and I^- compete with each other for •OH radicals, an increase in the dose-rate by a given factor does not result in linear increase in both the amount of I_2 and R•. The dose-rate dependence of organic iodide formation in LIRIC and IMOD is not as strong as it is in some of the other codes, which assume that the both formation of I_2 and the formation of organic iodides have separate and additive dependences on the dose-rate (see Reactions (22) through (27) below).

In LIRIC and IMOD, the concentration of organic species RH(aq) is assumed to be dependent upon its rate of accumulation in the aqueous phase as a result of dissolution from wetted or immersed painted surfaces (as well as on its rate of depletion by Reaction (14)). The rate of accumulation is described as a temperature dependent, first-order kinetic process:

$$[RH(aq)]_t = [RH(aq)]_\infty \cdot \left(1 - \exp\left(-k_{DIS} \cdot t\right)\right) \quad (19)$$

[4] The organic sub-models in LIRIC and IMOD differ only in the way they calculate OH concentration. In LIRIC, •OH concentration is modeled in detail using the full water radiolysis reaction set, whereas in IMOD, the •OH concentration is expressed using a simple algebraic formula. The algebraic formula in IMOD is however based on a steady-state analysis of the mechanistic model.

where $[RH(aq)]_t$ and $[RH(aq)]_\infty$ represent the concentrations of organic compound in the aqueous phase at time t, and when dissolution is complete, respectively, and k_{DIS} is the dissolution rate constant (s^{-1}). $[RH(aq)]_\infty$ ($mol \cdot dm^{-3}$) is determined by the initial amount of solvent available in the paint polymer to be released into a given volume of water and is a function of temperature, coating thickness and paint age. The rate constant k_{DIS} is also dependent upon these parameters.

IODE(NRIR) formulates organic iodide formation in the aqueous phase using a simple first order equation (see Reaction (20) below), and does not incorporate an organic solvent accumulation process into the model, instead, it assumes an initial [RH](aq) that is independent of temperature, and is user-defined. For this exercise, IODE NRIR assumed an initial concentration of 1×10^{-3} $mol \cdot dm^{-3}$ for all calculations. In addition, in IODE(NRIR) organic iodides decompose only by hydrolysis, (Reaction (17)), and not by radiolysis (Reaction (18)).

In IODE 5.0 (IRSN) and IMPAIR, organic iodide formation can occur both by aqueous-phase processes and heterogeneous processes:

(a) Aqueous homogeneous thermal process (I_2 and HOI):

$$I_2(aq) + 2\ CH_3R(aq) \rightleftarrows 2\ CH_3I(aq) + 2\ R(aq) \qquad (20a)$$

with the rate defined as:

$$d[CH_3I(aq)]/dt = k_{20a}\,[I_2(aq)]\,[CH_3R(aq)] - k_{-20a}\,[CH_3I(aq)] \qquad (21)$$

The IMPAIR code also considers the corresponding reaction with HOI:

$$HOI(aq) + CH_3R(aq) \rightleftarrows CH_3I(aq) + R(aq) \qquad (20b)$$

with the rate defined as:

$$d[CH_3I(aq)]/dt = k_{20b}\,[HOI(aq)]\,[CH_3R(aq)] - k_{-20b}\,[CH_3I(aq)] \qquad (21)$$

(b) Heterogeneous thermal and radiolytic process:

$$Paint + I_2(s) \text{ or } I^-(s) \rightleftarrows CH_3I(g,aq) + R(s) \qquad (22)$$

with the rate defined as,

in COCOSYS:

$$d[CH_3I]/dt = (A/V_g)\,(k_{22} + k_{22}^{rad}\,D)\,[H^+]^{0.24}\,(2\,[I_2(s)] + [I^-(s)]) \qquad (23a)$$

in IODE 5.0 (IRSN) and IODE 4.2:

$$d[CH_3I]/dt = (A/V_g)\,(k_{22} + k_{22}^{rad}\,D)\,[H^+]^{0.24}\,(2\,[I_2(aq)] + [I^-(aq)]) \qquad (23b)$$

where A is the total (dry and submerged) paint surface area, V is the volume of the gas phase, and s in brackets refers to deposited species.

Note that although Reaction (22) in IODE 5.0 (IRSN) is a surface process, the rate of production of CH_3I is formulated using the aqueous-phase concentrations of I_2 and I^- rather than the surface concentrations. The implicit assumption is that the surface concentrations of the iodine species are proportional to the aqueous concentrations.

The formulation of Equation (23) results in organic iodide formation being very pH dependent. This direct pH dependence, resulting from the $[H^+]^{0.24}$ term, is augmented by the dependence of I_2(aq) or I_2(s) on pH. . As a result, organic iodide formation is more strongly dependent on pH than it is in LIRIC and IMOD.

The dose-rate dependence of organic iodide formation according to equations (23a) and (23b) depends on how much iodide is predicted to be deposited on surfaces. The overall rates of organic iodide formation via Reactions (20) and (22) are proportional to the dose-rate because the rate of production of I_2 is dose-rate dependent. In addition, Reaction (22) has an extra dose-rate dependence resulting from the $k_{22}^{rad}D$ term. However, if appreciable I^- is deposited on the surface, and if k_{22} is larger than k_{22}^{rad}, there is a pathway to formation of organic iodides that is independent of the dose-rate.

The initial concentration of organic species $[CH_3R]$, is a user-defined input in both IODE 5.0 (IRSN) and IMPAIR.

Decomposition of CH_3I by hydrolysis, Reaction (17), is included in IODE 5.0 (IRSN) IMPAIR, IODE 4.2 and COCOSYS.

Many of the codes include radiolytic decomposition of organic iodides in both the gas and aqueous phases (Reaction 24).

$$CH_3I(g,aq) + h\nu \longleftrightarrow I_2(g,aq) + 2\ CH_3\bullet\ (g,\ aq) \quad (24)$$

$$-d[CH_3I]/dt = k_{24}\ D\ [CH_3I] - k_{-24}\ [I_2]\ [CH_3\bullet] \quad (25)$$

IODE 5.0 and 5.1 model both the radiolytic decomposition in aqueous and gaseous phase with I_2 being the product formed. The rate of destruction is of 1st order with respect to $[CH_3I]$ and is proportional to the dose rate.

IODE 5.1 has an organic formation model in the aqueous phase that is based on the same assumptions made in LIRIC and IMOD; i.e that the reaction of hydroxyl radicals with dissolved RH leads to the formation of organic radicals (R·), which then react with I_2 to form organic iodides. In this model, the first step is the dissolution in water of organic compounds released from the paints:

$$R_{paint} \rightarrow RH_{(aq)} \quad (26)$$

$d[RH(aq)]/dt = k_{11}\ A\ [R_{paint}]\ /V$ in $mol\cdot dm^{-1}\cdot s^{-1}$ with k_{11} in s^{-1}, A in dm^2, $[R_{paint}]$ which is the initial carbon compounds contain in the paint per unit of area ($3\ 10^{-6}$ $mol\cdot dm^{-2}$ as default value) and V the aqueous volume in dm^3.

The second step is that the organic radicals formed react with I_2 and O_2 in the competitive reactions:

$R^{\bullet} + I_2 \longrightarrow RI + \ldots$
(27a)

$R^{\bullet} + O_2 \longrightarrow RO^{\bullet} + \ldots$
(27b)

$d[RI(aq)]/dt = k_A D (\alpha [I_2]) (k_B [RH])/ (k_C + k_B [RH] + k_D [I^-])$ with D is the dose rate, in $Gy.s^{-1}$

k_A ($mol \cdot dm^{-3} \cdot Gy^{-1}$) is the production rate constant of the radical $OH^{\bullet}$, in
k_B ($mol^{-1} dm^{-3} \cdot s^{-1}$) is the destruction rate constant of $OH^{\bullet}$ due to the oxidation of organic compounds into radicals following to : $RH + OH^{\bullet} \rightarrow R^{\bullet} + H_2O$,
k_C (s^{-1})is the overall destruction rate of $OH^{\bullet}$ in water, in
k_D ($mol^{-1} dm^{-3} \cdot s^{-1}$) is the destruction rate constant of $OH^{\cdot}$ due to the oxidation of I^- and

$\alpha [I_2]$ represents the fraction of organic radical consumed by I_2, in competition with O_2

IODE 5.1(IRSN) and IMPAIR assume also that the organic iodides are produced by a surface process based on a model developed by Funke [2], which is similar to that in Reaction (22).

$Paint + DEP \underset{\leftarrow}{\rightarrow} CH_3I(g) + \ldots$
(28)

$d[CH_3I(g)]/dt = (A/V_g) (k_{29} [DEP]^{0.50} + k_{29}^{rad} D [DEP]^{0.43})$
(29)

where:

$[CH_3I(g)]$	= CH_3I concentration in the gas phase ($mol \cdot m^3$)
k_{29}^{rad}	= rate constant for radiation induced RI formation
k_{29}	= rate constant for thermal induced RI formation
[DEP]	= iodine deposited on dry paint ($mol \cdot m^2$)
A	= total dry painted surface area (m^2)
V_g	= gaseous volume (m^3)
D	= dose-rate ($Gy \cdot s^{-1}$).

For temperatures around 100°C, contributions by thermal processe are negligible except if the gas dose rate is small enough, i.e. $D < 0.01$ $Gy.s^{-1}$. The overall production rate is somewhat dependent upon pH and temperature, since the concentration of I_2 in either the gas or aqueous phase has some effect on the amount of iodine deposited on the surfaces. The concentrations of deposited species ($I_2(s)$ and $I^-(s)$) are calculated by the iodine absorption sub-model.

2.3 Interfacial Mass Transfer and Surface Adsorption

Mass transfer and surface adsorption (excluding adsorption on Ag) are modelled in a similar manner in all of the codes. The mass transfer approach uses a standard

two-resistance model. The values recommended for this exercise for the mass transfer coefficients and partition coefficients can be found in Appendix C (blind calculations) and Appendix D (open calculations). Adsorption of I_2 on containment surfaces (both wet and dry) is described as a first order process with recommended rate constants as given in Appendix D. Some of the codes also provide the option of modelling I^- absorption in the aqueous phase, and LIRIC and IMOD used this option for this exercise.

2.4 Condensation

The effect of the condensation of steam on iodine volatility is modelled in LIRIC and IMOD using a two-step kinetic scheme. Molecular iodine (but not organic iodides) is assumed to be absorbed into a condensing film covering the surfaces, in a simple first order process, identical to that of absorption. Once absorbed into the condensing steam, it is assumed to be hydrolysed to I^-, and returned to the sump by the condensate flow. Absorption of molecular iodine on non-immersed surfaces in the presence of steam is assumed to be slower than its absorption on the same surfaces under non-condensing conditions.

$$\frac{d([I_2(con)])}{dt} = k_{AD}^{cw} \cdot [I_2(g)] \cdot \frac{V_g}{V_{con}} \tag{30}$$

$$\frac{d([I_2(g)])}{dt} = -k_{AD}^{cw} \cdot [I_2(g)] \tag{31}$$

where V_{con} is the volume of the condensate on the wall in dm^3, V_g is the volume of the gas phase, and k_{AD}^{CW} is the rate constant for absorption of iodine in condensing water. k_{AD}^{CW} is further defined as:

$$k_{AD}^{CW}\ (s^{-1}) = v_{AD}^{CW} \cdot (A_{con}/V_g) \tag{32}$$

$$v_{AD}^{CW}\ (dm \cdot s^{-1}) = (7 \pm 2) \times 10^{-4} \tag{33}$$

where A_{con} is the surface area of the condensing water film in units of dm^2.

The mass transport rate of iodine from wall condensate to the aqueous phase depends on the condensation rate of water and therefore depends on the steam concentration, the temperature difference between the gas phase and the wall, and to a minor extent, on the type of surface. The process is incorporated as a first order process in both models:

$$\frac{d([I_2(con)])}{dt} = -k_{con} \cdot [I_2(con)] \tag{34}$$

$$\frac{d([I^-(aq)])}{dt} = 2\ k_{con} \cdot [I(con)] \cdot \frac{V_{con}}{V_{aq}} \tag{35}$$

$$k_{con}\ (s^{-1}) = F_{con}/V_{con} \tag{36}$$

where F_{con} is the flow rate of condensate going into the aqueous phase ($dm^3 \cdot s^{-1}$) and V_{con} is the volume of condensate on the walls in dm^3.

In IODE(NRIR), IODE(IRSN), and IMPAIR, the fraction of gaseous iodine removed by condensation and transported to the bulk water phase is assumed to be the same as the fraction of the mass of steam condensed into the bulk phase. These codes assume that organic iodides are also removed by steam condensation whereas LIRIC and IMOD do not. They also differ from LIRIC and IMOD in that they do not assume that I_2 and CH_3I are hydrolysed to I^-, rather these species remain in the same form when they are transferred to the bulk water phase.

Regardless of the model used, the condensation sub-model results in a first-order rate of removal of gaseous iodine species from the gas phase.

3. BLIND CALCULATIONS

The blind calculation exercise was one in which each of the participants were supplied with information about CAIMAN and RTF experiments, with a list of input and boundary conditions (pH, temperature, dose-rate, sampling schedule, etc.) This information is provided in Appendix C. Based on the information provided, participants performed blind calculations and submitted their results to IRSN and AECL. After the blind calculation results were submitted, the experimental results were distributed to each of the participants, who performed their own evaluation of their code performance against the experimental results. Selected plots of results for Phebus RTF1 and CAIMAN 97/01 are shown in Figures 1 – 6.

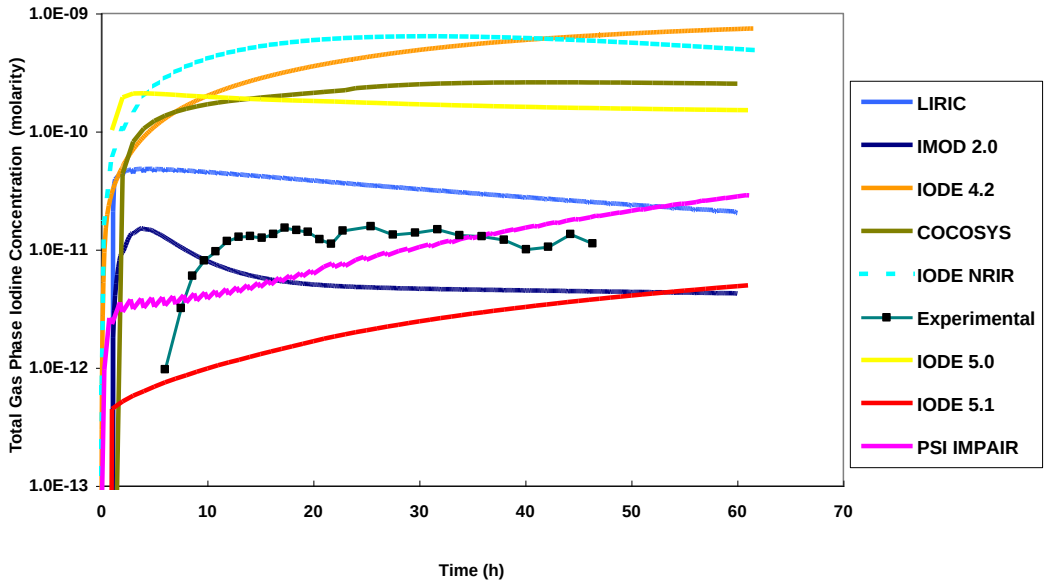

Figure 1: Total Gas Phase Iodine Concentration for CAIMAN 97/02 as Compared to Code Calculations (Blind).

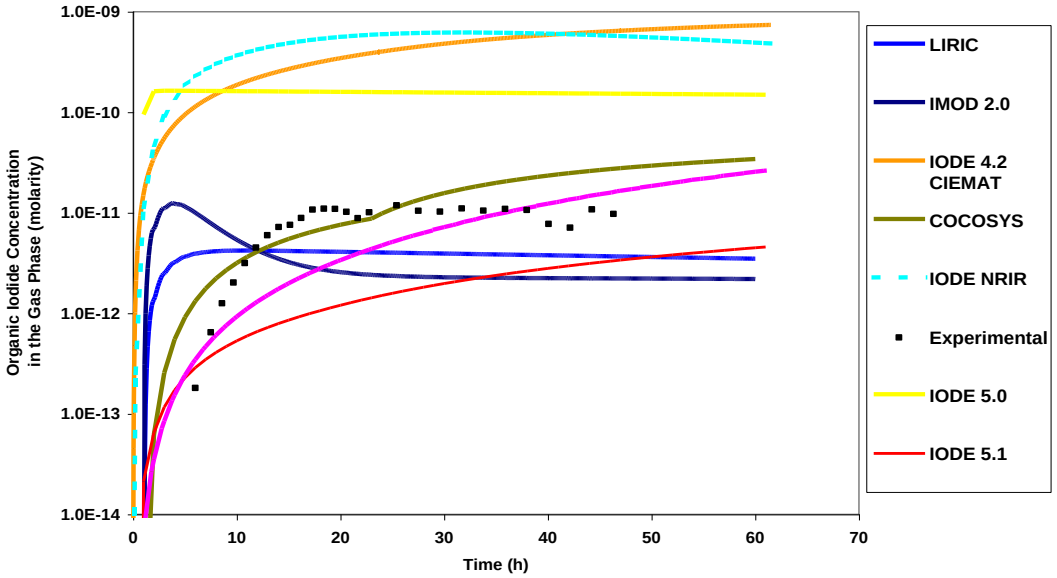

Figure 2: Total Gas Phase Organic Iodide Concentration for CAIMAN 97/02 as Compared to Code Calculations (Blind).

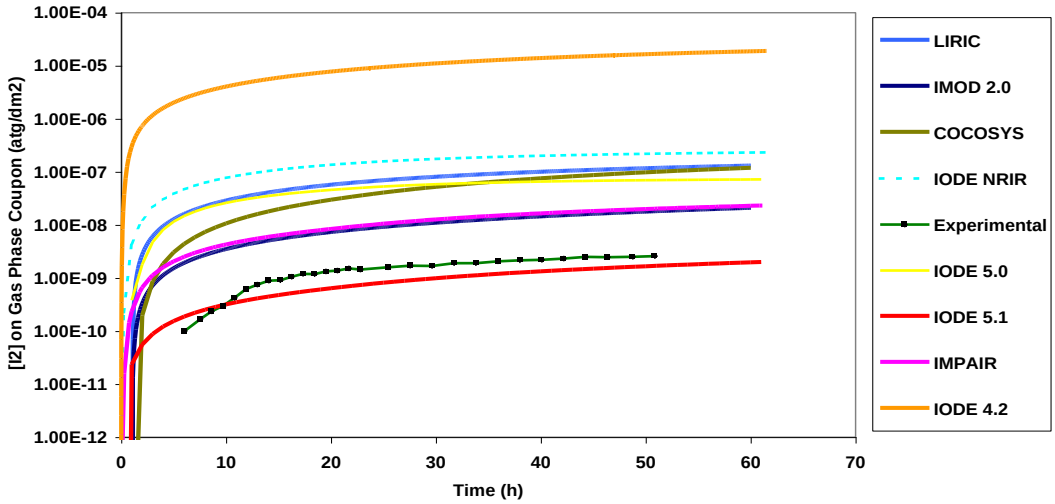

Figure 3: Total I_2 Adsorbed on Gas Phase Painted Coupons for CAIMAN 97/02 as Compared to Code Calculations (Blind).

As can be seen from the calculations for CAIMAN 97/02, there is a wide variation between code predictions. Gas phase iodine concentrations predicted by the codes vary by nearly three orders of magnitude (Figure 1). Equally large discrepancies exist for the predicted organic iodide concentrations (Figure 2). From analysis of the predicted quantities of I_2 in the gas phase on coupons exposed to the gas phase, it was concluded that most of the codes overestimated the I_2 production in the aqueous phase for this experiment.

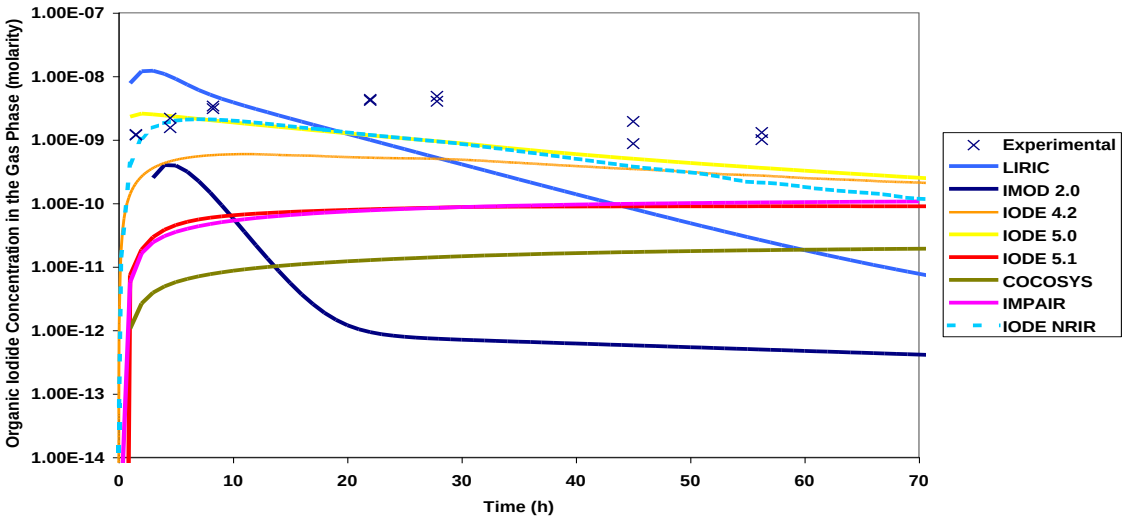

Figure 4: Total Gas Phase Organic Iodide Concentration for Phebus RTF1 as Compared to Code Calculations (Blind).

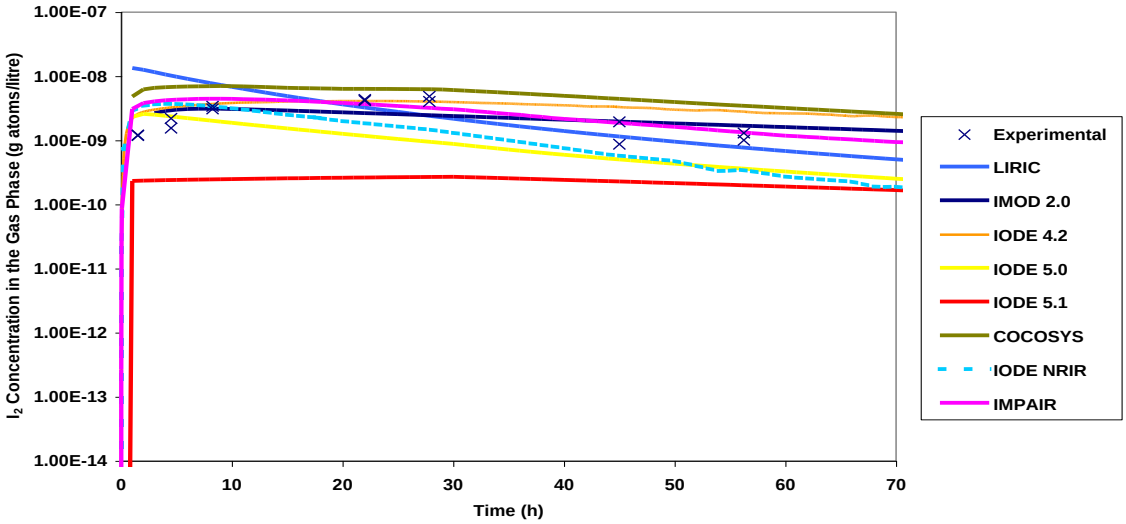

Figure 5: Total Gas Phase I_2 Concentrations for Phebus RTF1 as Compared to Code Calculations (Blind).

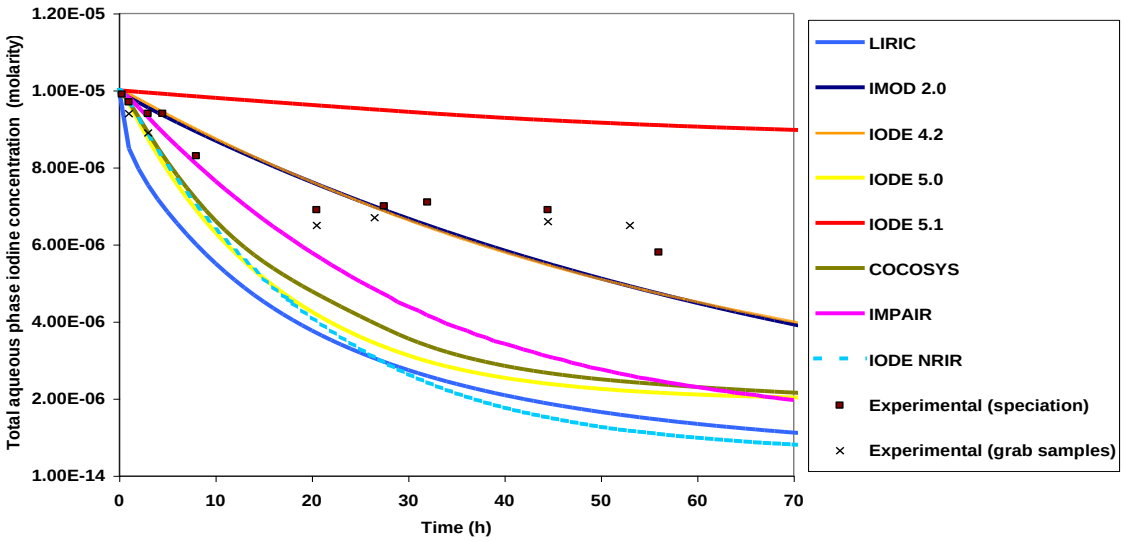

Figure 6: Total Calculated Aqueous Phase Iodine Concentration for Phebus RTF1 as Compared to Code Calculations (Blind).

Results from Phebus RTF1 also indicate that most of the codes predict that the overall production of I_2 in the aqueous phase is too high. Although the amount of I_2 predicted to be in the gas phase was not overestimated by the codes (Figure 5), most of them significantly underestimated the amount of iodine remaining in the aqueous phase. The codes predicted that I_2 formed in the aqueous phase was absorbed on gas or aqueous phase surfaces, depleting the aqueous phase concentration.

The blind calculations for CAIMAN 2001/01 and Phase 10 Test 1 were more difficult to analyze. This is due to a couple of factors.

- For Phase 10 Test 1, the pH was held at 10 for the first several hours, and then pH control was removed. Very few codes have a module for predicting pH changes due to organic dissolution and radiolytic degradation in the aqueous phase, therefore most participants "guessed" at the resulting pH profile. Since most overestimated the pH drop, the results are difficult to interpret.

- For CAIMAN 01/01, many participants received incorrect information regarding the presence of coupons in the aqueous phase. Consequently, many of the calculations incorporated aqueous phase adsorption onto coupons, and this skewed the results.

Plots of the total gas phase iodine concentrations predicted from these experiments are shown in Figures 7 and 8. As can be seen from the results, there are considerable differences between the code calculations with especially large discrepancies regarding the predicted organic iodide concentrations in the gas phase.

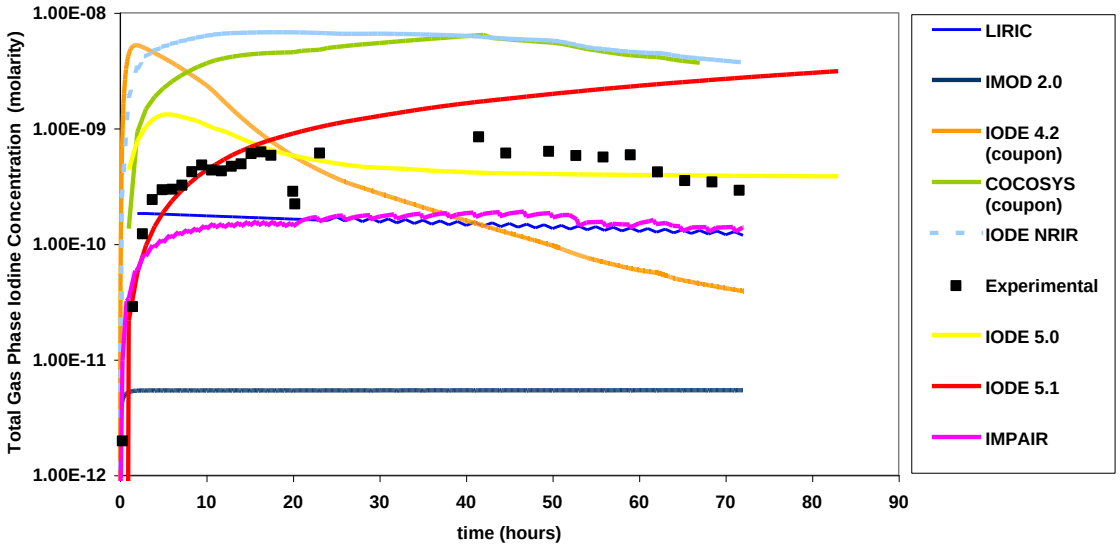

Figure 7: Total Gas Phase Iodine Concentration for CAIMAN 0101 as Compared to Code Calculations (Blind).

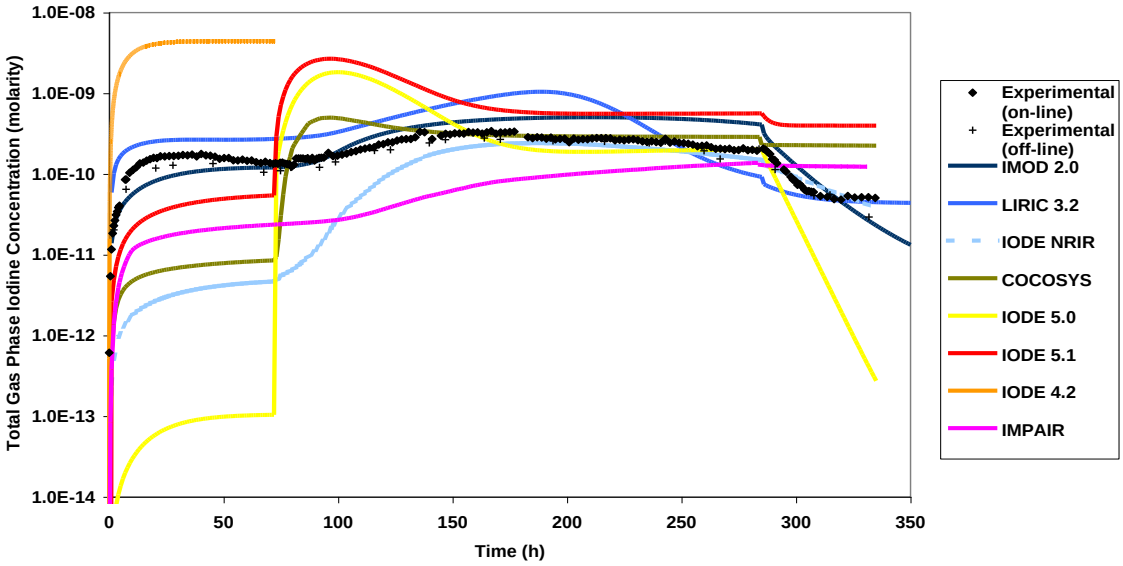

Figure 8: Total Gas Phase Iodine Concentration for Phase 10 Test 1 as Compared to Code Calculations (Blind).

3.1 Summary of Blind Calculation Results

Many of the parameters used in the blind calculations, such as adsorption/desorption rate constants and mass transfer coefficients, were very different from code to code, making an extensive evaluation of the blind calculations difficult. However, there are a few general observations that can be made. The most striking one is that there was a large scatter in the predicted gas phase iodine concentrations for every experiment. This would indicate that the genuine predictive capability of the codes, at this stage of the code comparison exercise, was not adequate. An additional observation regarding

the blind calculations is that most of the codes over-predicted the amount of I_2 formed in the aqueous phase under conditions of low pH (pH 5) and high temperatures (90ºC and higher). These conditions applied to both CAIMAN experiments and Phebus RTF1, where most codes predicted larger gas phase I_2 concentrations than were observed and/or that more I_2 was absorbed on surfaces than was observed. As the result of their predictions of large amounts of I_2 being absorbed on surfaces, most codes underestimated the amount of iodine in the aqueous phase (see for example results from Phebus RTF1 see Figure 6).

It was also noted that there was particularly poor agreement between code predictions and observed results of RTF Phase 10 Test 1. This is because, in a portion of the experiment, the pH was not controlled, and was allowed to decrease to the radiolytic oxidation of organic solvents (from the paint) to organic acids and CO_2. Most codes do not have the capability to predict pH changes as the result of this radiolysis process, and because they could not predict the pH, their predictions of volatile iodine production were also not good.

A summary of participants' evaluation of their codes' performance in the blind calculations follows:

GRS, COCOSYS/AIM

The results of the blind calculations were not in good agreement with the CAIMAN and RTF measurements made for the iodine species of radiological interest: the I_2 concentration in the gas phase was significantly overestimated: the CH_3I concentration in the gas phase was significantly underestimated. Several reaction coefficients recommended for use in the calculations differed significantly from AIM default values. These modifications and measurement uncertainties had to be taken into account when discussing the COCOSYS/AIM results

PSI/IMPAIR3

Calculated I_2 concentrations in the gas phase for CAIMAN 97/02 were in good agreement with measured concentrations. The amount of I_2 deposited on sump coupons was twice that of the measured value, whereas the fraction remaining in the water was half the experimental values. The organic iodide concentration was lower than that measured, but calculated and experimental numbers were in good agreement at the end of the experiment.

In Phebus RTF1, the amount of I_2 deposited on paint coupons was greatly over-predicted for both the gas and aqueous phase. The gas phase I_2 concentration was predicted well, but the organic iodide concentration was under-predicted by about ten times.

In RTF Phase 10 Test 1, I_2 in the gas phase was under-predicted by a factor of 10, CH_3I was slightly over-predicted and high molecular weight organic iodides were predicted reasonably well. There was more iodine in the aqueous phase than the experimentally measured value.

For CAIMAN 01/01, much more iodine was predicted to be absorbed on painted coupons in the gas phase than was observed. The gas phase I_2 concentration was predicted well, but both high and low molecular weight organic iodides were under-predicted.

CIEMAT IODE 4.2

Radiolytic reactions seem to play a key role in organic iodine chemistry according to IODE code formulation. All the cases analysed indicate that IODE modelling of aqueous I_2 production from I^- via radiation could be susceptible of some changes resulting in: an increase of I_2 formation under alkaline conditions and a decrease of I_2 formation under acid conditions. Under basic conditions, IODE modelling of heterogeneous organic iodide generation from wet painted surfaces seems to require a lower reaction rate. However, no clear trends have been observed with acid pHs.

IODE predictive capability may be considered adequate if a discrepancy of an order of magnitude in iodine gas phase concentration is seen as acceptable. IODE simulations worked better in RTF tests than in CAIMAN ones. In particular, CAIMAN 97/02 required to impose a time-dependent dose rate to fit data.

IRSN IODE 5.0 and 5.1

For CAIMAN 97/02, IODE 5.0 slightly over-predicts and IODE 5.1 slightly underpredicts gas phase I_2 concentrations. IODE 5.1 calculates organic iodide concentrations well, whereas IODE 5.0 over-predicts organic iodide concentrations. IODE 5.1 predictions of the total iodine concentrations in the aqueous phase and adsorbed on painted coupons are better than those of IODE 5.0.

For CAIMAN 01/01, IODE 5.0 predicted both CH_3I and I_2 concentrations better than IODE 5.1, but the trends predicted by IODE 5.1 were better. IODE 5.0 overestimated the amount of iodine deposited on painted coupons whereas IODE 5.1 predicted them well.

For Phebus RTF1, IODE 5.0 predicted the gas phase concentration better, but IODE 5.1 predicted the trend better, both codes predicted the gas phase iodine concentration to within an order of magnitude. IODE 5.0 underestimated the total aqueous phase iodine concentration whereas IODE 5.1 overestimated. In keeping with this observation, IODE 5.0 over-predicted the amount absorbed on aqueous coupons whereas IODE 5.1 predicted it well.

For RTF Phase 10 Test 1, during the first few hours when pH was maintained at 10, IODE 5.1 reproduced the gas phase concentrations of I_2 and CH_3I reasonably well.

AECL, LIRIC 3.3 and IMOD 2.0

For CAIMAN 97/02, IMOD 2.0 predicted I_2 well but underestimated the organic iodide concentration. The organic concentration predicted by the IMOD was such that organic impurities were introduced too rapidly and depleted too quickly relative to the experimental results. LIRIC calculations overestimated the amount of iodine

adsorbed on gas phase surfaces and the amount of I_2 in the gas phase. Organic iodide concentrations were over-predicted by LIRIC, and the code also predicted a much faster and shorter duration of release of organic compounds than was observed experimentally (by analysis of the total carbon content of the water).

For CAIMAN 01/01 IMOD underestimated both I_2 and organic iodide concentrations in the gas phase. LIRIC predicted the I_2 concentration well, but under-predicted organic iodide concentrations. LIRIC predictions regarding organic impurity concentrations in the aqueous phase were also much lower than those observed experimentally. This is one reason for its underestimation of organic iodide formation.

For Phebus RTF1, IMOD 2.0 predicted the total gas phase concentration well, but the predicted organic iodide concentration profile underwent too rapid a decrease compared to experimental results. LIRIC calculations predicted the gas phase I_2 concentrations well but overestimated the amount of I_2 adsorbed onto aqueous phase surfaces. LIRIC calculations also predicted too rapid a decrease in organic iodide concentrations, indicating that the organic impurities were introduced into the aqueous phase at too rapid a rate, and therefore decreased too rapidly.

For Phase 10 Test 1, both LIRIC and IMOD reproduced the concentrations of I_2 in the gas phase well. IMOD slightly over-predicted the amount of organic iodide in the gas phase, whereas LIRIC predicted them well.

3.2 General Observations of Blind Tests

The general consensus was that none of the codes could reproduce all of the experiments in a manner that satisfied the participants, but that with some model analysis and then some modifications, the codes should perform better.

4. OPTIMIZED CALCULATIONS

After the blind calculations were completed, and upon receiving experimentally measured data, the participants met to discuss the blind calculation results and strategies for code optimizations. At a meeting in Ottawa in September 2002, the participants decided upon criteria with which to judge their calculation results, and a list of "hard numbers" (deposition velocities and mass transfer coefficients) that were to be used in their code calculations. These are supplied in Appendix D.

4.1 Modifications Made For Optimized Calculations

For the blind calculations, most of the codes used their default parameters (e.g. rate constants for iodide oxidation), mass transfer coefficients and some parameters recommended at the introductory meeting (See Appendix C: Note to Participants). AECL performed calculations with LIRIC 3.3 and IMOD 2.0. IRSN performed calculations with both IODE 5.0 and IODE 5.1; for optimized calculations only IODE 5.1 was used. NRIR and CIEMAT performed calculations with their versions of IODE, GRS and PSI performed calculations with COCOSYS and IMPAIR

respectively. For the optimized calculations, a number of changes were implemented. These are outlined below:

PSI modifications:

- The rate coefficient for formation of organic iodide (HMWI) from painted surfaces in the gas phase was multiplied by 10.
- The model for formation of organic iodide from the paint in the aqueous phase (Funke model) was deactivated.
- A simple model with 4 fitted rate constants was introduced to replace Funke model.
- No radiolytic destruction of organic iodide in the gas phase (not enough gamma radiation adsorbed by the gas) was modelled for CAIMAN tests.
- The partition coefficient of high molecular weight organic iodides was set to be = 1000 × partition coefficient of CH_3I.

GRS modifications:

- Uncertainty of the organic iodide formation rate constant = +/- factor of 10, so it gives 2 decades on the $[CH_3I]_g$ – for these calculations, rate constant has been multiplied by 5.
- In order to obtain the recommended adsorption rate constants, GRS had to "decouple" adsorption and mass transfer. In COCOSYS, adsorption is represented by:

$$\frac{1}{k_{tot}} = \frac{1}{k_{AD}} + \frac{1}{k_{MT}}$$

  k_{AD} is the pure chemical adsorption/desorption rate coefficient and k_{MT} is the iodine mass transfer coefficient in the boundary layer. k_{MT} is the same parameter used for the mass transfer between gas and sump. The gas-side $k_{MT,g}$ is used for the adsorption/desorption processes in the gas phase and the water-side $k_{MT,w}$ is used for the processes in the water phase. In blind calculations COCOSYS used recommended adsorption rate constants in defining k_{AD} for various adsorption process. However, the recommended values for adsorption rate constants given by IRSN and AECL had already taken into account mass transfer, and hence were values of k_{tot} . In the optimized calculations, COCOSYS values were changed so that $k_{tot} = k_{AD}$. This resulted in much lower predicted iodine concentrations in the gas phase

CIEMAT modifications:

CIEMAT performed two calculations, one referred to as base case (BC) and another referred to as best estimate (BE). The differences between the two are:

- The rate constant for the radiolytic oxidation of iodide to iodine (k_7) was varied: $k_7=2.17.10^{-5}$ for the base case and $k_7=1.10^{-5}$ for the best estimate case.

- The exponent in the rate constant for formation of organic iodide in the sump (Reaction (22)) was varied:

$[CH_3I]/dt = (A/V_{aq}) (k_{22} + k_{22}^{rad} D) [H^+]^n (2 [I_2(aq)] + [I^-(aq)])$

For the base case the exponent was 0.24, for the best estimate, the exponent was 0.3. At pH=5, for the base case $(10^{-5})^{0.24} = 0.06$; for the best estimate case $(10^{-5})^{0.3} = 0.03$; the best estimate reduces the organic iodide production rate by a factor of two.

- For the CAIMAN experiments, the rate constants for adsorption of iodine on painted surfaces in the gas phase was $4\ 10^{-3}$ m·s-1 for the base case, and $2\ 10^{-3} m \cdot s^{-1}$ for the best estimate case.

AECL modifications:

- IMOD 2.1 was used in optimised calculations. IMOD 2.1 includes improved temperature dependences for the overall rate of production of I_2 and organic iodides in the aqueous phase. IMOD 2.1 predictions regarding steady-state aqueous I_2 concentrations are closer to those of LIRIC 3.3 than those of IMOD 2.0.

It was previously observed in RTF experiments [3] that LIRIC and IMOD overestimate the fraction of iodine in the form of I_2 for RTF experiments where the pH was less than 6, temperatures were 90 ºC, and where boric acid was present. When the same phenomena were observed for CAIMAN experiments, two trial approaches were taken to modify the codes.

- The first approach, shown in this section, was to use large values for the rate constants for adsorption and desorption of I_2 on immersed stainless steel, while maintaining the same overall rate constant and the quantity of I_2 adsorbed on the surface. The change had the desired effect of increasing the overall rate of conversion of I_2 to I^-, and reducing the concentration of I_2 in the aqueous phase. It resulted in very good agreement between calculated and experimental results. However, the magnitude of the rate constants required were inconsistent with what is understood about adsorption/desorption phenomena. For example, the overall adsorption rate constant required to obtain a good fit to CAIMAN 01/01 data was smaller than that used for CAIMAN 97/02. This modification is therefore not considered to be mechanistically sound.

- A more reasonable modification, involved the activation of a sub-model to account for the interaction of I_2 with impurities. This sub-model was reported previously [3] and gives results that are quantitatively the same as those involving adsorption/desorption on stainless steel surfaces. The model invokes an equilibrium between I_2, an impurity, and an I_2 impurity complex (such as an organic- I_2 charge transfer complex or an iodo-ketone). The modification is discussed briefly in Section (5) and Appendix A.

- Dissolution rate constants for both LIRIC and IMOD 2.1 were changed from their original default parameters. For all of the experiments

containing painted surfaces in the gas phase, solvent evaporation from the gas phase surfaces into the gas phase was assumed to occur at higher rates than those assumed previously. This had the results of increasing the amount, and prolonging the duration of the introduction of organic compounds into the aqueous phase. The changes were required to simulate the total carbon concentration measured in CAIMAN facility experiments.

- It should be noted that AECL calculations did not use the "hard values" for adsorption and desorption of I_2 on gas phase surfaces. The reasons for this are outlined in Section 4.4.

NRIR modifications:

There is no modification. These calculations are the same as the blind one.

IRSN modifications:

- The CH_3I destruction process linked to CH_3I formation (Funke model) had to be separated from the production because otherwise, I_2 produced by the destruction of ICH_3 is directly transferred to the painted surfaces.
- The destruction of I_2 by the radiolysis process in the aqueous phase had to be modified because when this reaction is activated, the reverse term is not null even the dose rate is zero (see equation 10b). So a test has been introduced to put to zero this rate when the dose rate is zero.
- Rp is necessary to calculate the homogeneous ICH_3 formation in the liquid phase. The default value is 3.10^{-6} mol/cm^2. It is linked to the surface of the painted coupons in the aqueous phase. In CAIMAN 2001/01, there is no coupon but the analysis of the total carbon in the solution shows that it is about 4 times higher than in CAIMAN 97/02. This is the reason why the value for Rp used in CAIMAN 2001/01 was equal to $3.0\ 10^{-5}$ kg as compared to $7.1\ 10^{-6}$ kg used in CAIMAN 97/02. In a future development of IODE, the organic released by the paints located in the gas phase and partially dissolved in the sump will be taken into account and this contribution will be automatically calculated.

4.2 Mass Balance at Test End

Tables 1 – 4 show the predicted mass balances at test end by the various codes as compared to the experimentally observed mass balances. Based on the criteria agreed to by the participants at an interim meeting for ISP-41 F, Phase 2 (Appendix D), the code predictions for the mass balance at test end were rated either a 1 or a 0. The criteria were:

- Gas phase iodine concentrations predicted to within a factor of 3
- Aqueous phase iodine concentrations predicted to within 20% and

- Fraction of gas phase concentration in the form of organic iodide predicted to within 20%.

After an initial analysis of the data, it was recognized that, in some circumstances, codes predicted the correct organic iodide fraction, despite the actual concentration being more than an order of magnitude over- or under-estimated. Conversely, in some cases, the organic iodide fraction was incorrectly predicted by the codes, yet the organic iodide concentration was correctly predicted. Because the concentration of organic iodides is an important parameter in accident analysis, it was decided that an additional criterion be set for the mass balance at test end. This criterion was:

- Total organic iodide concentration in the gas phase predicted to within a factor of 3.

Table 1: Mass Balance for Optimized Calculations: Phase 10 Test 1

	Total Aqueous Iodine			Total Gaseous Iodine			Gas Organic Iodide Fraction			Gas organic iodide concentration		
	Value	$(V_c-V_e)/V_e$	Rating	Value	V_c/V_e	Rating	Value	$(V_c-V_e)/V_e$	Rating	Value	V_c/V_e	Rating
Experimental	$2.3\ 10^{-6}$	--	--	$5.1\ 10^{-11}$ $4.2\ 10^{-11}$	--	--	0.942	--	--	$4.0\ 10^{-11}$	--	--
COCOSYS	$8.3\ 10^{-6}$	+260%	0	$2.0\ 10^{-10}$	3.9	0	0.967	2.6%	1	$1.9\ 10^{-10}$	4.8	0
IODE 4.2 BC	$4.6\ 10^{-6}$	+100%	0	$1.1\ 10^{-9}$	22	0	1.00	6%	1	$1.1\ 10^{-9}$	28	0
IODE 4.2 BE	$6.2\ 10^{-6}$	170%	0	3.810^{-10}	74	0	1.00	6%	1	$3.8\ 10^{-10}$	28	0
LIRIC	$2.4\ 10^{-6}$	4%	1	$1.2\ 10^{-10}$	2.5	1	0.999	6%	1	$1.2\ 10^{-10}$	2.8	1
IMOD	$2.4\ 10^{-6}$	4%	1	$3.5\ 10^{-10}$	6.6	0	1.00	6%	1	$3.5\ 10^{-10}$	8.3	0
IMPAIR	$2.5\ 10^{-6}$	9%	1	1.810^{-10}	3.6	0	1.00	6%	1	$1.8\ 10^{-10}$	4.5	0
IODE 5.1	$7.5\ 10^{-6}$	226%	0	1.110^{-10}	2.2	1	0.994	6%	1	$1.1\ 10^{-10}$	2.8	1
IODE NRIR	$2.4\ 10^{-6}$	4%	1	$3.8\ 10^{-11}$	0.9	1	01.00	6%	1	$3.8\ 10^{-11}$	0.95	1

Table 2: Mass Balance for Optimized Calculations: Phebus RTF1

	Total Aqueous Iodine			Total Gaseous Iodine			Gas Organic Iodide Fraction			Gas organic iodide concentration		
	Value	$(V_c-V_e)/V_e$	Rating	Value	V_c/V_e	Rating	Value	$(V_c-V_e)/V_e$	Rating	Value	V_c/V_e	Rating
Experimental	$5\ 10^{-6}$	--	--	$2.0\ 10^{-9}$ $6.2\ 10^{-10}$	--	--	0.494	--	--	$9\ 10^{-10}$	--	--
COCOSYS	$8.3\ 10^{-6}$	+66%	0	$4.9\ 10^{-9}$	2.5	1	0.004	-99%	0	$1.9\ 10^{-11}$	.021	0
IODE 4.2 BE	$6.4\ 10^{-6}$	+28%	0	$1.2\ 10^{-9}$	0.6	1	0.133	-73%	0	$1.6\ 10^{-10}$	0.18	0
IODE 4.2 BC	$3.8\ 10^{-6}$	-24%	1	$1.7\ 10^{-9}$	0.9	1	0.118	-76%	0	$2.0\ 10^{-10}$	0.22	0
LIRIC	$5.5\ 10^{-6}$	+10%	1	$1.2\ 10^{-8}$	6	0	0.027	-95%	0	$3.3\ 10^{-10}$	0.37	1
IMOD	$5.6\ 10^{-6}$	+12%	1	$1.4\ 10^{-8}$	7	0	0.016	-97%	0	$2.3\ 10^{-10}$	0.26	0
IMPAIR	$8.3\ 10^{-6}$	+66%	0	$6.5\ 10^{-9}$	3.3	0	0.988	+100%	0	$6.5\ 10^{-9}$	7.2	0
IODE 5.1	$8.1\ 10^{-6}$	+62%	0	$3.1\ 10^{-10}$	0.5	1	0.303	-38%	0	$8.7\ 10^{-11}$	0.10	0
IODE NRIR	$7.9\ 10^{-7}$	-84%	0	$4.5\ 10^{-10}$	0.7	1	0.240	-50%	0	1.110^{-10}	0.12	0

Table 5: Mass Balance for Optimized Calculations: CAIMAN 97/02

Organisation	Total aqueous iodine			Total gaseous iodine			Gas organic iodine fraction			Gas organic iodide concentration		
	Value	$(V_c-V_e)/V_e$	Rating	Value	V_c/V_e	Rating	Value	$(V_c-V_e)/V_e$	Rating	Value	V_c/V_e	Rating
Experimental data	$6.9\ 10^{-6}$	-	-	$1.1\ 10^{-11}$	-	-	0.86	-	-	9.910^{-12}		
COCOSYS (no IO_3-g)	$8.6\ 10^{-6}$	+24%	0	$2.0\ 10^{-10}$	18	0	0.68	-20%	1	$1.4\ 10^{-10}$	14	0
COCOSYS (IO_3-g)				$3.1\ 10^{-10}$	28	0	0.45	-48%	0			
IODE 4.2 BC	$5.0\ 10^{-6}$	-6.2%	1	$1.4\ 10^{-10}$	13	0	0.97	+13%	1	$1.8\ 10^{-10}$	18	0
IODE 4.2 BE	$7.2\ 10^{-6}$	+4.3%	1	$1.2\ 10^{-10}$	7	0	0.93	+8%	1	$1.1\ 10^{-10}$	9	0
AECL (LIRIC)	$7.5\ 10^{-6}$	+9%	1	$3.1\ 10^{-11}$	2.8	1	0.78	-9%	1	$2.5\ 10^{-11}$	2.5	1
AECL (IMOD)	$7.2\ 10^{-6}$	+4%	1	$3.8\ 10^{-11}$	3.5	0	0.76	-11%	1	$2.8\ 10^{-11}$	2.8	1
PSI	$8.8\ 10^{-6}$	+28%	0	$2.9\ 10^{-10}$	26	0	0.98	+14%	1	$2.9\ 10^{-10}$	29	0
IRSN	$9.9\ 10^{-6}$	+44%	0	$1.1\ 10^{-11}$	1	1	0.90	+5%	1	$9.9\ 10^{-12}$	1	1
NRI	$1.49\ 10^{-6}$	-78%	0	$5.9\ 10^{-10}$	54	0	0.98	+14%	1	5.710^{-10}	57	0

Table 4: Mass Balance for Optimized Calculations: CAIMAN 01/01

Organisation	Total aqueous iodine			Total gaseous iodine			Gas organic iodine fraction			Gas organic iodide concentration		
	Value	$(V_c-V_e)/V_e$	Rating	Value	V_c/V_e	Rating	Value	$(V_c-V_e)/V_e$	Rating	Value	V_c/V_e	Rating
Experimental	$3.7\ 10^{-5}$	-	-	$2.9\ 10^{-10}$	-	-	0.885	-	-	$2.6\ 10^{-10}$	--	--
COCOSYS (no IO_3-g)	$3.8\ 10^{-5}$	+3%	1	$5.5\ 10^{-10}$	1.9	1	0.517	-41%	0	$2.8\ 10^{-10}$	1.1	1
COCOSYS (IO_3-g)				$2.3\ 10^{-9}$	7.8	0	0.127	-85%	0	$2.9\ 10^{-10}$	1.1	1
IODE 4.2 BE	$2.6\ 10^{-5}$	-38%	0	$4.3\ 10^{-10}$	0.7	1	0.969	+9%	1	$1.9\ 10^{-10}$	0.73	1
IODE 4.2 BC	$1.7\ 10^{-5}$	-54%	0	$4.2\ 10^{-10}$	0.6	1	0.884	0%	1	$3.1\ 10^{-10}$	1.2	1
AECL (LIRIC)	$3.9\ 10^{-5}$	+4%	1	$1.9\ 10^{-10}$	0.7	1	0.849	-4.5%	1	$1.6\ 10^{-10}$	0.61	1
AECL (IMOD)	$3.9\ 10^{-5}$	+4%	1	$3.1\ 10^{-10}$	1.1	1	0.954	+2.3%	1	$2.9\ 10^{-10}$	1.1	1
PSI	$3.9\ 10^{-5}$	+4%	1	$2.8\ 10^{-9}$	9.6	0	0.993	+12%	1	$2.8\ 10^{-10}$	1.1	1
IRSN	$4.0\ 10^{-5}$	+8%	1	$1.6\ 10^{-10}$	0.5	1	0.966	+9%	1	$1.6\ 10^{-10}$	0.62	1
NRI	$1.1\ 10^{-5}$	-70%	0	$3.7\ 10^{-9}$	12.9	0	0.939	+6%	1	$3.5\ 10^{-9}$	13	0

From analysis of Tables 1 – 4, it is clear that none of the codes can predict all 4 of the important parameters for each test to within the established criteria set by the exercise. To summarize the results:

Phase 10 Test 1;

- 4 out of 8 of the codes reproduced the aqueous phase iodine concentration
- 3 out of 8 reproduced the total gas phase iodine concentration
- 8 out of 8 reproduced the gas phase organic fraction and
- 3 out of 8 reproduce the gas phase organic iodide concentration.

Phebus RTF1;

- 3 out of 8 of the codes reproduced the aqueous phase concentration
- 5 out of 8 reproduced the total gas phase concentration
- 0 out of 8 reproduced the gas phase organic iodide fraction and
- 1 out of 8 reproduced the gas phase organic iodide concentration.
- .

CAIMAN 97/02;

- 4 out of 8 of the codes reproduced the aqueous phase concentration
- 2 out of 8 reproduced the total gas phase iodine concentration
- 8 out of 8 reproduced the organic iodide fraction and
- 3 out of 8 reproduced the gas phase organic iodide concentration.

CAIMAN 01/01;

- 5 out of 8 of the codes reproduced the aqueous phase concentration (and gas phase coupon data)
- 6 out of 8 reproduced the total gas phase iodine concentration
- 7 out of 8 reproduced the organic iodide fraction and
- 7 out of 8 reproduced the gas phase organic iodide concentration.

4.3 Analysis of Trends

Although the predicted mass balance at test end is some indication of whether a code's performance is adequate, its ability to predict trends is also important. Consequently, the next section analyzes code performance based on their ability to predict the correct trends observed experimentally. A somewhat subjective criterion was used to evaluate the trends, and this criterion was whether or not the time vs. concentration profile was a similar shape to the experimental results. Quantitative agreement was also used as a criterion. If the agreement between calculated and experimental values for the total gas phase and organic iodide concentration was within a factor of three throughout the majority of the experiment, the quantitative agreement was considered to be good. If the agreement between calculated and experimental values for the amount of iodine adsorbed on gas phase coupons was within a factor of three, or the amount of iodine in the aqueous phase was within 20%, the agreement was also considered to be good. The prediction of the steady-state concentration of I_2 (or distribution between I^- and I_2) in the aqueous phase is essential to each code's ability to predict iodine volatility, therefore, in the discussion below,

much attention is focussed on determining whether or not the code calculations indicate that it correctly predicts the concentration of I_2 in the aqueous phase.

Phase 10 Test 1

Figures 9-11 show the optimized code calculations compared to experimental measurements of the total iodine concentration in the gas phase, the total organic iodide concentration in the gas phase and the total iodine concentration in the aqueous phase for RTF Phase 10 Test 1. It should be noted that the mass balance derived for Phase 10 Test 1 was not closed; only 70% of the iodine inventory was accounted for. Nonetheless, the gas phase and aqueous phase concentrations for this experiment are considered to be reliable measurements, since they were based on two independent measurements for each set of data. The difficulty in closing the mass balance was due to uneven distribution of iodine on the vessel surfaces at the end of the experiment (e.g. stratified iodine adsorption on gas phase painted surfaces), which made it impossible to properly estimate the iodine adsorbed on these surfaces. The assumption is that all of the iodine unaccounted for was adsorbed either on the vessel gas phase or aqueous phase surfaces. Monitoring of the vessel enclosure during the experiment ensured that none of the iodine inventory was leaked out of the facility during the experiment.

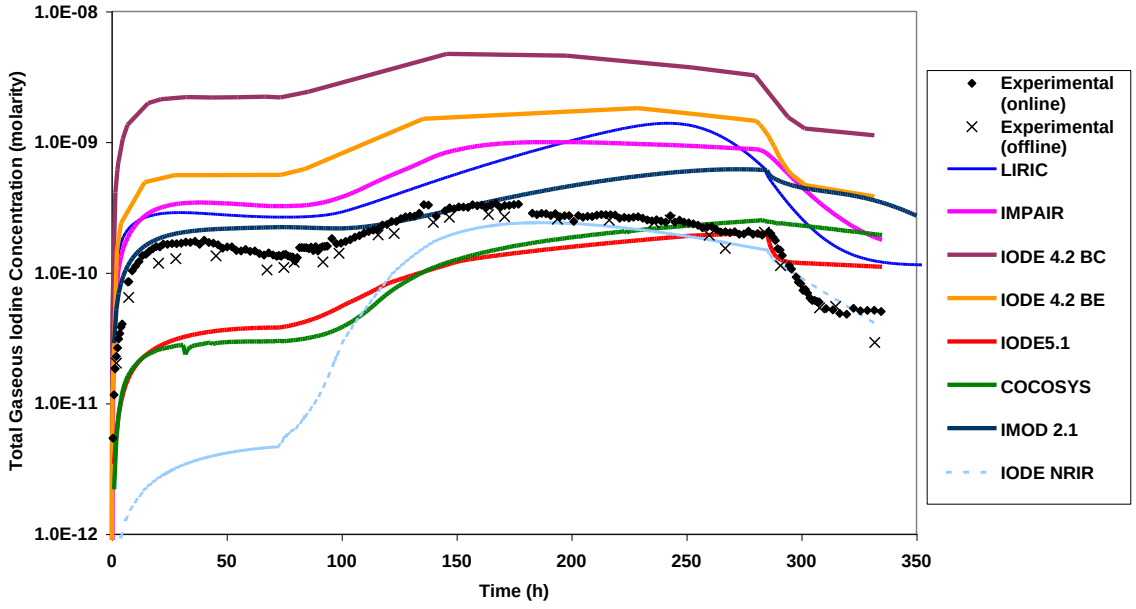

Figure 9: Total Gas Phase Iodine Concentration for RTF Phase 10 Test 1 as Compared to Code Calculations (Optimized). Note that NRIR blind calculations are shown.

The optimized calculations for Phase 10 Test 1 show a marked improvement over the blind calculations. The better agreement between the optimized calculations and the blind calculations arises to some extent from the fact that the codes IMPAIR, IODE 4.2, COCOSYS and IODE 5.1 perform much better when the correct pH profile is supplied as input.

As can be seen from Figure 9, both IODE 5.1 and COCOSYS under-predict iodine volatility during the pH 10 stage of the test (between 0 and 75 h), whereas IODE 4.2 CIEMAT (both cases) over-predicts. IODE 5.1 and COCOSYS also under-predict iodine volatility during the time where pH is uncontrolled, with all of the other codes over-predicting. Finally, during the final pH 10 stage, all of the codes over-predict iodine volatility.

The trends in iodine volatility predicted by each of the codes are generally reasonable. With the exception of the initial stages of the experiment, all of the codes predict overall iodine volatility to within an order of magnitude.

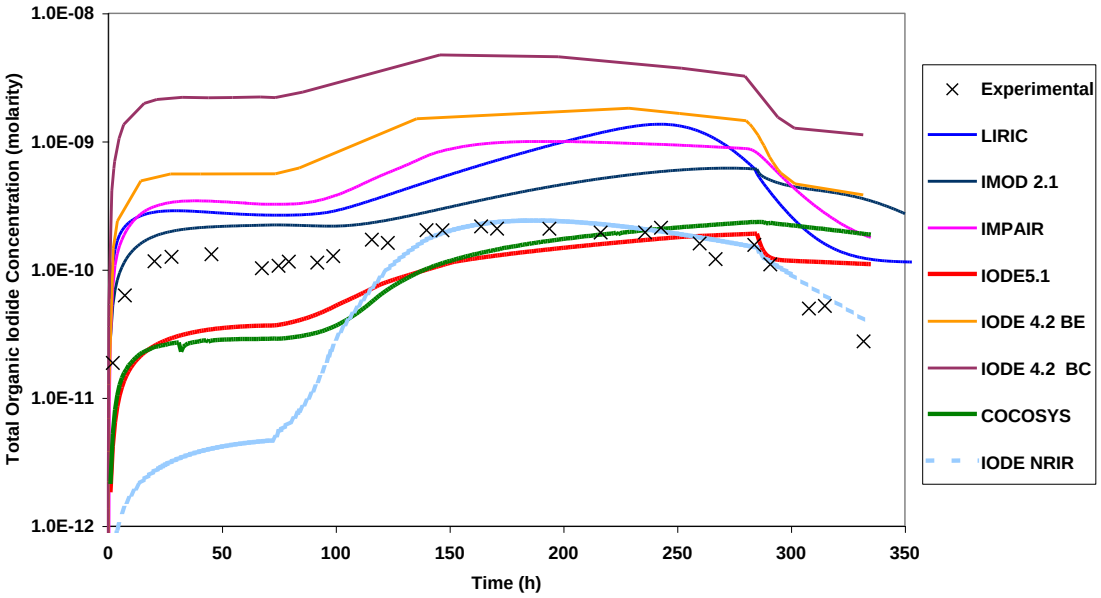

Figure 10. Total Gas Phase Organic Iodide Concentration for RTF Phase 10 Test 1 as Compared to Code Calculations (Optimized). Note that NRIR blind calculations are shown.

In Phase 10 Test 1, the gas phase iodine concentration was dominated by organic iodides. For this reason, all of the statements regarding the code predictions of overall iodine volatility apply to their predictions of the organic iodide concentrations. All of the codes predict the correct general trend, with COCOSYS and IODE under-predicting slightly, and the rest of the codes over-predicting (Figure 10).

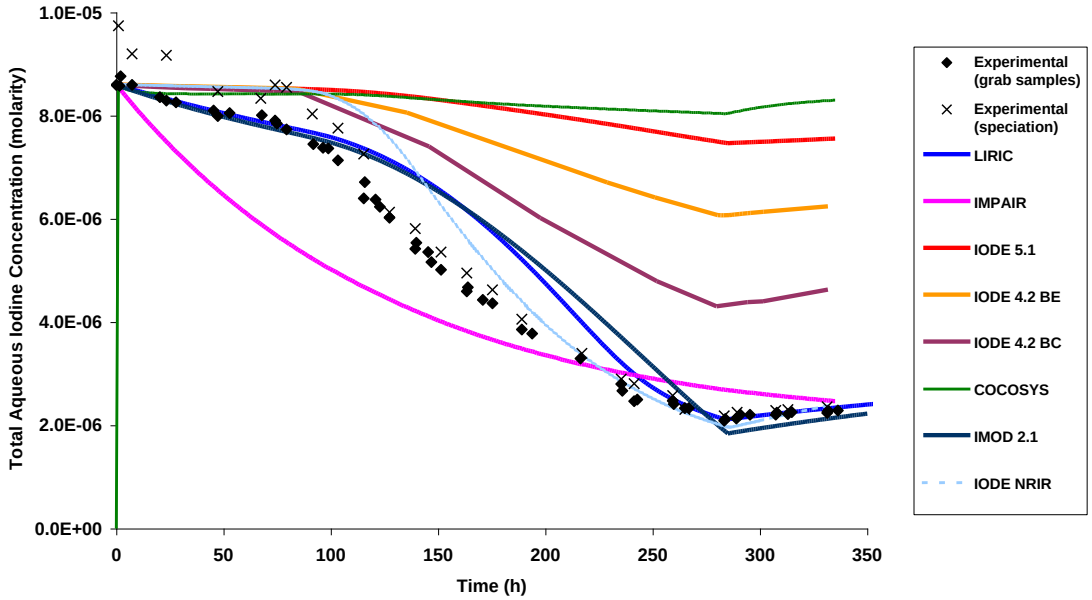

Figure 11. Total Aqueous Phase Iodine Concentration for RTF Phase 10 Test 1 as Compared to Code Calculations (Optimized). Note that NRIR blind calculations are shown.

In general, the behaviour of the aqueous iodine concentration is not well predicted by the codes (see Figure 11).

Figure 11 shows that, with the exception of IMPAIR, LIRIC and IMOD 2.1, the concentration of aqueous iodine species is overestimated by more than 50% at test end.
The code predictions regarding aqueous phase concentrations can be rationalized by their predictions regarding the amount of I_2 in the aqueous phase and the rate at which it is absorbed on surfaces. The overestimation of iodine in the aqueous phase during the experiments can be attributed partially to the difference in the adsorption/desorption rate constants used in the codes for adsorption of I_2 in the aqueous phase. From Table 5, it can be seen that COCOSYS uses a lower adsorption rate for I_2 in the aqueous phase than either LIRIC or IMOD, with approximately the same desorption rate (it is the ratio of the two that affects the amount of iodine adsorbed on the surface). IODE 5.1 uses a slower adsorption rate and a higher desorption rate, and also does not use adsorption of I^- in the aqueous phase. Therefore, these codes predict a greater fraction of iodine inventory in the aqueous phase at test end partially because they also underestimate the adsorption of iodine on aqueous phase surfaces. However, for RTF experiments, the I_2 behaviour in the aqueous phase is mirrored by its behaviour in the gas phase, because mass transfer is rapid enough that pseudo-equilibrium between the gas and aqueous phase I_2 concentrations is reached relatively rapidly (Note that this is not the case for CAIMAN experiments). Figures 12 and 13 show that most of the codes (IMPAIR excepted) predict similar amounts of I_2 in the gas and aqueous phase. If these codes increased the extent of adsorption on I_2 on surfaces significantly, in order to attain the correct aqueous phase concentrations, it is possible that their predictions of the gas phase I_2 concentrations would be decreased (however, this is not always the case, see the calculations made for PHEBUS/RTF1 with IODE 5.1 in Appendix A). Note that

IMPAIR calculations which uses the higher end of the recommended range of adsorption values and the lower end of the desorption values, predicts that there is too much iodine adsorbed on surfaces. Consequently, IMPAIR predictions of the aqueous phase I_2 concentrations are very low, and the code predicts that essentially no I_2 reaches the gas phase.

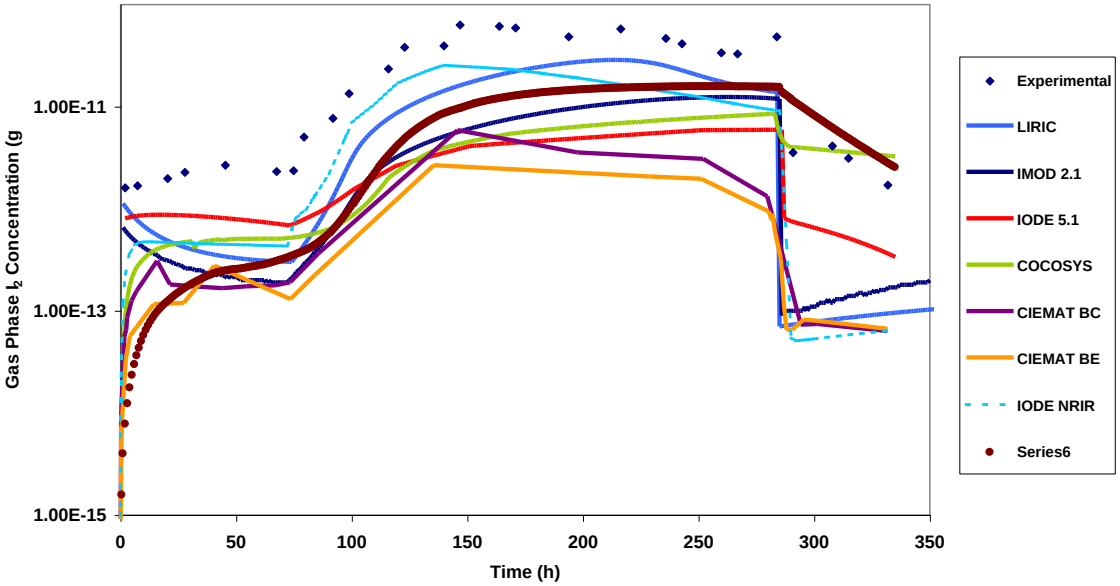

Figure 12: Gas Phase I_2 Concentration for RTF Phase 10 Test 1 as Compared to Code Calculations (Optimized). Note that NRIR blind calculations are shown.

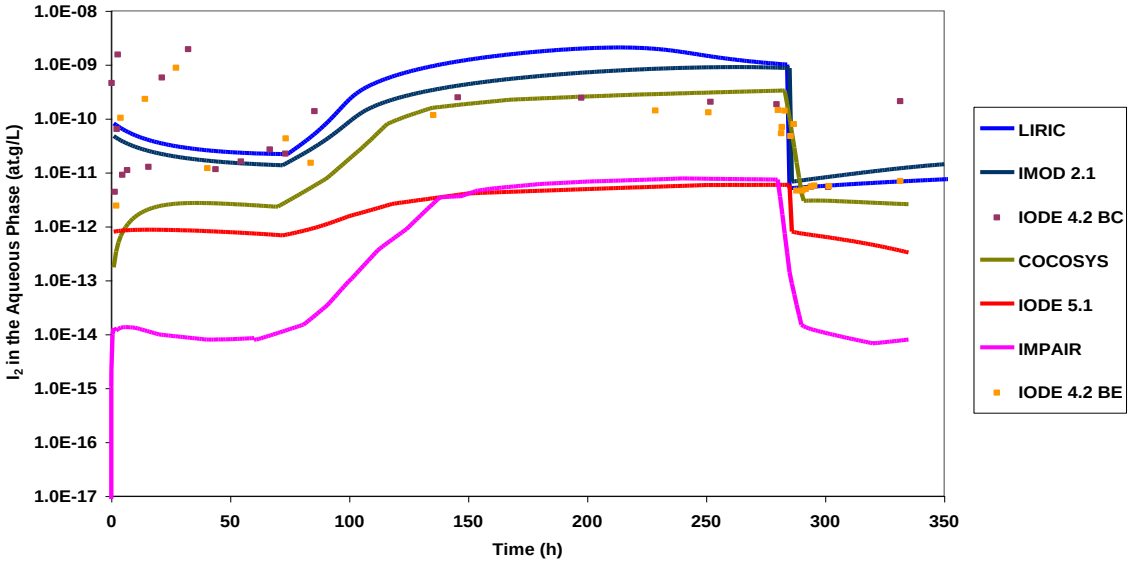

Figure 13: Aqueous Phase I_2 Concentrations for RTF Phase 10 Test 1 as Predicted by Code Calculations (Optimized).

Table 5: Adsorption Rate Constants Used in Phase 10 Test 1.

	Recommended [a]	IODE 5.1	COCOSYS	LIRIC	IMOD 2.1	IODE 4.2 BE	IMPAIR	IODE NRIR
$K_{ads}I_2aq$ ($m \cdot s^{-1}$)	$8\ 10^{-4}$	$2\ 10^{-4}$	$2\ 10^{-4}$	$4\ 10^{-4}$	$6\ 10^{-4}$	$8\ 10^{-4}$	$1.6\ 10^{-3}$	$4\ 10^{-4}$
$K_{des}I_2aq$ (s^{-1})	510^{-7}	$5\ 10^{-7}$	$5\ 10^{-7}$	$2.5\ 10^{-7}$	$2.5\ 10^{-7}$	$5\ 10^{-7}$	$2.5\ 10^{-7}$	$2.5\ 10^{-7}$
$K_{ads}I^-aq$ ($m \cdot s^{-1}$)	$4\ 10^{-8}$	0	$4\ 10^{-8}$	$2\ 10^{-8}$	$2\ 10^{-8}$	0	$8\ 10^{-8}$	$2\ 10^{-8}$
$K_{des}I^-aq$ (s^{-1})	$1\ 10^{-6}$	0	$1\ 10^{-6}$	$2\ 10^{-6}$	$1\ 10^{-6}$	0	$5\ 10^{-7}$	$2\ 10^{-6}$
$K_{ads}I_2gp$ ($m \cdot s^{-1}$)	$6\ 10^{-4}$	$6\ 10^{-4}$	$6\ 10^{-4}$	$6\ 10^{-4}$	$6\ 10^{-4}$	$6\ 10^{-4}$	$1.2\ 10^{-3}$	$6\ 10^{-4}$
$K_{des}I_2gp$ (s^{-1})	0	0	0	0	0	0	0	0
$K_{L\text{-}G}\ I_2$ ($m \cdot s^{-1}$)	$7\ 10^{-5}$	$1.4\ 10^{-4}$	$7\ 10^{-5}$	$7\ 10^{-5}$	$7\ 10^{-5}$	$7\ 10^{-5}$		$7\ 10^{-5}$
$K_{L\text{-}G}\ CH_3I$($m \cdot s^{-1}$)	$8\ 10^{-5}$	$1.6\ 10^{-4}$	$8\ 10^{-5}$	$8\ 10^{-5}$	$8\ 10^{-5}$	$8\ 10^{-5}$		$8\ 10^{-5}$

[a] A factor of two uncertainty is assigned to all of these numbers.

A final observation about the results from Phase 10 Test 1 is that both IODE 5.1 and COCOSYS underestimate both the gas phase I_2 and organic iodide concentration at the beginning of the experiment. It is likely that the codes underestimate the organic iodide production rate at the beginning of the experiment because they underestimate the rate of aqueous phase production I_2.

PHEBUS 1

Figures 14 through 17 show the calculated versus experimental results for PHEBUS RTF1.

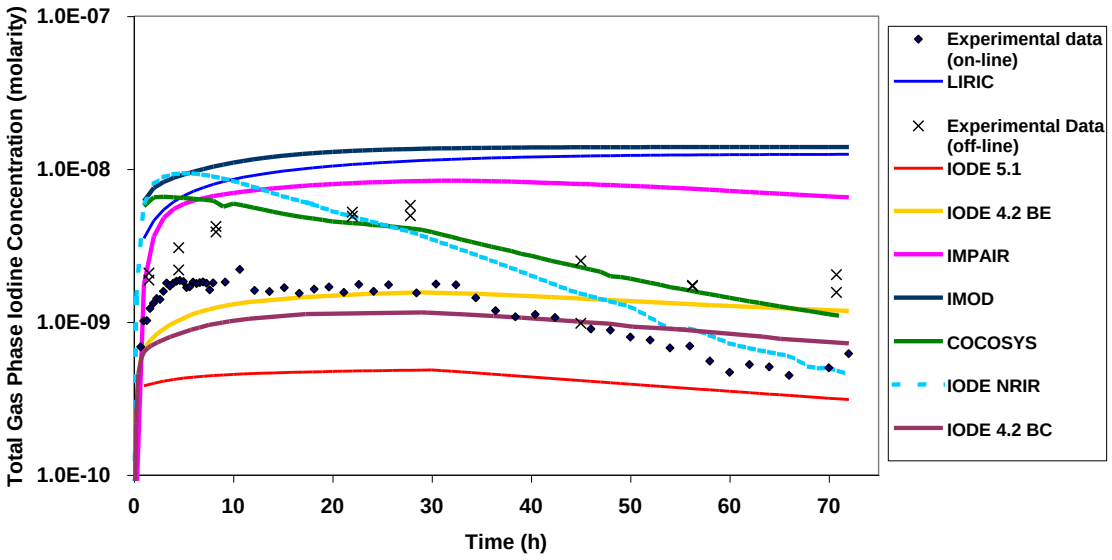

Figure 14: Total Gas Phase Iodine Concentration for Phebus RTF1 as Compared to Code Calculations (Optimized). Note that NRIR blind calculations are shown.

As one can see from Figure 14, there is some difference between analysis methods (a maximum of a factor of 2.5 between on-line and off-line measurements) for the experimentally measured total gas phase iodine concentrations. For analysis of the trends in this experiment, if the calculated results agreed to within a factor of three to either the on-line or off-line experimental measurements, the agreement was deemed

to be good. LIRIC and IMOD are higher by a factor of five at the end of the experiment and therefore do not satisfy this criterion. IODE 5.1 under-predicts iodine volatility by a factor of four during the initial stages of the experiment and therefore its agreement was also not considered to be good.

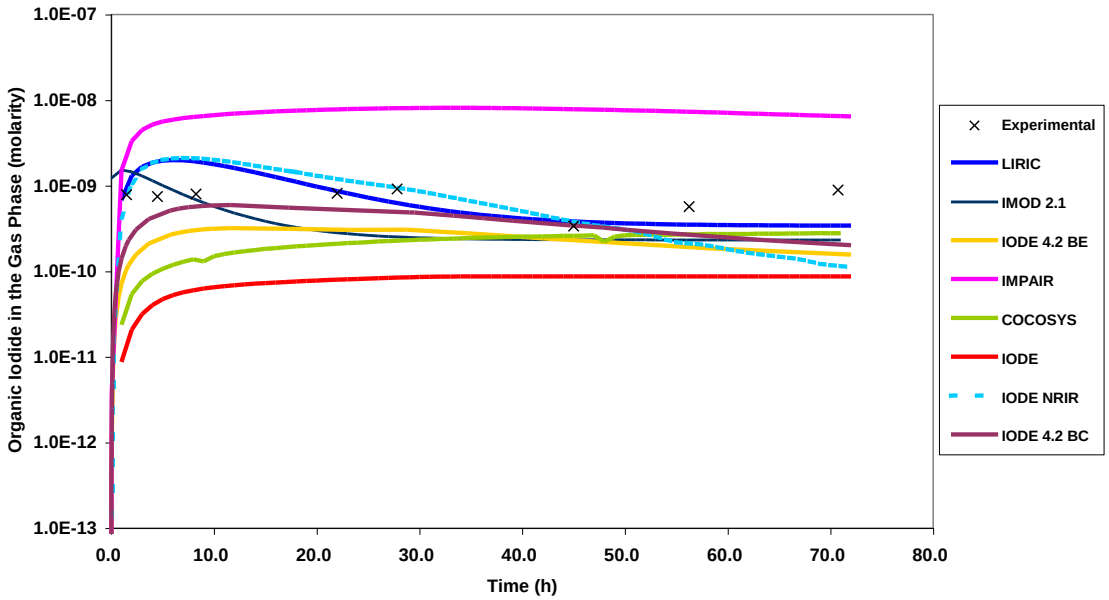

Figure 15: Total Gas Phase Organic Iodide Concentration for Phebus RTF1 as Compared to Code Calculations (Optimized). Note that NRIR blind calculations are shown.

The organic iodide concentrations predicted by each of the codes for PHEBUS RTF1 are shown in Figure 15. The agreement between code calculations and experimental results is not as good as for the total iodine concentrations. IODE 5.1 underestimates the organic iodide concentration by more than an order of magnitude, with the poorest agreement during the first 40 h of the experiment. IMPAIR overestimates the amount by more than an order of magnitude.

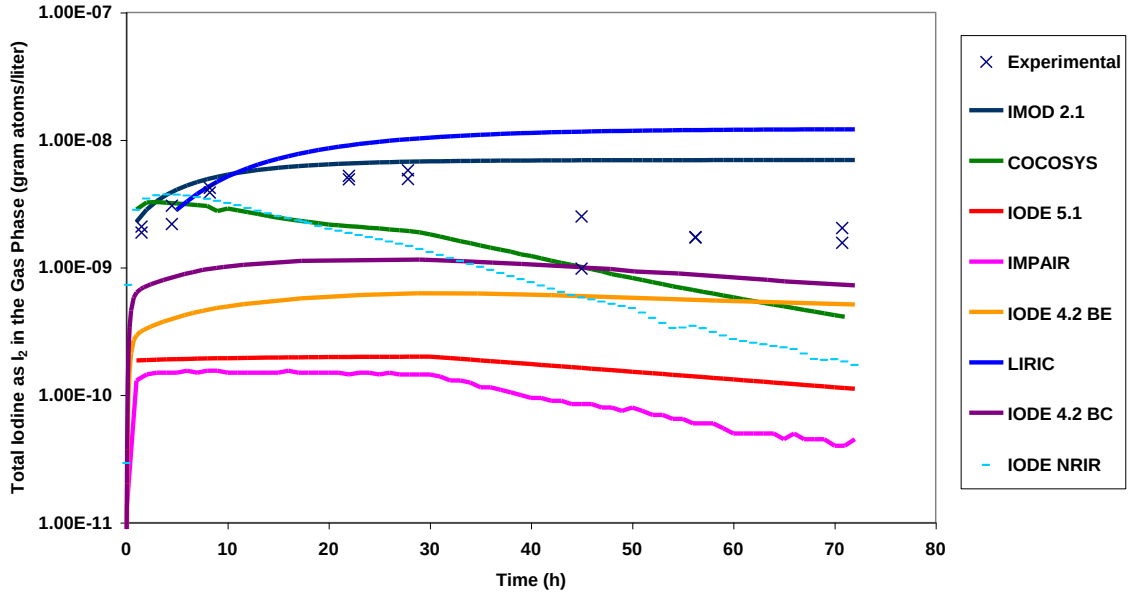

Figure 16: Gas Phase I_2 Concentration for Phebus RTF1 as Compared to Code Calculations (Optimized). Note that NRIR blind calculations are shown.

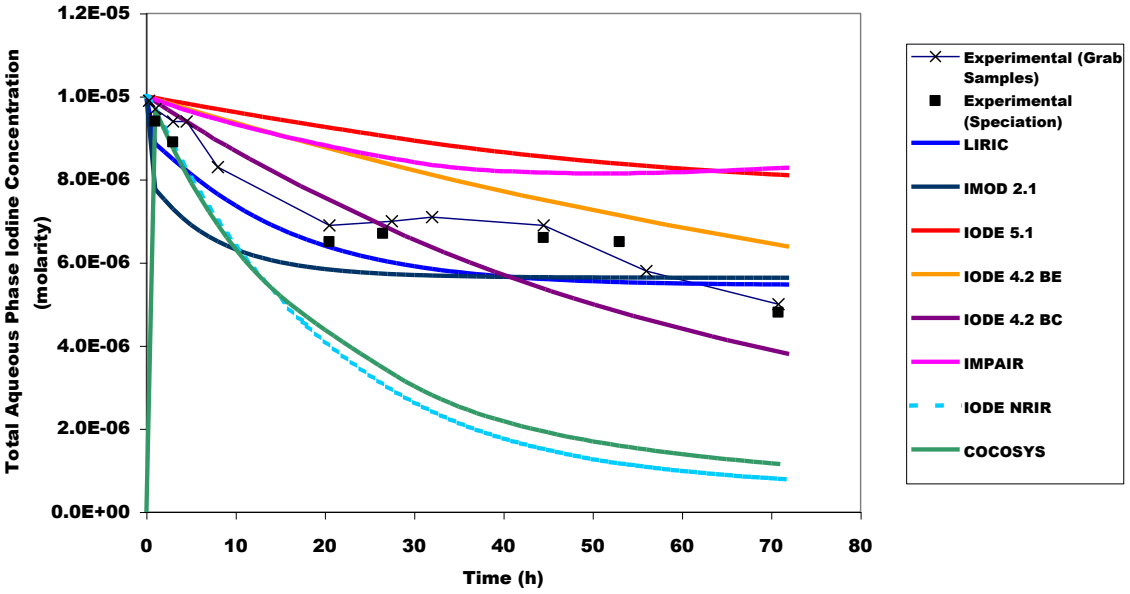

Figure 17: Total Aqueous Phase Iodine Concentration for Phebus RTF1 as Compared to Code Calculations (Optimized). Note that NRIR blind calculations are shown.

The predicted gas phase I_2 concentrations are shown in Figure 16 and the aqueous phase total iodine concentrations are shown in Figure 17. COCOSYS calculations show about the right amount of I_2 in the gas phase (slightly underestimating), and

underestimate the total aqueous phase iodine concentration. This indicates that, in COCOSYS calculations there is an overestimation of the amount of I_2 adsorbed on surfaces (either the amount of I_2 is overestimated, or the overall absorption rate is overestimated). LIRIC and IMOD on the other hand overestimate the I_2 in the gas phase but predict the total aqueous phase concentrations well. This also indicates an overall aqueous phase production rate for I_2 that is too large. IODE 4.2 (CIEMAT) calculations appear to slightly underestimate the gaseous I_2 concentration, but predict the aqueous phase concentration reasonably well.

NRIR predicts the initial I_2 concentration in the gas phase well, but the concentration is predicted to decrease much more rapidly than observed experimentally. NRIR also overestimates the amount of iodine lost from the aqueous phase. The agreement between experimental data and NRIR predictions might also be improved by decreasing the rate of adsorption of I_2 on surfaces. Both IODE 5.1 and IMPAIR underestimate the amount of I_2 in the gas phase, and the amount of iodine absorbed on surfaces (i.e. they overestimate the amount of iodine in the aqueous phase). This indicates that they are underestimating the overall rate of production of I_2 in the aqueous phase
The code predictions for I_2 in the aqueous phase are shown in Figure 18.

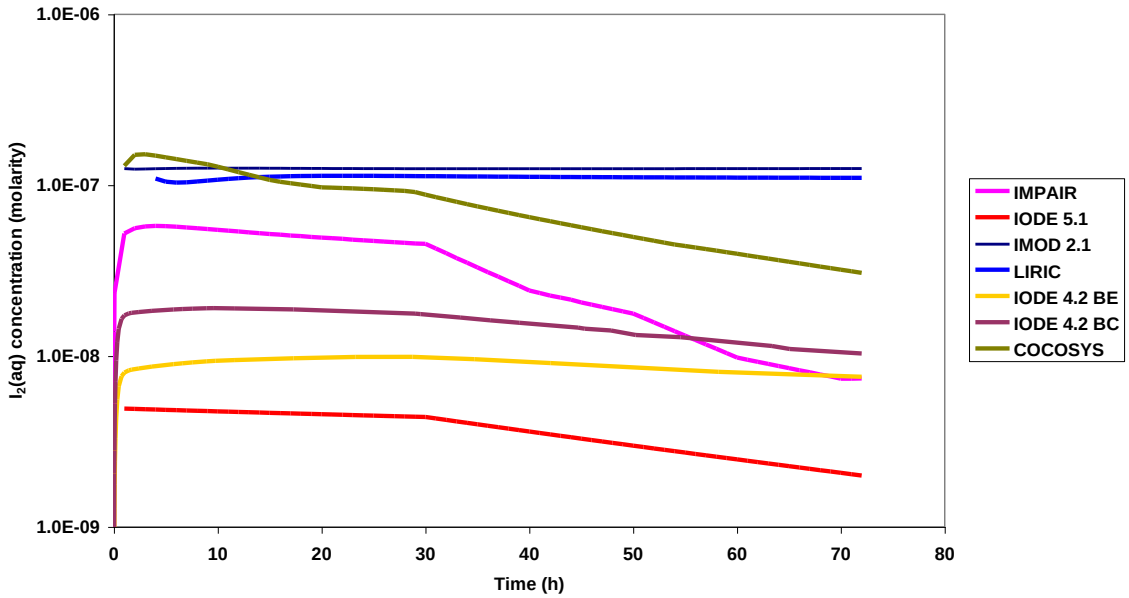

Figure 18: Aqueous Phase I_2 Concentrations for Phebus RTF1 as Predicted by Code Calculations (Optimized). Note that NRIR blind calculations are shown.

Consistent with the interpretation of the gas phase results, LIRIC, IMOD and COCOSYS predict significantly higher aqueous phase I_2 concentrations than any of the other codes

A final note regarding the Phebus RTF1 predictions is that IMPAIR greatly overestimates the organic iodide concentration, yet it apparently predicts lower

aqueous phase I_2 concentrations than were attained experimentally. This indicates that the organic iodide production rate in IMPAIR is too high.

Table 6: Adsorption Rate Constants Used in Phebus RTF1.

	Recommended[a]	IODE 5.1	COCOSYS	LIRIC	IMOD 2.1	IODE 4.2 BE	IMPAIR	NRIR
$K_{ads}I_2aqss$ ($m \cdot s^{-1}$)	$<2\ 10^{-6}$	$2\ 10^{-6}$	0	$1\ 10^{-2}$	$2\ 10^{-2}$	0	0	$<2\ 10^{-6}$
$K_{des}I_2aqss$ (s^{-1})	$<2\ 10^{-6}$	0	0	$4\ 10^{-2}$	$4\ 10^{-2}$	0	0	$<2\ 10^{-6}$
$K_{ads}I_2aqp$ ($m \cdot s^{-1}$)	$8\ 10^{-4}$	$8\ 10^{-4}$	$2\ 10^{-4}$	$2\ 10^{-4}$	$2\ 10^{-4}$	$8\ 10^{-4}$	$4\ 10^{-4}$	$8\ 10^{-4}$
$K_{des}I_2aqp$ (s^{-1})	$5\ 10^{-7}$	$5\ 10^{-7}$	$5\ 10^{-7}$	$1\ 10^{-4}$	$1\ 10^{-4}$	$5\ 10^{-7}$	$1\ 10^{-6}$	$5\ 10^{-7}$
$K_{ads}I^-aqp$ ($m \cdot s^{-1}$)	$4\ 10^{-8}$	0	$4\ 10^{-8}$	$4\ 10^{-8}$	$4\ 10^{-8}$	0	$8\ 10^{-8}$	$4\ 10^{-8}$
$K_{des}I^-aqp$ (s^{-1})	$1\ 10^{-6}$	0	$1\ 10^{-6}$	$1\ 10^{-6}$	$1\ 10^{-6}$	0	$5\ 10^{-7}$	$1\ 10^{-6}$
$K_{ads}I_2gss$ ($m \cdot s^{-1}$)	$1\ 10^{-4}$	$1\ 10^{-4}$	$1\ 10^{-4}$	$2\ 10^{-4}$	$2\ 10^{-4}$	$2\ 10^{-4}$	$1\ 10^{-4}$	$1\ 10^{-4}$
$K_{des}I_2gss$ (s^{-1})	$5\ 10^{-5}$	$1\ 10^{-5}$	$3.6\ 10^{-5}$	$1\ 10^{-4}$	$1\ 10^{-4}$	$4.9\ 10^{-5}$	$1\ 10^{-5}$	$5\ 10^{-5}$
$K_{ads}I_2gp$ ($m \cdot s^{-1}$)	$4.5\ 10^{-3}$	$4\ 10^{-3}$	$4.5\ 10^{-3}$	$4\ 10^{-3}$	$4\ 10^{-3}$	$2.25\ 10^{-3}$	$6.5\ 10^{-3}$	$4.5\ 10^{-3}$
$K_{des}I_2gp$ (s^{-1})	0	0	0	$1\ 10^{-4}$	$1\ 10^{-4}$	0	0	0
$K_{L\text{-}G}\ I_2$ ($m \cdot s^{-1}$)	$5.5\ 10^{-5}$	$9.2\ 10^{-5}$	$5.5\ 10^{-5}$	$5.5\ 10^{-5}$	$5.5\ 10^{-5}$	$5.5\ 10^{-5}$	1.10^{-5}	$5.5\ 10^{-5}$
$K_{L\text{-}G}\ CH_3I$ ($m \cdot s^{-1}$)	$8.3\ 10^{-5}$	$1.4\ 10^{-4}$	$8.3\ 10^{-5}$	$8.3\ 10^{-5}$	$8.3\ 10^{-5}$	$8.3\ 10^{-5}$	$1.5.10^{-5}$	$8.3\ 10^{-5}$

[a] A factor of two uncertainty is assigned to all of these numbers.

CAIMAN 97/02

The total gas phase iodine concentration for CAIMAN Test 97/02 is shown in Figure 19, along with the concentrations predicted by the various codes. One of the first things to note is that the gas phase accumulation at the beginning of the experiment appears to be delayed relative to the accumulation observed in the other experiments and the accumulation predicted by each of the codes. It has been suggested by the operator of the CAIMAN facility that there may have been a time lag between the start of the experiment (when the gamma source was placed inside the vessel) and the introduction of the labelled iodide solution. The starting point for the experiment in this case would be 5 hours later that time zero shown in the plots above. This would explain the divergence between the initial gas phase accumulation rate in CAIMAN 97/02 with that of CAIMAN 01/01. It would also explain the failure of all of the codes to simulate the first 10 h of the experiment. Note also that the concentrations observed during the first part of the experiment are very low, (10^{-11} – 10^{-12} $mol \cdot dm^3$). Under these conditions, adsorption on sampling lines leading to the filters, or stratification of the gas phase iodine concentrations could lead to uncertainties in the measured concentrations

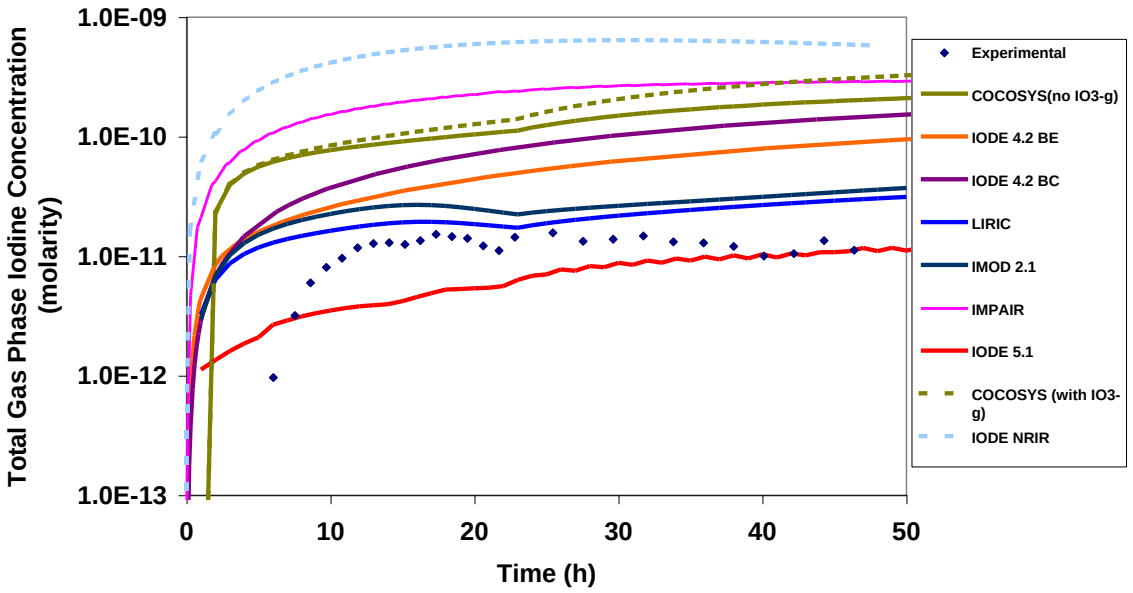

Figure 19: Total Gas Phase Iodine Concentration for CAIMAN 97/02 as Compared to Code Calculations (Optimized). Note that NRIR blind calculations are shown.

In general, the codes overestimate the total amount of iodine in the gas phase, however IODE 5.1 underestimates slightly. IODE 5.1, IMOD, LIRIC and IODE 4.2 BE predict the gas phase iodine concentration to within an order of magnitude at all times, whereas the other codes significantly overestimate the concentration. All of the codes except IODE NRIR predict that the total iodine concentration in the gas phase will gradually increase with time up until the end of the experiment, whereas the experimental data show a fairly constant concentration.

Before a comparison of the predicted versus experimental gas phase I_2 concentrations, it should be noted that, in CAIMAN facility experiments is that in comparison to RTF experiments, it is more difficult to draw conclusions regarding the production rate of I_2 in the aqueous phase from the gas phase I_2 concentrations. In RTF experiments a qualitative judgement can be made regarding aqueous phase I_2 concentrations by examination of the behaviour of the gas phase I_2 concentrations and the aqueous phase iodine concentration. Any I_2 produced in the aqueous phase rapidly appears in the gas phase, and losses of I_2 in either phase due to adsorption manifest themselves immediately by a decrease in the concentration in the aqueous phase. Interfacial mass transfer in CAIMAN facility experiments is slower than in RTF experiments however due to a small interfacial surface area in the former, and significant gas and aqueous phase recirculation in the latter. In CAIMAN facility experiments, small changes in the amount of adsorption/desorption on gas phase surfaces could influence observed gas phase I_2 concentrations without changing the aqueous phase concentrations significantly. In practical terms this could mean that a code could predict I_2 concentrations in the gas phase that were significantly higher or lower than those observed, even if the aqueous phase I_2 concentrations were predicted correctly. Conversely, the gas phase I_2 concentrations might match well with the experimentally observed concentrations, but the aqueous phase I_2 concentrations could be over- or underestimated. It is therefore more difficult to make assumptions regarding whether

the codes are producing the correct amount of I_2 in the aqueous phase based on observations of the predicted gas phase concentrations. The code must demonstrate that it predicts the gas phase I_2 concentration and the amount of iodine deposited on gas phase coupons and walls well, in order to demonstrate that it predicts the aqueous phase I_2 concentration correctly.

The predicted and experimental gas phase I_2, and I_2 adsorbed on painted coupons are shown in Figures 20 and 21. COCOSYS and IODE NRIR significantly overestimate both the I_2 concentration in the gas phase, and the amount of I_2 adsorbed on gas phase coupons. IODE 4.2 (both versions) and IMPAIR calculate the correct amount of I_2 in the gas phase, but significantly over-predict the amount of I_2 on the gas phase coupons. These observations indicate that the aqueous phase I_2 concentrations predicted by all of these codes are too high. IODE 5.1 slightly underestimates (by a factor of 5 to 6) the amount of I_2 in the gas phase during the initial stage (0 –10 h) of the test and IMOD and LIRIC underestimate by a factor of 10 in the same time frame. LIRIC, IMOD and IODE 5.1 predict the correct amount of I_2 adsorbed on the coupons. These observations indicate that all three of these codes may slightly underestimate aqueous phase I_2 concentrations.

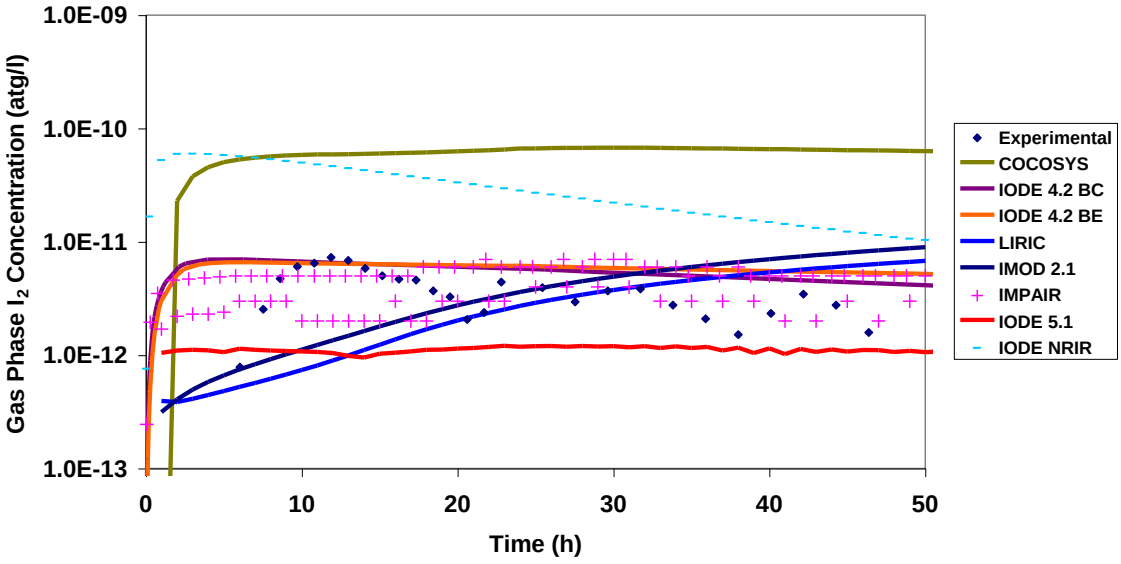

Figure 20: Gas Phase I_2 Concentration for CAIMAN 97/02 as Compared to Code Calculations (Optimized). Note that NRIR blind calculations are shown.

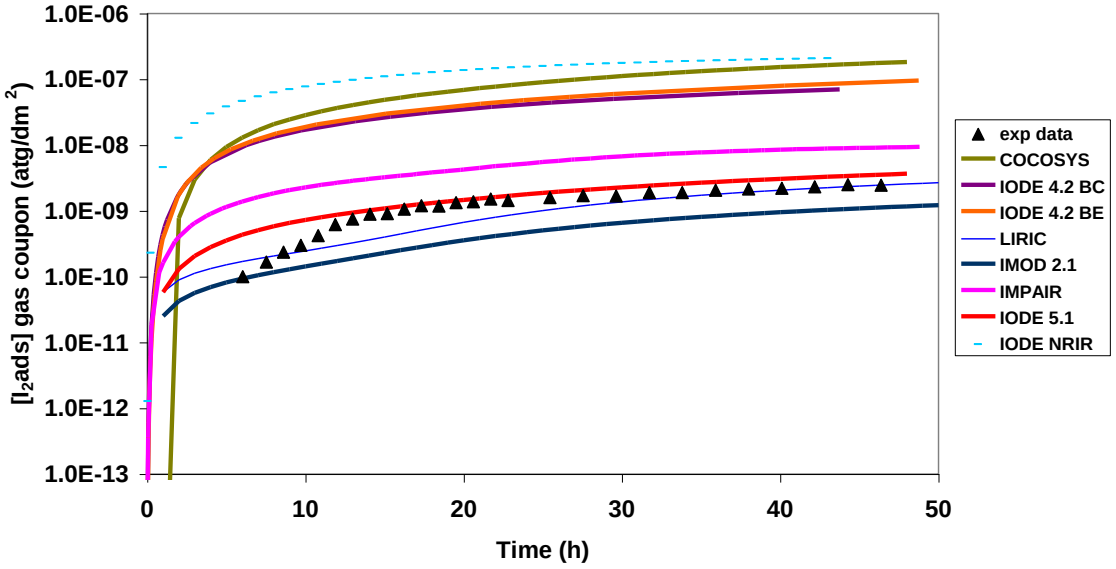

Figure 21: Concentration of I_2 adsorbed on Gas Phase Paint Coupons for CAIMAN 97/02 as Compared to Code Calculations (Optimized).

The gas phase I_2 concentration profile predicted by LIRIC and IMOD is quite different from the one observed experimentally. The initial slow accumulation of I_2, predicted by these codes (first 20 h) is a phenomenon associated with aqueous phase radiolytic decomposition of organic compounds and the resulting competition between organic compounds and I^- for ·OH radical. CAIMAN facility experiments provided data regarding the total carbon concentration as a function of time, and this information was used to estimate release of organic compounds from painted surfaces to model the experiment. LIRIC and IMOD predict that when organics are released from the paint in the initial stage of the test, they scavenge ·OH radical to form organic radicals, and this reaction competes with, and suppresses the radiolytic oxidation of I^- to I_2. However, as the organic compounds are decomposed, and their source is gradually depleted, the ·OH radical concentration recovers from this scavenging, resulting in an increase of the rate of oxidation of I^- to I_2.

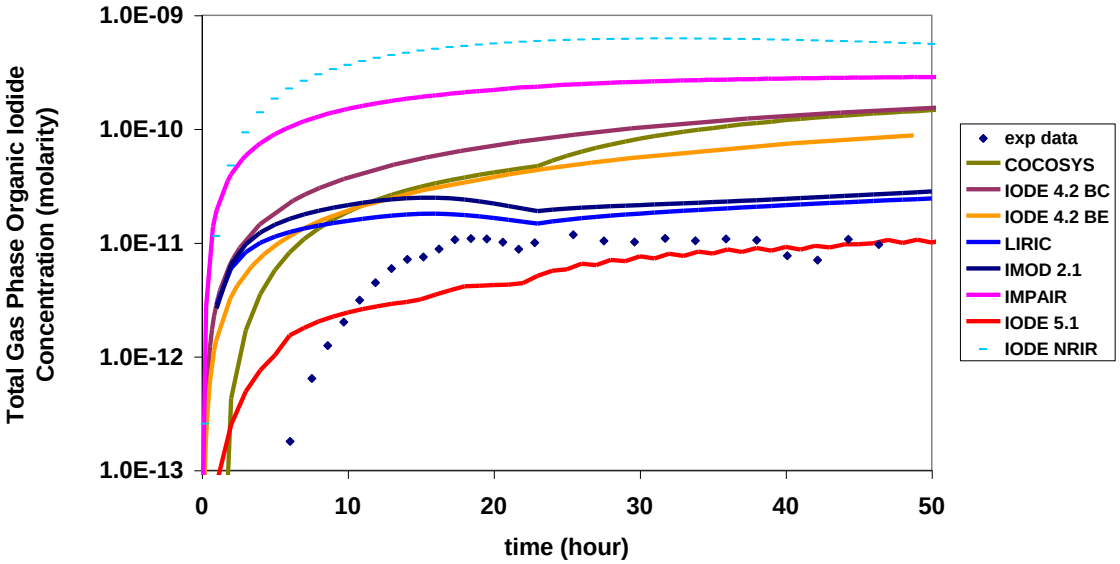

Figure 22: Total Gas Phase Organic Iodide Concentration for CAIMAN 97/02 as Compared to Code Calculations (Optimized).

As noted above, all of the codes predict that the total gas phase iodine concentration increases gradually with time at the end of the experiment, whereas the experimental results show that a steady-state concentration is reached. The gas phase organic iodide concentration predicted by each of the codes also shows the same increasing trend at test end, in contrast to the experimental data (Figure 22). It should be noted that there is some uncertainty regarding the Maypack measurements during the last part of the experiment. At 20 h there was an electrical outage resulting in condensation in the filter which may have affected the efficiency of the Maypacks, this may have led to an underestimation of the gas phase concentration [see Appendix B]. There is also an inherent in the Maypack measurements during the latter portions of the test because the total amount of iodine absorbed on the filters by this time is much larger than the incremental quantity added by each sampling Therefore, it may be that the code predictions are showing the correct trends.

IMPAIR, COCOSYS, IODE 4.2 and IODE 5.1 all invoke a heterogeneous surface process for organic iodide formation (some use both heterogeneous and homogeneous processes). For heterogeneous processes, as more iodine is deposited on painted surfaces (in this case it is primarily the aqueous phase painted surfaces), the organic iodide formation rate increases, and the gas phase organic iodide concentration increases. Note that for IODE 5.1, the main process that leads to the presence of organic iodides in the gas phase, is homogeneous aqueous phase processes, because of the low dose rate in the gas phase.

In the case of LIRIC, IMOD and NRIR, organic iodide formation is by aqueous phase processes alone. In LIRIC and IMOD, the source of organic materials used in simulating the experiments was based on leaching of solvents from immersed paints, and slow evaporation of solvents from paints exposed to the gas phase. LIRIC and IMOD predict that the source of organic material from immersed paints contributes the most to the organic concentration in the aqueous phase at the beginning of the

experiment, but that this source is significantly depleted by the end of the test. Both models predict that the aqueous phase organic concentration reaches a minimum concentration at about 30 h. After this there is a very slow, but steady accumulation of organic compounds into the aqueous phase due to evaporation from painted surfaces in the gas phase (followed by interfacial mass transfer to the aqueous phase). The organic concentration in the aqueous phase is predicted to increase during this stage, hence the organic iodide concentration increases.

For IODE NRIR, the source of organic compounds in the aqueous phase maintains a constant concentration of organic in the aqueous phase. However, NRIR predicts a large amount of I_2 is deposited on the gas phase coupon, resulting in a depletion of iodine and I_2 in the aqueous phase. Therefore, NRIR predicts that the organic iodide production rate will decrease at the end of the experiment.

The amount of I_2 in the aqueous phase as predicted by each of the codes, is shown in Figure 23. One can see that COCOSYS calculations overestimate I_2 in the liquid phase compared to the other codes. This result can be linked to its overestimation of I_2 in the gas phase. Thus, in these conditions, COCOSYS modeling of radiolytic I_2 formation could be improved to obtain a better agreement with experimental values for the I_2 concentration in the gas phase. In contrast, it can be noted that IODE 5.1 underestimates I_2 in the aqueous phase, consistent with its under-prediction of I2 in the gas phase. Some additional IODE 5.1 calculations have been made with the modification of I_2 radiolytic destruction process activation energy (see Appendix A). This modification gives much better results and could be adopted for the future code version.

It is interesting that LIRIC and IMOD predict a slow increase in I_2 concentration in the gas phase at the end of the experiment, but both predict that the aqueous phase I_2 concentration during this period decreases slightly (see Figure 23). Calculations of other parameters, such as the iodine absorbed on aqueous phase stainless steel surfaces suggest that this is because the codes predict that the system has not yet reached a steady state partitioning between the gas and aqueous phases, and surfaces exposed to these phases. The overall trend is that volatile I_2 is still moving from the aqueous phase, and aqueous phase surfaces to the gas phase and gas phase surfaces to attain a steady-state partitioning.

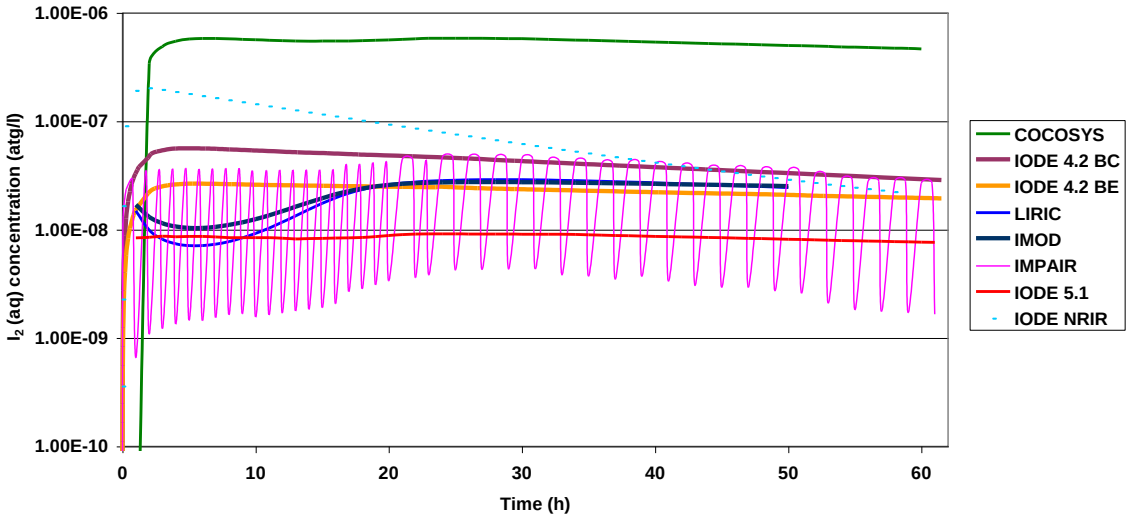

Figure 23: Aqueous Phase I_2 Concentrations for CAIMAN 97/02 as Predicted by Code Calculations (Optimized).

Table 7: Rate Constants Used in CAIMAN 97/02

	Recommended [a]	IODE 5.1	COCOSYS	LIRIC	IMOD 2.1	IODE 4.2 BE	IMPAIR	NRIR
$K_{ads}I_2aqp$ ($m{\cdot}s^{-1}$)	$2.5\ 10^{-4}$	$1.\ 10^{-4}$	4.10^{-6}	3.10^{-4}	3.10^{-4}	1.10^{-4}	1.10^{-4}	2.10^{-4}
$K_{des}I_2aqp$ (s^{-1})	-	0	2.10^{-6}	1.10^{-6}	2.10^{-7}	0	1.10^{-6}	5.10^{-7}
$K_{des}I^-aqp/I_2$ ads (s^{-1})	-	-	$3.57.10^{-5}$			-	$8.6.10^{-7}$	-
$K_{ads}I^-aqp$ ($m{\cdot}s^{-1}$)	-	0	$7.3.10^{-7}$	-	-	-	2.10^{-8}	-
$K_{des}I^-aqp$ (s^{-1})	-	0	4.10^{-5}	-	-	-	2.10^{-6}	-
$K_{ads}I_2aqss$ ($m{\cdot}s^{-1}$)	negligible	1.10^{-8}	-	2.10^{-2}	2.10^{-2}	0	0	0
$K_{des}I_2aqss$ (s^{-1})	negligible	0	-	5.10^{-1}*	5.10^{-1}*	0	0	0
$I_2 \rightarrow I^-$ (ss adsaq) ($m{\cdot}s^{-1}$)	-	-	$8.46.10^{-7}$	-	-	-	$7.9.10^{-7}$	-
$K_{ads}I^-aqss$ ($m{\cdot}s^{-1}$)	negligible	0	-	2.10^{-8}	2.10^{-8}	-	0	-
$K_{des}I^-aqss$ (s^{-1})	negligible	0	-	1.10^{-6}	1.10^{-6}	-	0	-
$K_{ads}I_2gp$ ($m{\cdot}s^{-1}$)	$4\ 10^{-3}$	$2\ 10^{-3}$	2.10^{-3}	$4.5.10^{-3}$	$4.5.10^{-3}$	2.10^{-3}	2.10^{-3}	4.10^{-3}
$K_{des}I_2gp$ (s^{-1})	-	0	1.10^{-6}	1.10^{-4}	1.10^{-4}	0	0	0
$K_{ads}I_2gss$ ($m{\cdot}s^{-1}$)	negligible	1.10^{-5}	1.10^{-4}	2.10^{-4}	2.10^{-4}	0	5.10^{-7}	1.10^{-4}
$K_{des}I_2gss$ (s^{-1})	negligible	1.10^{-6}	$8.34.10^{-5}$	$3.2.10^{-4}$	$3.2.10^{-4}$	0	$7.1.10^{-5}$	9.10^{-5}
$K_{L\text{-}G}\ I_2$ ($m{\cdot}s^{-1}$)	1.10^{-5}	1.10^{-5}	$8.3.10^{-6}$	$3.5.10^{-6}$	$3.5.10^{-6}$	1.10^{-5}	1.10^{-5}	5.10^{-5}
$K_{L\text{-}G}\ ICH_3$ ($m{\cdot}s^{-1}$)	1.510^{-5}	1.510^{-5}	$9.7.10^{-6}$	$5.3.10^{-6}$	$5.3.10^{-6}$	$1.5.10^{-5}$	$1.5.10^{-5}$	5.10^{-5}

CAIMAN 01/01

The experimental and predicted total gas phase iodine concentration observed in CAIMAN 01/01 is shown in Figure 24. In general, all of the codes predicted the concentration profile well. Improved concentration profiles were obtained from codes in which the pH profile observed in the experiment (pH rising from around 4.8 to 5.5 after 40 h) was used as input, rather than assuming a constant pH. COCOSYS, LIRIC and IMOD predictions all used an altered pH profile for the calculations shown in this experiment.

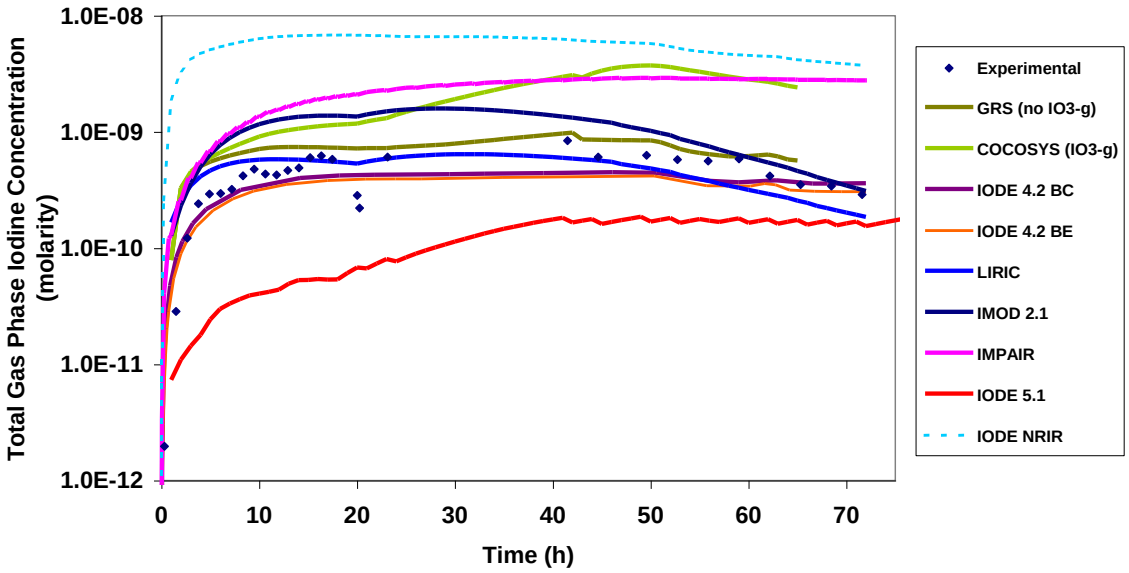

Figure 24: Total Gas Phase Iodine Concentration for CAIMAN 2001/01 as Compared to Code Calculations (Optimized).

The code predictions for this experiment fall into three categories. IODE 5.1 (IRSN) underestimate the total gas phase concentrations, whereas IMPAIR, COCOSYS (with IO_3^-) and IODE NRIR overestimate. COCOSYS calculations performed without IO_3^- production in the gas phase predict the experimental data well, as do LIRIC and IMOD and IODE 4.2 (CIEMAT) (both cases)

Predictions for organic iodide concentration are compared to experimental data in Figure 25. IMPAIR and IODE NRIR overestimate organic iodide formation by factors of 5-10 and 10 –50 respectively, whereas COCOSYS, IODE 5.1 and IODE 4.2 BE (CIEMAT) underestimate it by a factor of 5 to 10.

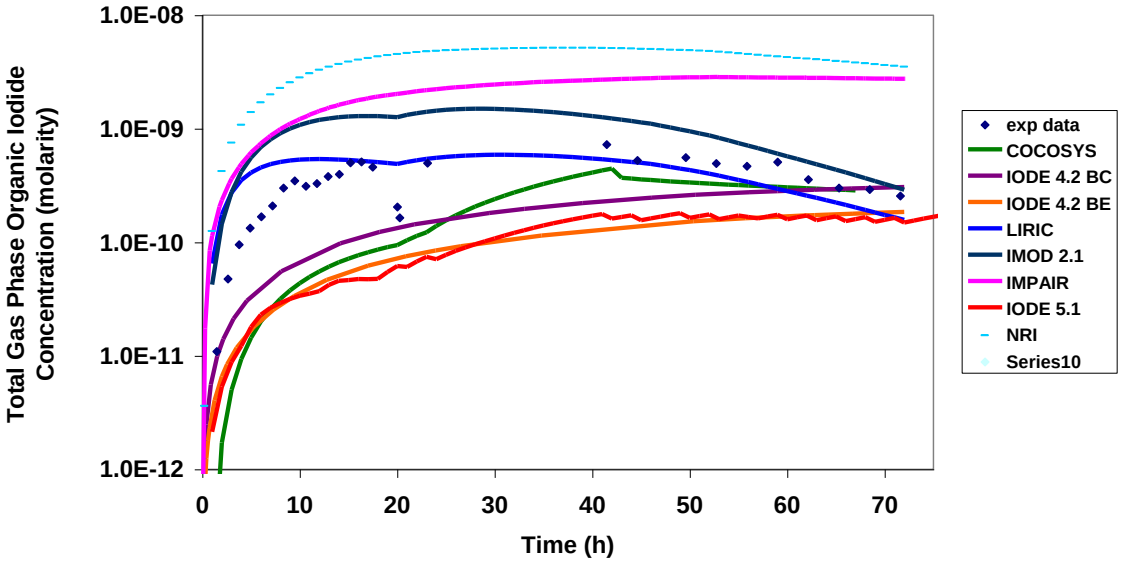

Figure 25: Total Gas Phase Organic Iodide Concentration for CAIMAN 2001/01 as Compared to Code Calculations (Optimized).

The gas phase I_2 concentrations predicted by each of the codes is shown in Figure 26, and the amount predicted to be absorbed on surfaces in Figure 27. IODE 5.1 underestimates the I_2 concentrations both in the gas phase and on the gas phase coupons; therefore it is assumed that it also underestimates the aqueous phase I_2 concentration. This explains the low organic iodide concentrations predicted by IODE 5.1. Conversely, IODE NRIR predicts too much I_2 in the gas phase; hence it also over-predicts the organic iodide formation rate, leading to high organic iodide concentrations and high iodine volatility. IODE 4.2 and COCOSYS predict gas phase I_2 concentrations relatively well, and over-predict I_2 adsorption on gas phase surfaces. This indicates that they over-predict the aqueous phase I_2 concentration. Despite this, they significantly underestimate organic iodide production at the beginning of the test. This suggests that the organic iodide production rate in COCOSYS and IODE 4.2 is too low.

In IMPAIR an assumption is made that there is a constant source of organic radicals in the aqueous phase available for production of organic iodide. The assumed concentration is obviously too high, because it appears to results in a consistently high prediction of organic iodide concentration in the gas phase for most of the experiments.

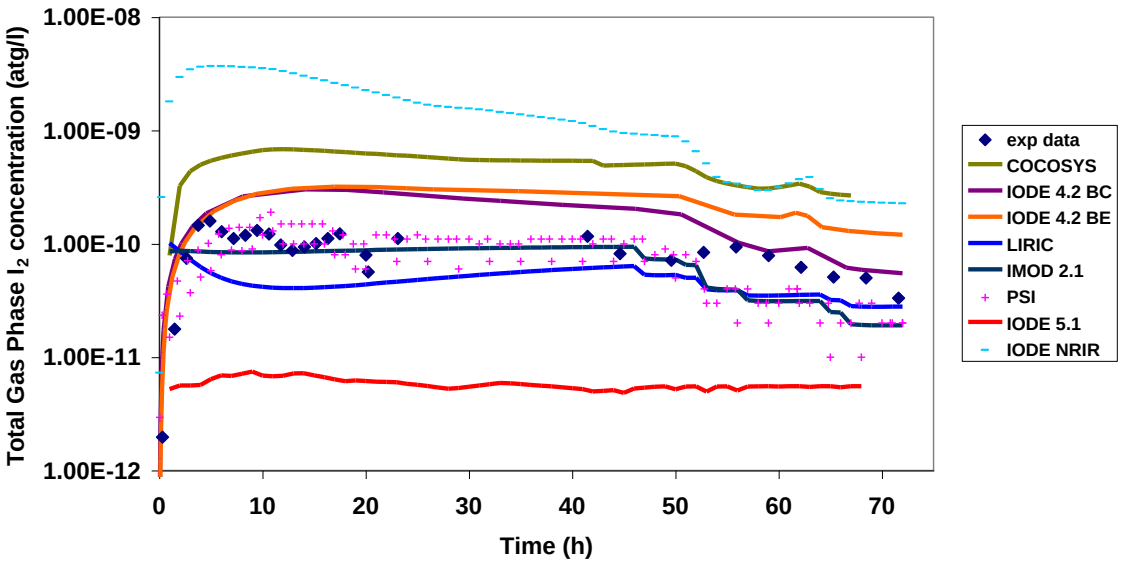

Figure 26: Gas Phase I_2 Concentration for CAIMAN 2001/01 as Compared to Code Calculations (Optimized).

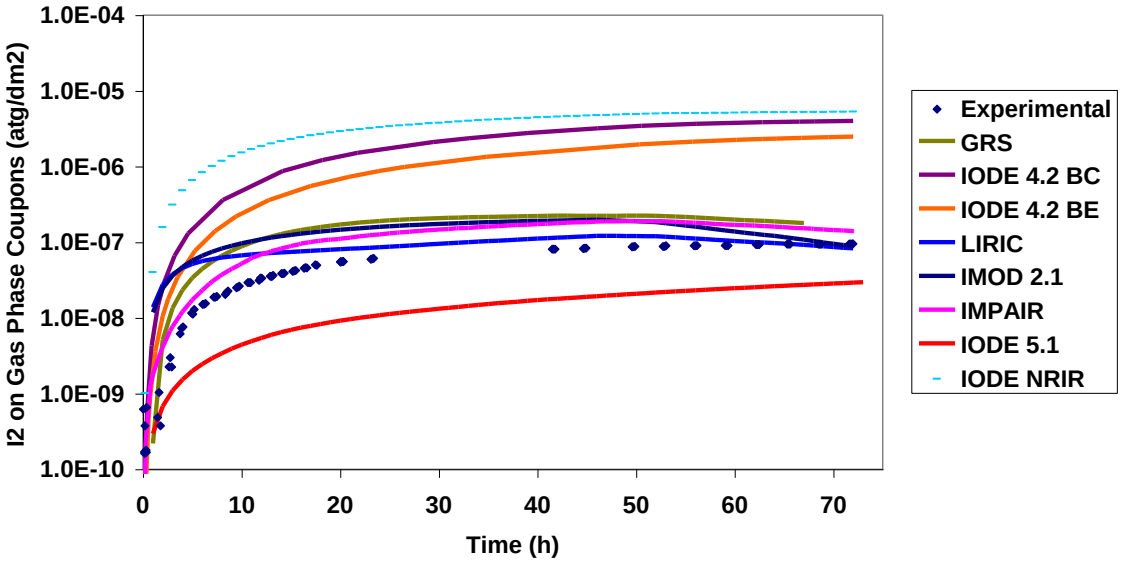

Figure 27: Concentration of I_2 adsorbed on Gas Phase Paint Coupons for CAIMAN 2001/01 as Compared to Code Calculations (Optimized).

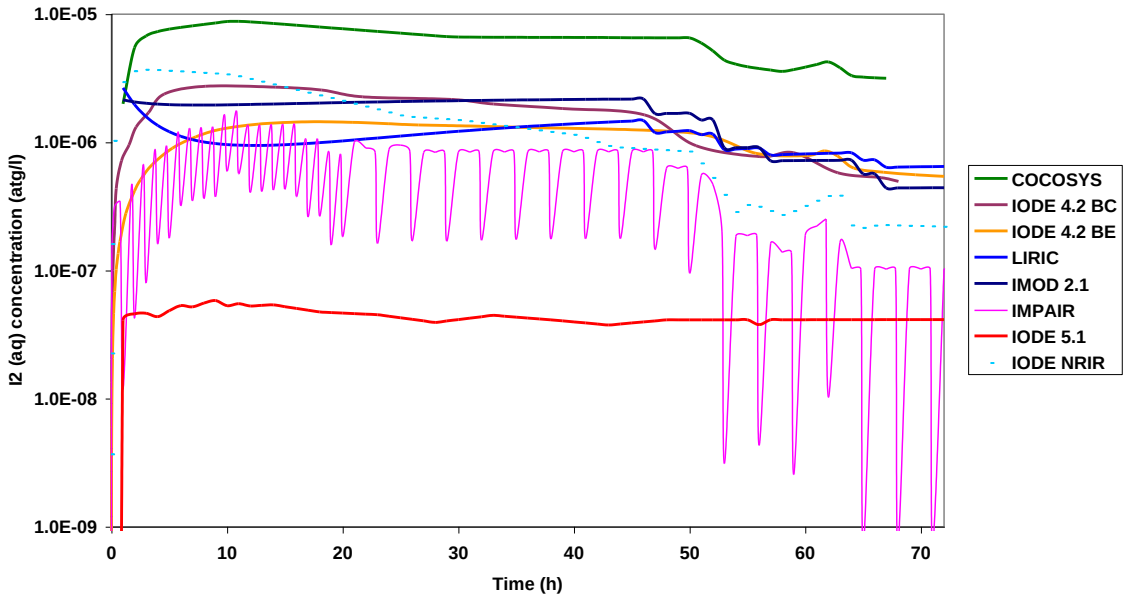

Figure 28: Aqueous Phase I_2 Concentrations for CAIMAN 01/01 as Predicted by Code Calculations (Optimized).

Figure 28 shows the calculated concentrations for I_2 in the aqueous phase. There is a good agreement between the different codes except COCOSYS, which overestimates, and IODE 5.1, which underestimates, I_2(aq) compared to the other codes. These two codes also over- and under-estimate gas phase I_2 concentrations. It is more difficult to rationalize some of the other results. For example, IODE 4.2, IODE NRIR, LIRIC and IMOD all show about the same amount of I_2 in the aqueous phase. Despite this, IODE 4.2 and IODE NRIR overestimate I_2 in the gas phase and LIRIC and IMOD do not.

IODE 4.2 and IODE NRIR calculations use a larger interfacial mass transfer coefficient than do LIRIC and IMOD (see Table 8). However, this is not the reason for the difference in the amount of I_2 transferred to the gas phase. A sensitivity study showed that if the mass transfer coefficient in LIRIC and IMOD is increased from 7.5 10^{-6} to $1e^{-5}$ $m \cdot s^{-1}$, the gas phase I_2 concentration increases by only 20%. It appears that the difference between these code predictions is that in IODE 4.2 and IODE NRIR, it is predicted that most of the I_2 is transferred out of the sump, where it deposits on painted surfaces in the gas phase (IODE NRIR predicts about 75% of the inventory on the gas phase coupon, and IODE 4.2 BE about 34%, experimental data indicate 10%). In LIRIC and IMOD however, although the steady state I_2(aq) concentration is similar, there is competition between transfer of iodine into the gas phase, and rapid adsorption/desorption of I_2 on aqueous phase surfaces, with the latter being much more rapid. LIRIC and IMOD predict that only 13 and 15% of the inventory, respectively are deposited on the gas phase coupon at the end of the experiment.

Table 8: Rate Constants Used in CAIMAN 2001/01

	Recommended [a]	IODE 5.1	COCOSYS	LIRIC	IMOD 2.1	IODE 4.2 BE	IMPAIR	NRIR
$K_{ads}I_2$aqss ($m \cdot s^{-1}$)	negligible	1.10^{-8}	-	5.10^{-4}	2.10^{-3}	0	0	0
$K_{des}I_2$aqss (s^{-1})	negligible	0	-	4.10^{-1}*	4.10^{-1}*	0	0	0
$I_2 \rightarrow I^-$ (ss adsaq) ($m \cdot s^{-1}$)	-	-	$7.9.10^{-7}$	-	-	-	$3.2.10^{-6}$	-
$K_{ads}I^-$aqss ($m \cdot s^{-1}$)	-	-	-	0	0	-	0	-
$K_{des}I^-$aqss (s^{-1})	-	-	-	0	0	-	0	-
$K_{ads}I_2$gp ($m \cdot s^{-1}$)	4.10^{-3}	2.10^{-3}	2.10^{-3}	$4.5.10^{-3}$	$4.5.10^{-3}$	2.10^{-3}	2.10^{-3}	$1.3.10^{-3}$
$K_{des}I_2$gp (s^{-1})	-	0	1.10^{-6}	2.10^{-5}	2.10^{-5}	0	0	0
$K_{ads}I_2$gss ($m \cdot s^{-1}$)	negligible	1.10^{-5}	1.10^{-4}	2.10^{-4}	2.10^{-4}	0	5.10^{-5}	1.10^{-4}
$K_{des}I_2$gss (s^{-1})	negligible	1.10^{-6}	$1.06.10^{-4}$	$7.3.10^{-4}$	$3.7.10^{-4}$	0	1.10^{-5}	$4.8.10^{-4}$
$K_{L\text{-}G}$ I_2 ($m \cdot s^{-1}$)	1.10^{-5}	1.10^{-5}	$8.3.10^{-6}$	$7.2.10^{-6}$	$7.2.10^{-6}$	1.10^{-5}	1.10^{-5}	5.10^{-5}
$K_{L\text{-}G}$ ICH_3 ($m \cdot s^{-1}$)	1.510^{-5}	1.510^{-5}	$9.7.10^{-6}$	$1.1.10^{-5}$	$1.1.10^{-5}$	$1.5.10^{-5}$	$1.5.10^{-5}$	5.10^{-5}

* : desorbed as I^-

4.4 Comparison of Rate Constants

A comparison of some of the rate constants used in various calculations show that there are some anomalies. These are identified and explained in the following discussion.

Table 9: I_2 Adsorption Rate Constants ($m \cdot s^{-1}$) on Stainless Steel in the Aqueous Phase

	IODE 5.1	COCOSYS	LIRIC	IMOD	IODE 4.2 BE	IMPAIR	NRI
RTF 1	2.10^{-6}	0	2.10^{-2}	6.10^{-2}	0	0	0
CAIMAN 97/02	1.10^{-8}	0	2.10^{-2}	6.10^{-2}	0	0	0
CAIMAN 01/01	1.10^{-8}	0	5.10^{-4}	2.10^{-3}	0	0	0

Table 9 shows that IODE 5.1 used a higher adsorption rate constant for PHEBUS/RTF 1 in comparison to the one used for the CAIMAN tests. This is justified because the measured amount of iodine adsorbed on the stainless steel surfaces in the RTF experiment (8.5%) was much higher than in the CAIMAN experiments (0.85 and 0.05% for 97/02 and 01/01 respectively). The measured amount of iodine on stainless steel surfaces in this experiment may also have significantly underestimated the amount of iodine absorbed on the stainless steel surfaces. The mass balance for Phebus RTF1 was not closed; 13% of the iodine inventory was unaccounted for. It likely that the portion of iodine inventory that was unaccounted for could have been absorbed in localized “hot spots” on the aqueous phase stainless steel surfaces.

Note that there are differences in the adsorption rate constants used by LIRIC, IMOD and those used by other codes. The large rate constants used in LIRIC and IMOD for adsorption of I_2 on stainless steel surfaces was to test whether rapid conversion of I2 to I- on stainless steel surfaces could explain why experimentally observed I_2 concentrations were always much lower than code predictions for Phebus RTF1 and the CAIMAN experiments. However, as mentioned previously [Section 4.1], there is no satisfactory mechanistic explanation for the necessity of LIRIC and IMOD calculations to require a smaller adsorption rate constant for CAIMAN 01/01 than for PHEBUS RTF1 and CAIMAN 97/02. For this reason, subsequent optimisation calculations used an alternative sub-model, involving impurities, to produce similar results, but with more consistent rate constants.

Table 10: I_2 Desorption Rate Constant on Stainless Steel in the Aqueous Phase

	IODE	COCOSYS	LIRIC	IMOD	IODE 4.2 BE	IMPAIR	NRI
RTF 1	0	0	4.10^{-2}	4.10^{-2}	0	0	?
CAIMAN 97/02 ($I_2 \rightarrow I^-$)	0	$8.5.10^{-7}$	5.10^{-1}	5.10^{-1}	0	$7.9.10^{-7}$	0
CAIMAN 01/01 ($I_2 \rightarrow I^-$)	0	$7.9.10^{-7}$	4.10^{-1}	4.10^{-1}	0	$3.2.10^{-6}$	0

For LIRIC and IMOD calculations the value used for k_{des} for PHEBUS/RTF 1 is lower in comparison to the CAIMAN tests (the adsorption rate is the same, see Table 9 above). The use of an increased overall adsorption rate for PHEBUS RTF results is consistent with the greater amount of iodine absorbed on stainless steel surfaces in Phebus RTF1.

Table 11: I_2 adsorption rate constant on painted surfaces in the aqueous phase

	IODE	COCOSYS	LIRIC	IMOD	IODE 4.2 BE	IMPAIR	NRI
Phase 10 Test 1	2.10^{-4}	2.10^{-4}	4.10^{-4}	6.10^{-4}	8.10^{-4}	$1.6.10^{-3}$	4.10^{-4}
Phebus RTF 1	8.10^{-4}	2.10^{-4}	2.10^{-4}	2.10^{-4}	8.10^{-4}	4.10^{-4}	?
CAIMAN 97/02	1.10^{-4}	4.10^{-6}	3.10^{-4}	3.10^{-4}	1.10^{-4}	1.10^{-4}	2.10^{-4}

IMPAIR code used a higher rate constant for Phase 10 Test 1 than for Phebus RTF1 and CAIMAN 97/02 despite the fact that the temperature in the former (60ºC) was lower that the others. This could be justified because the paint type for Phase 10 Test 1 is different that the type used in the other experiments. Although the overall adsorption rate observed for Phebus RTF1 could be different from that observed for CAIMAN 97/02, because of differences in mass transfer between the two experiments, there is no satisfactory explanation as to why the absorption rate

coefficient used for Phebus RTF1 should be different than that used for CAIMAN 97/02, because the paint type and temperature is the same.

COCOSYS used a very low rate constant for CAIMAN 97/02 in comparison to that used for Phase 10 Test 1 and Phebus RTF1. However, the rate constant provided in the table for COCOSYS calculations is comprised of both chemical adsorption and mass transfer to the surface. Mass transfer to the surface is lower for CAIMAN 97/02, thus the rate constant reported in the table is lower. The actual rate constant for chemical absorption used in the calculations conforms to the recommended value.

Table 12: I_2 Desorption Rate Constant on Painted Surfaces in the Aqueous Phase

	IODE	COCOSYS	LIRIC	IMOD	IODE 4.2 BE	IMPAIR	NRI
Test 1	5.10^{-7}	2.10^{-6}	$2.5.10^{-7}$	$2.5.10^{-7}$	5.10^{-7}	$2.5.10^{-7}$	$2.5.10^{-7}$
RTF 1	5.10^{-7}	2.10^{-6}	1.10^{-4}	1.10^{-4}	5.10^{-7}	1.10^{-6}	?
CAIMAN 97/02	0	2.10^{-6}	1.10^{-6}	2.10^{-7}	0	1.10^{-6}	5.10^{-7}

LIRIC and IMOD calculations require the use of a larger desorption rate constant to achieve the same overall rate of adsorption for PHEBUS/RTF 1 as compared to CAIMAN tests, despite the fact that the paint surface is the same as that for the CAIMAN tests. This indicates that the predicted I_2 concentration in the aqueous phase for LIRIC and IMOD calculations of Phebus RTF1 is too high, an observation consistent with Figure 16 (I_2 in the gas phase for Phebus RTF1)

Table 13: I_2 Desorption Rate Constant on Painted Surfaces in the Gas Phase

	IODE	COCOSYS	LIRIC	IMOD	IODE 4.2 BE	IMPAIR	NRI
Test 1	0	0	0	0	0	0	0
RTF 1	0	0	1.10^{-4}	1.10^{-4}	0	0	?
CAIMAN 97/02	0	1.10^{-6}	1.10^{-4}	1.10^{-4}	0	0	0
CAIMAN 01/01	0	1.10^{-6}	2.10^{-5}	1.10^{-4}	0	0	0

The desorption rate constants used by LIRIC and IMOD are large relative to those used by others codes. The LIRIC and IMOD models use a higher desorption rate constant for the Ripolin paint used in these experiments because a non-linear least squares analysis of CAIMAN 97/02 and 01/01 data, using data for adsorption on the gas phase coupons, and measured I_2 concentrations in the gas phase, indicated that the "hard value" recommended for the overall iodine adsorption rate constant (Appendix D) was too high by a factor of 5 to 10. The recommended adsorption rate constant to be used for modelling these experiments was 4×10^{-3} m·s^{-1} ($\pm$ a factor of 2) and this value assumed that there was no desorption. However non-linear least squares analysis of the CAIMAN 01/01 and 97/02 data found that values of $k_{ads} = 8 \times 10^{-4}$

$m \cdot s^{-1}$ $k_{des} = 1 \times 10^{-5}$ s^{-1}, and $k_{ads} = 5 \times 10^{-4}$, $k_{des} = 1 \times 10^{-5}$ s^{-1} respectively, produced best fits to the adsorption data. For the modelling studies therefore, LIRIC and IMOD used the recommended value for the adsorption rate constant, but they incorporated a desorption rate constant. The overall absorption rate constant used for their calculations was therefore different from the "hard value because in an attempt to make the overall adsorption rate constant consistent with that derived from the experimental data. A plot of the CAIMAN adsorption data along with the non-linear least squares fit to the data is shown in Figure 29.

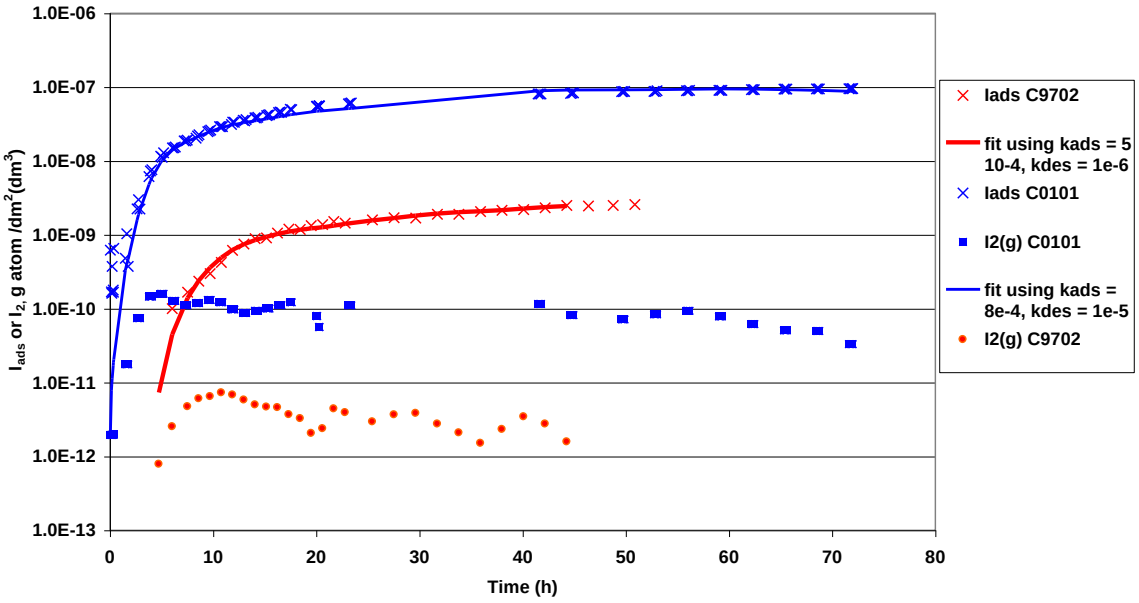

Figure 29: Gas Phase I_2 concentrations and Iodine Adsorbed on Gas Phase Coupons for CAIMAN 97/02 and 01/01. Solid lines show best fits to the data using non-linear least squares regression analysis.

4.5 Summary Of Trends

Overall summaries of the trends predicted by each code as compared to the experimental data are shown in Tables 14– 17.

Table 14: Summary of Trends for RTF Phase 10 Test 1

Code	General Trend of Gas Phase	Aqueous phase profile	Organic Iodide Profile	I_2 profile
COCOSYS	Qualitative: curve shape good. Underestimates initial pH 10 stage by a factor of 5	Qualitative: curve shape poor Overestimates by 300 %	Qualitative: curve shape good. Underestimates initial pH 10 stage by a factor of 5	Qualitative: curve shape good Underestimates by a factor of 5 –10
IODE 4.2 BE	Qualitative: curve shape good. Overestimates by a factor of 5 -10	Qualitative: curve shape poor Overestimates by 200 %	Qualitative: curve shape good. Overestimates by a factor of 5 -10	Qualitative: curve shape good Underestimates by a factor of 10
IODE 4.2 BC	Qualitative: curve shape good. Overestimates by a factor of 10 - 50	Qualitative: curve shape okay Overestimates by 100 %	Qualitative: curve shape good. Overestimates by a factor of 10 - 50	Qualitative: curve shape good Underestimates by a factor of 10
AECL (LIRIC)	Qualitative: curve shape good. Overestimates by a factor of 2 - 5	Qualitative: curve shape good. Quantitative agreement good.	Qualitative: curve shape good. Overestimates by a factor of 2 - 5	Qualitative: curve shape good Underestimates by a factor of 5 -10
AECL (IMOD)	Qualitative: curve shape good. Overestimates by a factor of 2	Qualitative: curve shape good Quantitative agreement good.	Qualitative: curve shape good. Overestimates by a factor of 2	Qualitative: curve shape good Underestimates by a factor of 5
PSI IMPAIR	Qualitative: curve shape good. Overestimates by a factor of 2	Qualitative: curve shape okay Underestimates by 20% at beginning of test	Qualitative: curve shape good Overestimates amount by a factor of 3 - 5	Qualitative: curve shape poor Underestimates by orders of magnitude.
IRSN IODE 5.1	Qualitative: curve shape good. Underestimates by a factor of 3 during initial stage	Qualitative: curve shape poor Overestimates by 250%. (see appendix A)	Qualitative: curve shape good. Underestimates by a factor of 3 during initial stage.	Qualitative: curve shape good Underestimates by a factor of 3 - 10.
NRI IODE	Qualitative: curve shape okay. Underestimates by a factor of 30 during initial stage	Qualitative: curve shape good Quantitative agreement good.	Qualitative: curve shape okay. Underestimates by a factor of 30 during initial stage	Qualitative: curve shape good Underestimates by a factor of 5 -10

Table 15: Summary of Trends for Phebus RTF1

Code	General Trend of Gas Phase	Aqueous phase profile	Organic Iodide Profile	I_2 profile
COCOSYS	Qualitative: curve shape good. Overestimates by a factor of 3 - 5	Qualitative: curve shape poor Underestimates by 60 – 70 %	Qualitative: curve shape good. Underestimates by 2 orders of magnitude.	Qualitative: curve shape good. Quantitative agreement good

				overestimates slightly
IODE 4.2 IODE BE	Qualitative: curve shape good. Underestimates by a factor of 2.	Qualitative curve shape good Overestimates by 30%	Qualitative: curve shape good. Quantitative agreement good.	Qualitative: curve shape good Underestimates by a factor of 2 – 5.
IODE 4.2 IODE BC	Qualitative: curve shape good. Overestimates by a factor of 2.	Qualitative: curve shape good Underestimates by 30%	Qualitative: curve shape good. Quantitative agreement good.	Qualitative: curve shape okay Quantitative agreement good, underestimates slightly.
AECL (LIRIC)	Qualitative: curve shape good. Overestimates by a factor of 3 - 5	Qualitative: curve shape good. Quantitative agreement good.	Qualitative: curve shape good. Quantitative agreement good.	Qualitative: curve shape good Overestimates by about a factor of five.
AECL (IMOD)	Qualitative: curve shape good. Overestimates by a factor of 3 - 5	Qualitative: curve shape good Quantitative agreement good.	Qualitative: curve shape good. Quantitative agreement good.	Qualitative: curve shape good Quantitative agreement good.
PSI IMPAIR	Qualitative: curve shape good. Quantitative agreement good.	Qualitative: curve shape poor Overestimates by 80%.	Qualitative: curve shape good Overestimates amount by a factor of 10 -50	Qualitative: curve shape good Underestimates by a factor of 25.
IRSN IODE 5.1	Qualitative: curve shape good. Underestimates by a factor of 3 to 4.	Qualitative: curve shape poor Overestimates by 80%.(see appendix A)	Qualitative: curve shape okay Underestimates by a factor of 3 - 20.	Qualitative: curve shape good Underestimates by a factor of 5 – 10.
NRI IODE	Qualitative: curve shape poor Overestimates by a factor of 5 at beginning.	Qualitative: curve shape poor Underestimates by 80%.	Qualitative: curve shape poor Overestimates by a factor of 5 at beginning.	Qualitative: curve shape okay Underestimates by a factor of 5 at end.

Table 16: Summary of Trends for Caiman 97/02:

Code	**General Trend of Gas Phase**	**Gas Paint Adsorption profile**	**Organic Iodide Profile**	**I_2 profile**
COCOSYS (no IO_3-g)	Qualitative: wrong trend at beginning and end, Overestimates at beginning, and a factor of 5 –10 at end	Qualitative: curve shape good Overestimates by 2 orders of magnitude	Qualitative: wrong trend at beginning and end, Overestimates at beginning, and a factor of 5 –10 at end	Qualitative: good agreement Overestimates by 50
COCOSYS (IO_3-g)				
IODE 4.2 BC	Qualitative: wrong trend at beginning and end, Overestimates at beginning and a factor of 5 –10 at end	Qualitative: curve shape good Overestimates by more than an order of magnitude	Qualitative: wrong trend at beginning and end, Overestimates at beginning and a factor of 5 –10 at end	Qualitative: curve shape good Quantitative agreement good.

IODE 4.2 IODE BE	Qualitative: wrong trend at beginning and end, Overestimates at beginning and a factor of 5 at end	Qualitative: curve shape good Overestimates by more than an order of magnitude	Qualitative: wrong trend at beginning and end, Overestimates at beginning and a factor of 5 at end	Qualitative: curve shape good Quantitative agreement good.
AECL (LIRIC)	Qualitative: wrong trend at beginning and end, Overestimates at beginning and slightly at end	Qualitative: curve shape good Quantitative agreement good.	Qualitative: wrong trend at beginning and end, Overestimates at beginning and slightly at end	Qualitative: curve shape poor Underestimates by a factor of 10 at beginning of test.
AECL (IMOD)	Qualitative: wrong trend at beginning and end, Overestimates at beginning and slightly at end	Qualitative: curve shape good Quantitative agreement good.	Qualitative: wrong trend at beginning and end, Overestimates at beginning and slightly at end	Qualitative: curve shape poor Underestimates by a factor of 10 at beginning of test.
PSI IMPAIR	Qualitative: curve shape okay Overestimates amount by a factor of 50	Qualitative: curve shape good Overestimates by a factor of 5.	Qualitative: curve shape okay Overestimates amount by a factor of 50	Qualitative: curve shape good Quantitative agreement good.
IRSN IODE 5.1	Qualitative: curve shape okay Overestimates at beginning and underestimates slightly during the middle of the test.	Qualitative: curve shape good Quantitative agreement good.	Qualitative: curve shape okay Overestimates at beginning and underestimates slightly during the middle of the test.	Qualitative: curve shape good Underestimates by a factor of 10 at beginning of test and slightly at end of test
NRI IODE	Qualitative: curve shape good Overestimates by a factor of 100.	Qualitative: curve shape good Overestimates by 2 orders of magnitude	Qualitative: curve shape good Overestimates by a factor of 100.	Qualitative: curve shape okay Overestimates a factor of 50 at beginning and about 5 at end.

Table 17: Summary of Trends for Caiman 01/01

Code	**General Trend of Gas Phase**	**Gas Paint Adsorption profile**	**Organic Iodide Profile**	**I_2 profile**
COCOSYS (no IO_3-g)	Qualitative: curve shape good Quantitative agreement good	Qualitative: curve shape good Quantitative agreement good	Qualitative: curve shape okay Underestimates by more than a factor of 10 during initial 10 h.	Qualitative: curve shape good Overestimates by a factor of 5 -10.
COCOSYS (IO_3-g)	Qualitative: curve shape poor Overestimates amounts by a factor of 5 -10			
IODE 4.2 BE	Qualitative: curve shape okay Underestimates amounts by a factor of 5 -10	Qualitative: curve shape good Overestimates by a factor of 10	Qualitative: curve shape okay Underestimates by a factor of 10 during initial 10 h.	Qualitative: curve shape good Overestimates by a factor of 3
IODE 4.2 IODE BC	Qualitative: curve shape okay Underestimates amounts by a factor of 5 -10	Qualitative: curve shape good Overestimates by a 3 – 4 orders of magnitude	Qualitative: curve shape okay Underestimates by a factor of 5 during initial 10 h.	Qualitative: curve shape good Overestimates by a factor of 3 initially, but not at end

AECL (LIRIC)	Qualitative: curve shape good Quantitative agreement good	Qualitative: curve shape good Quantitative agreement good	Qualitative: curve shape good Quantitative agreement good	Qualitative: curve shape good Quantitative agreement good
AECL (IMOD)	Qualitative: curve shape good Overestimates by a factor of 2	Qualitative: curve shape good Quantitative agreement good	Qualitative: curve shape good Quantitative agreement good	Qualitative: curve shape good Quantitative agreement good
PSI IMPAIR	Qualitative: curve shape good Overestimates amounts by a factor of 5 -10	Qualitative: curve shape good Quantitative agreement good	Qualitative: curve shape good Overestimates amount by a factor of 5-10	Qualitative: curve shape good Quantitative agreement good
IRSN IODE 5.1	Qualitative: curve shape okay Underestimates amounts by a factor of 5 -50	Qualitative: curve shape okay Underestimates by a factor of 5 during initial 10 h.	Qualitative: curve shape okay Underestimates by a factor of 5 during initial 10 h.	Qualitative: curve shape good Underestimates by a factor of 50
NRI IODE	Qualitative: curve shape good Overestimates amounts by a factor of 10 -50	Qualitative: curve shape okay Overestimates by a factor of 10 to 50.	Qualitative: curve shape okay Overestimates by a factor of 10 to 50.	Qualitative: curve shape okay Overestimates by a factor of 10 to 50.

From the tables, some general trends regarding each code calculation can be seen. Most of the codes overestimate I_2 production in the aqueous phase for Phebus RTF1, CAIMAN 01/01 and CAIMAN 97/02, and underestimate I_2 production in the aqueous phase for Phase 10 Test 1.[5] These are summarized as follows.

COCOSYS

- overestimates I_2 for pH 5 and 90 and 110ºC. Organic iodide concentrations are underestimated, or overestimated to a far less extent under the same conditions.
- At pH 8 – 10, and 60ºC COCOSYS underestimates I_2 concentrations and underestimates organic iodide concentrations slightly.
- Overall, COCOSYS appears to slightly underestimate organic iodide production rates

IODE 4.2. (CIEMAT)

- Based on predicted adsorption on gas phase surfaces and predicted gas phase I_2 concentrations both BE and BC overestimate aqueous phase I_2 in CAIMAN experiments. They also overestimate organic iodide formation, but not as significantly.

- In Phebus RTF1, IODE 4.2 BE overestimates aqueous phase concentration and underestimates I_2, indicating that it underestimates I_2 in the aqueous phase. IODE 4.2 BC slightly underestimates the gas phase I_2 concentration but this is offset by its underestimation of the aqueous phase total iodine concentration (indicates that too much I_2 is absorbing on surfaces) so its aqueous phase I_2 concentration is probably about right. The organic iodide concentration predicted for this test are about right.

- Both IODE 4.2 BC and BE underestimates I_2 concentrations in Phase 10 Test 1 but significantly overestimate organic iodide concentrations.

IMPAIR

- In CAIMAN tests PSI predicts the gas phase I_2 concentration and the adsorption on gas painted surfaces well, so it is assumed that it predicts aqueous phase I_2 concentrations well. Organic iodide formation is significantly overestimated in CAIMAN 97/02 and somewhat overestimated in CAIMAN 01/01
- In Phebus RTF1, IMPAIR underestimates the I_2 concentration in the gas phase but also underestimates the amount of iodine in the aqueous phase because it predicts that too much I_2 is absorbed on aqueous phase surfaces. Its predictions of the rate of production of I_2 in the

[5] RTF Phase 10 Test 1 is outside of the range of conditions thought to be representative of PWR severe accident conditions, and it is the view of some participants that this experiment should not be used to validate codes for severe accident analysis.

aqueous phase are probably about right. Organic iodide concentrations in the gas phase are significantly overestimated.

- In Phase 10 Test 1 I_2 in the gas phase is underestimated significantly, but the aqueous phase iodine concentration is about right. It appears that the aqueous phase I_2 concentrations are underestimated. Despite this, organic iodide concentrations in the gas phase are overestimated.
- In general, for a given I_2 concentrations, organic iodide production is overestimated.

IODE 5.1(IRSN)

- Underestimates gas phase I_2 slightly in CAIMAN 97/02, Phebus RTF1, and Phase 10 Test 1. It also underestimates organic iodide concentrations by a similar amount, indicating that the underestimation of organic iodide concentrations is a consequence of I_2 underestimation. In CAIMAN 0101, it significantly underestimates gas phase I_2 concentrations but underestimates organic iodide concentrations less.
- In general it appears that IODE 5.1 correctly predicts the appropriate organic iodide concentrations for a given I_2 concentration and underpredicts I_2 formed by radiolytic process.

LIRIC 3.3/IMOD 2.1

- Slightly overestimates I_2 in the aqueous phase for Phebus RTF1. The organic iodide concentration is about right. In CAIMAN 97/02 the amount of I_2 is about right, but the trend is wrong, organic iodide concentrations are slightly overestimated. In CAIMAN 01/01 both organic iodide concentrations and I_2 concentrations are predicted well.
- In Phase 10 Test 1, the gas phase I_2 concentration is underestimated slightly but organic iodide concentration is slightly overestimated. Overall, the codes perform well in the experiment.
- In general it appears that LIRIC and IMOD correctly predict the appropriate organic iodide concentrations for a given I_2 concentration and overpredict I_2.

IODE NRIR

- Overestimates the aqueous phase I_2 concentrations in CAIMAN experiments (and perhaps in Phebus RTF 1)
- Underestimates I_2 concentrations in Phase 10 Test 1.
- For a given predicted I_2 concentrations, organic iodide production is overestimated.

It should be noted that the apparent over- or under-prediction of $I_2(g)$ by some of the codes may be the result of the recommended value for the interfacial mass transfer coefficient being too high. The recommended values were based on best estimates, but were not measured for each experiment.

5. FURTHER CODE IMPROVEMENTS

Despite the improvement in agreement between code predictions and experimental results in the first set of optimized calculations, a number of suggestions for further improvements to code calculations were made, and participants were invited to further improve their calculations should they desire. The additional calculations are presented in detail in Appendix A. Full details are given in the appendices, briefly, the most important modifications made were:

- IODE 5.1 calculations for CAIMAN 01/01, CAIMAN 97/02 and PHEBUS/RTF1 were repeated with a lower activation energy for the conversion of I_2 to I-. The results are in much better agreement with experimental results when this modification is implemented. IODE 5.1 calculations for Phebus RTF1 were also repeated to demonstrate that changing the adsorption/desorption rate constant for I_2 on stainless steel surfaces could improve the calculated aqueous phase iodine concentration.

- IMOD 2.1 calculations for all tests were repeated using a sub-model for I_2 interaction with impurities, rather than rapid adsorption/desorption of I_2 on stainless steel surfaces. The impurity sub-model can be switched on and off, and is a more consistent model than the adsorption/desorption model, because the same rate constants (both adsorption/desorption an d impurity rate constants) can be used for all of the tests. The repeated calculations for CAIMAN 97/02 also assumed a time lag between the start of the experiment and introduction of the iodine source, since experimentalists confirmed that this could have been the reason for the delay in accumulation of iodine in the gas phase observed in the experiment.

- COCOSYS calculations were repeated increasing the thermal and the radiation induced CH_3I release in the water phase by a factor 5 for all tests, and the pH-dependency of the radiolytic oxidation of iodide to I_2 and IO_3^- to I_2 in the water phase was reduced. Additionally some of the adsorption/desorption rate constants were modified within their uncertainty margins.

- IMPAIR calculations were repeated for RTF P10T1 and CAIMAN 01/01 using smaller rate constants for organic iodide formation in the aqueous phase, and changing the rate of radiolytic oxidation of iodine. A similar approach will be attempted for the other two experiments. It should be noted that a consistent set of rate constants for organic iodide formation and the radiolytic oxidation of iodine which give a “best fit” to all four of the experiments have not yet been determined for IMPAIR.

The gas phase concentrations predicted by IMOD 2.1, IODE 5.1, COCOSYS, and IMPAIR for CAIMAN 0101 with additional improvements are shown in Figure 30. Total gas phase concentrations for Phebus RTF1 as predicted by IMOD 2.1, IODE 5.1, COCOSYS with additional improvements are shown in Figure 31. As can be seen from the figures, the additional improvements to the codes improve the agreement between code predictions and experimental data.

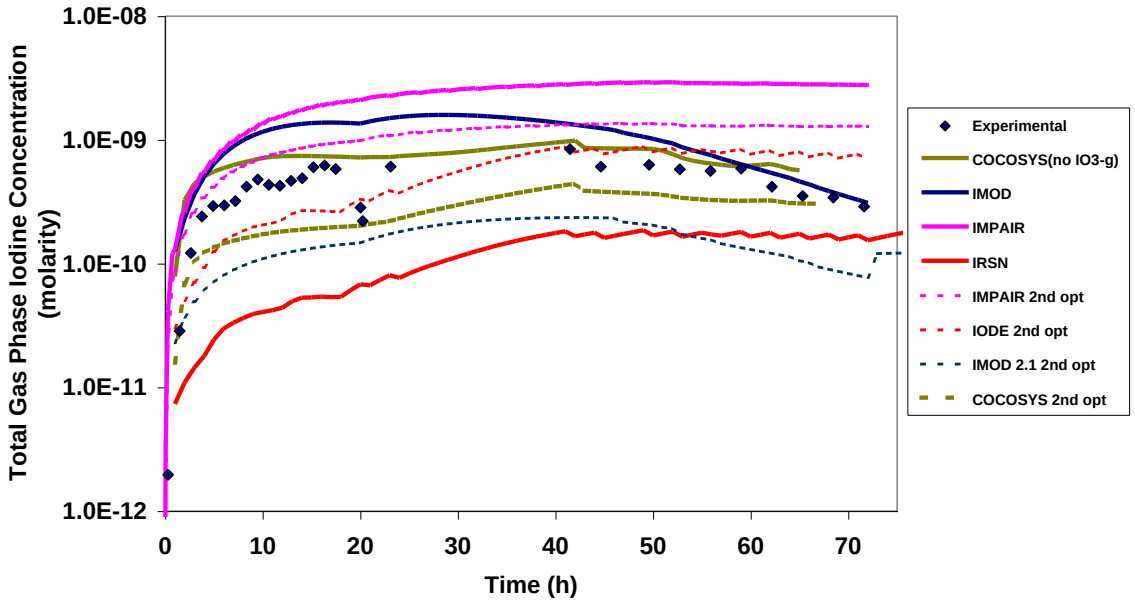

Figure 30: Total Gas Phase Iodine Concentration for CAIMAN 2001/01 as Compared to Code Calculations (2nd Optimization).

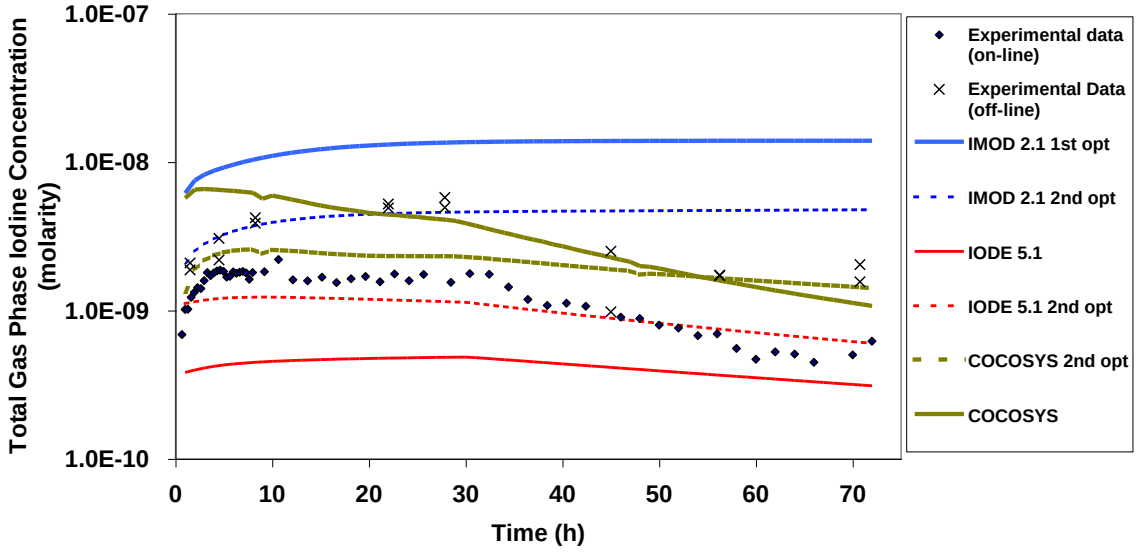

Figure 31: Total Gas Phase Iodine Concentration for Phebus RTF1 as Compared to Code Calculations (2nd Optimization).

For IMOD 2.1 and COCOSYS, all four tests were re-calculated. IODE 5.1 re-calculated three experiments, both CAIMAN facility experiments and Phebus RTF1, and IMPAIR re-calculated CAIMAN 01/01 and P10T1.

6. CONCLUSIONS

The code comparison exercise demonstrated that, in general, all of the iodine behaviour codes predict the correct trends regarding iodine volatility. In the blind calculations, there was a very large discrepancy between quantitative code results. Open calculations improved the quantitative agreement between calculations and experimental data, and between the various codes by allowing:

- Some changes in the models (e.g. PSI's organic model, AECL's new version of IMOD, IMOD 2.1)
- Some modifications in the "hard parameters" of the models (e.g. CIEMAT modifications of the rate constant for adsorption on the gas phase paint) and
- A better estimate of the input parameters (pH profiles for P10T1 required by some of the codes, organic dissolution rate constants for LIRIC, IMOD and IODE 5.1).

In the open calculations, there were still significant discrepancies between model predictions and experimental results. None of the codes predicted all of the important parameters for all four of the tests to within the criteria determined for this exercise on the basis of experimental uncertainties. The results are summarized completely in Section (4). As an example, the results at test end for CAIMAN 97/02 and Phebus RTF1 are presented here.

CAIMAN 97/02;

- 4 out of 8 of the codes reproduced the aqueous phase concentration,
- 2 out of 8 reproduced the total gas phase iodine concentration,
- 8 out of 8 reproduced the organic iodide fraction, and
- 3 out of 8 reproduced the gas phase organic iodide concentration

Phebus RTF1;

- 3 out of 8 of the codes reproduced the aqueous phase concentration,
- 5 out of 8 reproduced the total gas phase concentration,
- 0 out of 8 reproduced the gas phase organic iodide fraction, and
- 1 out of 8 reproduced the gas phase organic iodide concentration.

The optimized calculations demonstrated that many of the codes predict the overall rate of production of I_2(aq) differently. The general trend was that most codes overestimated the overall rate of production of I_2(aq) at pH 5, and 90 and 110º C (CAIMAN 97/02 and 01/01 and Phebus RTF1), but underestimated the overall rate of production of I_2(aq) at higher pH and 60ºC (RTF Phase 10 Test 1).

In order to properly assess organic iodide formation models, the I_2(aq), the I_2(g), and the amount of adsorbed iodine (or aqueous iodine) must be well predicted. Because the codes predicted the overall I_2 production rate differently, there were difficulties assessing the performance of the organic iodide sub-models in each of the codes. Nonetheless, some general observations of organic iodide production rates were made. It appears that COCOSYS slightly underestimates organic iodide production rates, whereas IMPAIR and IODE NRIR overestimate. IODE 4.2 appears to overestimate organic iodide production rates at high pH values, but predicts well at

lower pH values. LIRIC, IMOD and IODE 5.1 appear to produce the appropriate amount of organic iodide for a given predicted I_2 concentration.

One of the problems in predicting organic iodide concentrations is that, for homogeneous aqueous phase processes, the organic iodide formation depends on the quantity of organic impurities in the liquid phase, this organic amount is mainly released from the paints, a parameter that is difficult to predict. For ISP calculations, it was possible for participants to estimate the concentration, because there was information available on measured total carbon (CAIMAN) or organic impurity concentrations (RTF). However, for reactor applications it is uncertain whether the default values for organic impurities in each of the iodine codes are adequate for the prediction of organic iodide production. In CAIMAN experiments, although the ratios of painted surface to volume are similar to those encountered in the reactors and it can be assumed that the organic amount measured from the paints is representative of a severe accident situation, there may also be additional sources of organics. Furthermore, the gas phase dose-rate under accident conditions is considerably higher than those in CAIMAN experiments.

The final phase of ISP41 has provided an unique opportunity to compare codes against previously unavailable experiments performed over a wide range of initial conditions. The exercise was used to evaluate the reliability of various codes for prediction of iodine volatility from simple but realistic analytical experiments, providing participants with an opportunity to identify their code's weaknesses, and test various approaches to improving these weaknesses. The exercise should also be used by each organization to identify areas where additional experiments, or analysis of additional experimental data or may be required. It is clear that analysis of additional experiments are required for improvements to be made in the ability of the iodine behaviour models to simulate the overall rate of production of I_2 by radiolytic processes. This needs to be accomplished before organic iodide sub-models are further developed, and a full evaluation of the importance of various organic iodide formation processes (aqueous phase or gas phase surfaces) is made.

From the simulations of PHEBUS RTF1, and CAIMAN 97/02, the experiments identified by the participants as being most representative of reactor accident conditions, it is evident that there is still some work to be done to improve the iodine behaviour codes so that they can be used confidently as predictive tools for reactor applications. A few of the participants have provided information regarding further code improvements that have been investigated since the optimization exercises were performed. These improvements demonstrate that better agreement between code calculations and experimental data can be achieved by making adjustments to the existing codes, and using consistent modeling approaches. It is imperative, however, that these modifications be validated over a wide range of experimental conditions.

Depending upon the application, additional information may be required in order that the iodine behaviour codes can be used as predictive tools for reactor accident scenarios. This additional information could include such things as:

- reactor and accident specific information regarding thermalhydraulic parameters for the determination of mass transfer and the adsorption-desorption rate constants (these parameters were fixed in this exercise)

- information regarding the presence of other fission products, and control rod materials,
- the qualification of the source of iodine released into containment.

Further code improvements are expected to be an on-going process for each organization as a result of this ISP-41 exercise, and as new experimental data becomes available. The participants in this ISP are encouraged to apply their optimized models to calculations of RTF tests (e.g. ACE RTF, and Phebus RTF) and other experiments available in the literature.

7. REFERENCES

1. J. Ball, G. Glowa, J. Wren, A.Rydl, C. Poletiko, Y. Billarand, F. Ewig, F. Funke, A. Hidaka, R. Gauntt, R. Cripps, B. Herrero, J. Royen, "ISP 41 Containment Iodine Computer Code Exercise Based on a Radioiodine Test Facility (RTF) Experiment," NEA/CSNI Report, R(2000)6/ Volume 1 (2000).
2. J. Ball, G. Glowa, J. Wren, F. Ewig, S.Dickenson, Y. Billarand, L. Cantrel, A. Rydl and J. Royen, "International Standard Problem (ISP) No. 41 Follow Up Exercise: Containment Iodine Computer Code Exercise: Parametric Studies," Atomic Energy of Canada Ltd. Report, AECL-12124. 2001.
3. J.C. Wren, G. Glowa and J.M. Ball, "A Simplified Iodine Chemistry and Transportation Model: Model Description and Some Validation Calculations", in Proceedings of OECD Workshop on Iodine Aspects of Severe Accident Management Vantaa, Finland, May 18-20, 1999, NEA/CSNI/R(99)7, pp. 327 - 341, Committee on the Safety of Nuclear Installations/Organization for Economic Cooperation and Development (1999).
4. J.C. Wren, G.A. Glowa and J.M. Ball, "Summary of PHEBUS RTF Programme", in Proceedings of the 4th PHEBUS Seminar, Marseille, France, March 20-21, (2000).

APPENDIX A: Further Code Improvements and Sensitivity Studies:

A1: LIRIC 3.3 and IMOD 2.1 Calculations (J.M. Ball)

In several reported calculations of Phebus RTF experiments using IMOD 2.0 [3], it was observed that IMOD 2.0 overestimated the fraction of iodine in the form of I_2 when the pH was less than 6, temperatures were 90 ºC, and where boric acid was present. Blind calculations performed for this exercise established that this phenomenom was not just limited to RTF experiments, nor was it limited to IMOD 2.0 predictions. LIRIC 3.3 and IMOD 2.0 calculations of CAIMAN facility experiments also over-predicted I_2 concentrations at pH 5 and 90 and 110º C. It appears as if both LIRIC and IMOD require modifications to decrease the overall rate of production of I_2 under these conditions.

Consequently, two trial approaches were taken to modify the codes. The first approach, shown in the main text, was to use large values for the rate constants for adsorption and desorption of I_2 on immersed stainless steel, while maintaining the same overall rate constant and the quantity of I_2 adsorbed on the surface. The change had the desired effect of increasing the overall rate of conversion of I_2 to I^-, and reducing the concentration of I_2 in the aqueous phase. It resulted in very good agreement between calculated and experimental results. However, the magnitude of the rate constants required for each of the tests were inconsistent with what is understood about adsorption/desorption phenomena.

A second set of optimized calculations performed with both LIRIC 3.3 and IMOD 2.1 are reported here. These calculations were performed by activating a sub-model within the codes [3,4], which describes the interaction of aqueous phase I_2 with organic impurities. The rapid adsorption/desorption of I_2 on stainless steel surfaces used in the first set of optimized calculations were not employed in these calculations. Use of the impurity sub-model provides a more satisfactory method for changing the aqueous phase I_2 concentration, because:

1) It allows for the use of consistent rate constants for all of the experiments (both adsorption/desorption and impurity rate constants)
2) It is based on a wide range of literature observations that I_2 forms a variety of co-ordination and charge transfer complexes with organic compounds in the aqueous phase, and that formation of these species is an equilibrium process. Many of these species are highly water soluble, and are therefore assumed to be non-volatile. Charge transfer complexes between I_2 and organic compounds have been observed for various ketones, benzene and substituted aromatic complexes. Many of the organic compounds observed in RTF experiments (including Phebus RTF1, using ripolin paint) could be capable of forming such complexes.

None of the default rate constants for the radiolysis of iodine species or organic compounds was changed in IMOD 2.1 and LIRIC 3.3 for the second optimization. The models and parameters for dissolution of solvents from containment paints were also kept the same. The only change in the codes, aside from those in adsorption/desorption rate constants listed in Table A1, was that the sub-model previously reported in Reference 3 and 4 was activated. This sub-model was modified from that reported in

the references, to incorporate a temperature dependence. The reactions in the impurity sub-model are:

Impurity + I_2 = I_2IMP A1)
Impurity → decomposition products A2)

Reaction A1 is an equilibrium. For the optimization exercises, the rate constant k_{A1} was described as :

k_{A1} (dm3·mol^{-1}·s^{-1}) = 1.2×10^6 × exp (3406 ×(1/298 –1/T)) with k_{-A1} = 6 s^{-1}. A3)

The expression used for Reaction A2 was
k_{A2} (s^{-1}) = 6×10^{-11} × exp (16256 ×(1/298 –1/T)) A4)

The concentration of impurity assumed for each experiment was 1 × 10^{-4} mol·dm^{-3}.

Table A1 lists the adsorption/desorption rate constant used in the calculations. Note that deviations from the recommended rate constants were used for desorption from gas phase painted surfaces (reasons are provided in Section (4.4) main text). Slightly higher desorption rate constants were also required for aqueous painted surfaces. Note also that, although the current calculations used an adsorption rate constant for I_2 on stainless steel surfaces that is larger than the recommended value of 2 × 10^{-6} m·s^{-1}, they also incorporate a significant desorption rate constant. The overall rate constant for adsorption, resulting from the use of the adsorption/desorption rate constants given in Table A1 is similar to that generated by use of an adsorption rate constant of 2 × 10^{-6} m·s^{-1}, and a desorption rate constant of 0.

Table A1: Rate Constants Used for IMOD 2.1 Optimized Calculations.

	Pheb RTF1 (recommended)	CAIMAN 9702 (recommended)	CAIMAN 0101(recommended)
$K_{ads}I_2$aqss (m·s^{-1})	7 10^{-5} (k_{ads} <2e-6 overall)	7 10^{-5} (<2e-6 overall)	7 10^{-5} (<2e-6 overall)
$K_{des}I_2$aqss (s^{-1})	5 10^{-5} (k_{ads} <2e-6 overall)	2 10^{-3} (k_{ads} <2e-6 overall)	2 10^{-3} (k_{ads} <2e-6 overall)
$K_{ads}I_2$aqp (m·s^{-1})	4 10^{-4} (8 10^{-4})	4 10^{-4} (8 10^{-4})	0
$K_{des}I_2$aqp (s^{-1})	5 10^{-6} (5 10^{-7})	5 10^{-6} (5 10^{-7})	0
$K_{ads}I^-$aqp (m·s^{-1})	2 10^{-8} (4 10^{-8})	2 10^{-8} (4 10^{-8})	0
$K_{des}I^-$aqp (s^{-1})	1 10^{-6} (1 10^{-6})	1 10^{-6} (1 10^{-6})	0
$K_{ads}I_2$gss (m·s^{-1})	2 10^{-4} (1 10^{-4})	2 10^{-4} (1 10^{-4})	2 10^{-4} (1 10^{-4})
$K_{des}I_2$gss (s^{-1})	5 10^{-5} (5 10^{-5})	5 10^{-5} (5 10^{-5})	5 10^{-5} (5 10^{-5})
$K_{ads}I_2$gp (m·s^{-1})	2 10^{-3} (4.5 10^{-3})	2 10^{-3} (4.5 10^{-3})	2 10^{-3} (4.5 10^{-3})
$K_{des}I_2$gp (s^{-1})	1 10^{-5} (0)	2 10^{-5} (0)	2 10^{-5} (0)
$K_{L\text{-}G}$ I_2 (m·s^{-1})	5.5 10^{-5} (5.5 10^{-5})	7.5 10^{-6} (1 10^{-5})	7.5 10^{-6} (1 10^{-5})
$K_{L\text{-}G}$ CH_3I(m·s^{-1})	8.3 10^{-5} (8.3 10^{-5})	1.1 10^{-5} (1.5 10^{-5})	1.1 10^{-5} (1.5 10^{-5})

Figures A1 – A9 show selected IMOD 2.1 calculation results for Phebus RTF1, CAIMAN 0101, and CAIMAN 9702 using the first optimization method, and the second. Note that results for RTF Phase 10 Test 1 are not shown. Neither of the optimization methods used have any effect on predictions for RTF P10T1. There were

no aqueous phase stainless steel surfaces in this experiment, therefore I_2 adsorption/desorption on the surfaces could not be invoked. It was also found that use of the impurity model does not affect the aqueous phase I_2 concentrations predicted for P10T1. In the higher temperatures and lower pH values of the other experiments, the use of the impurity model results in more I2 being retained in the aqueous phase because it is "tied-up" as an impurity complex. At the lower temperature (60ºC) and higher pH values employed for P10T1, the aqueous phase I_2 behaviour concentration is dominated primarily by the rate of production of I_2 from I^- to $\cdot OH$, and rapid conversion of I_2 to I^- by hydrolysis, reaction with H_2O_2, and reaction with O_2^-. Using the rate constants reported in A3 and A4, the overall rate of formation of an I_2 impurity complex is much to slow to compete with the conversion of I_2 to I^- by these aforementioned processes.

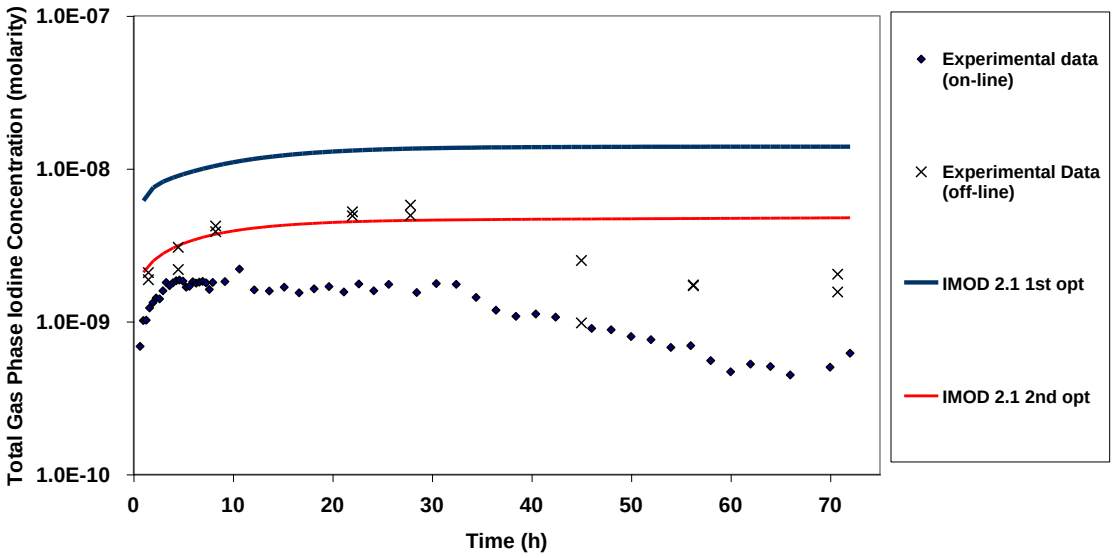

Figure A1: Total Gas Phase Iodine Concentration for Phebus RTF1 as Compared to IMOD 2.1 Code Calculations (1st and 2nd optimization).

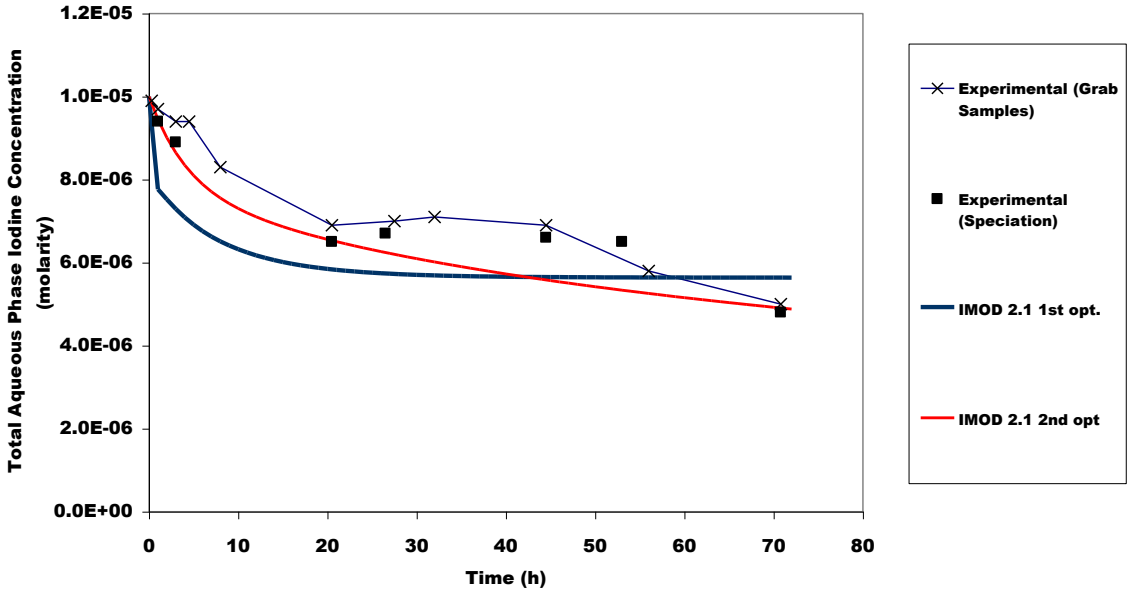

Figure A2: Total Aqueous Phase Iodine Concentration for Phebus RTF1 as Compared to IMOD 2.1 Code Calculations (1st and 2nd optimization).

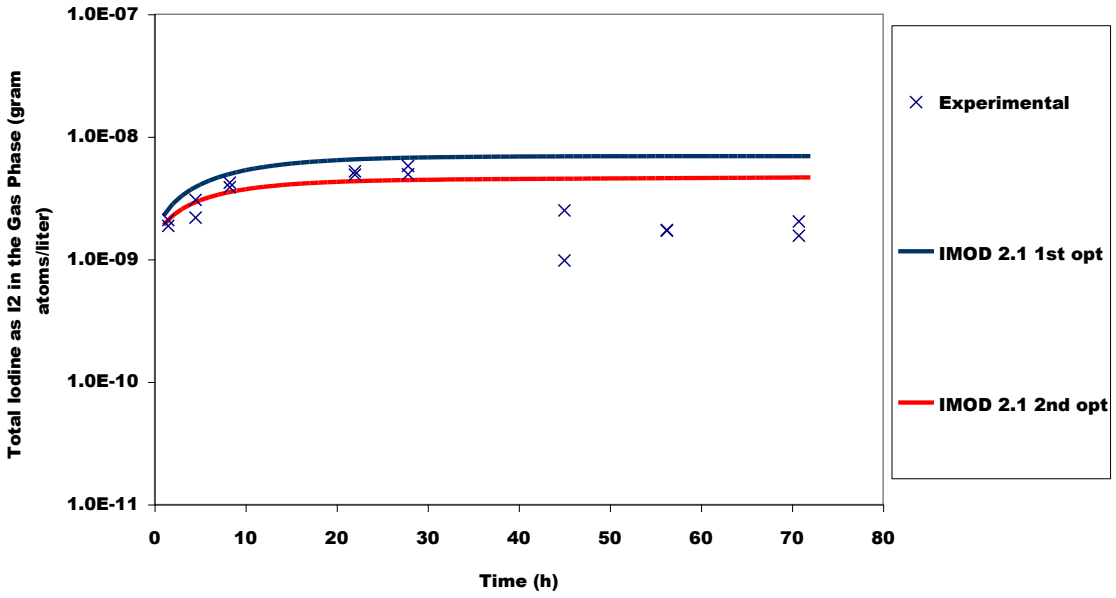

Figure A3: I_2 in the Gas Phase for Phebus RTF1 as Compared to IMOD 2.1 Code Caculations (1st and 2nd optimization).

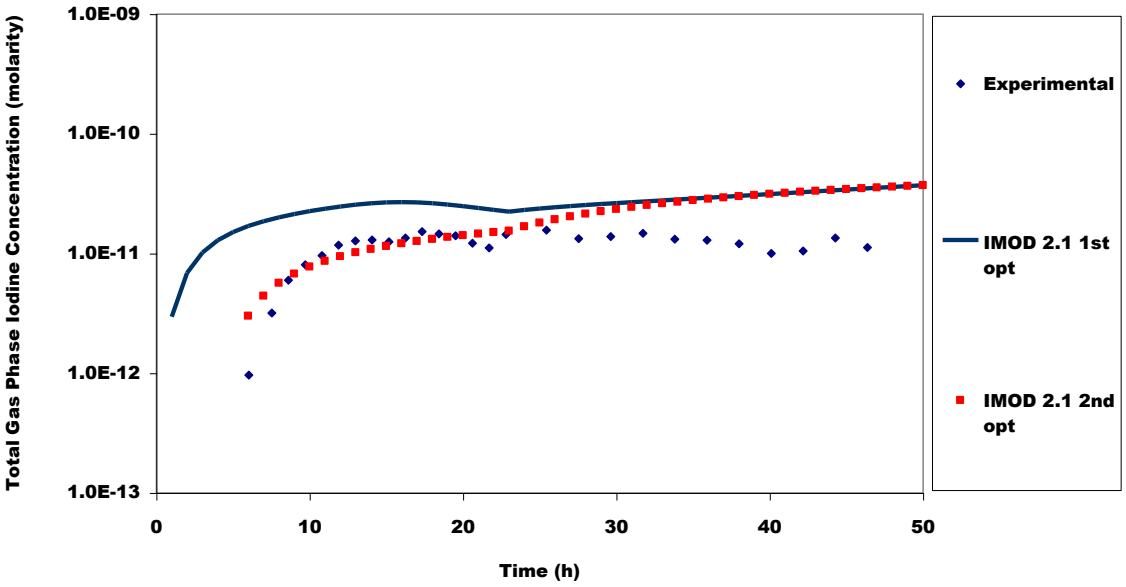

Figure A4: Total Gas Phase Iodine Concentration for CAIMAN 9702 as Compared to IMOD 2.1 Code Calculations (1st and 2nd optimization).

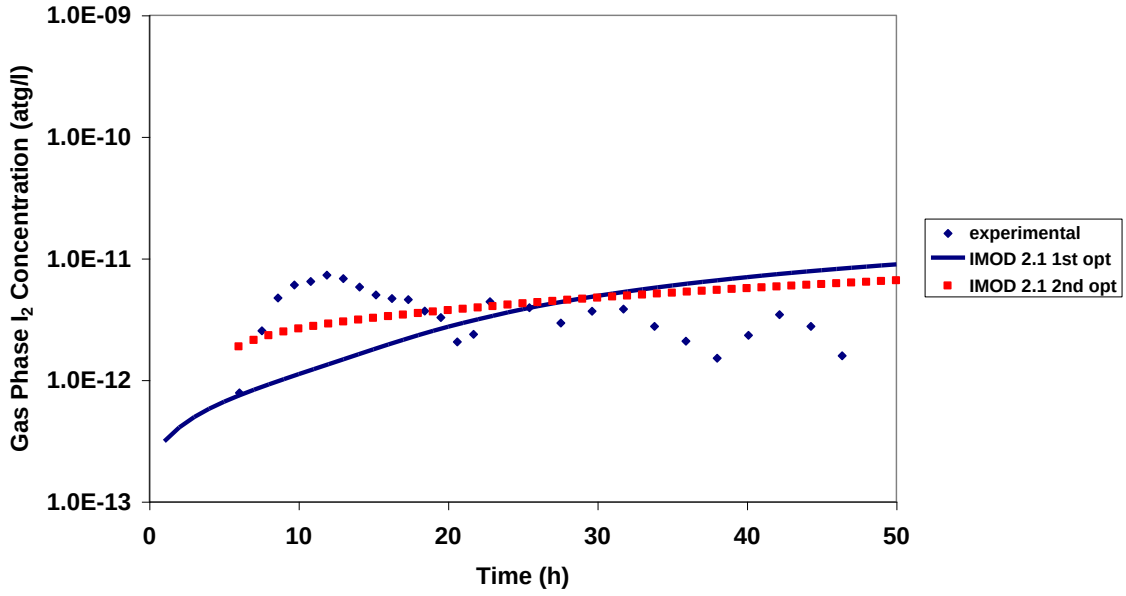

Figure A5: I_2 in the Gas Phase for CAIMAN 9702 as Compared to IMOD 2.1 Code Caculations (1st and 2nd optimization).

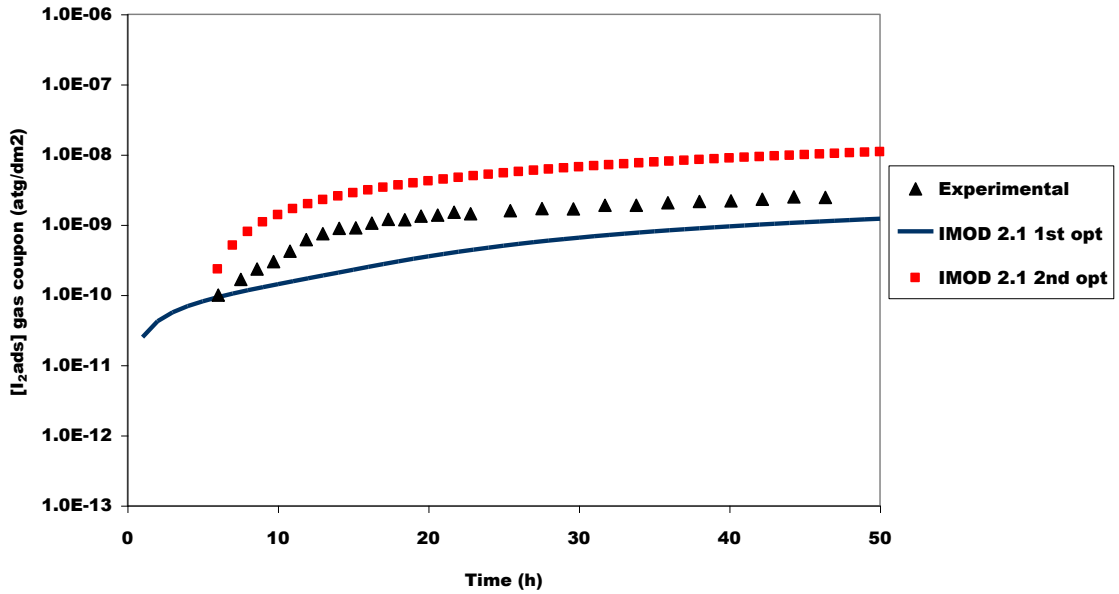

Figure A6: Total I_2 Adsorbed on Painted Coupon for CAIMAN 9702 as Compared to IMOD 2.1 Code Calculations (1st and 2nd optimization).

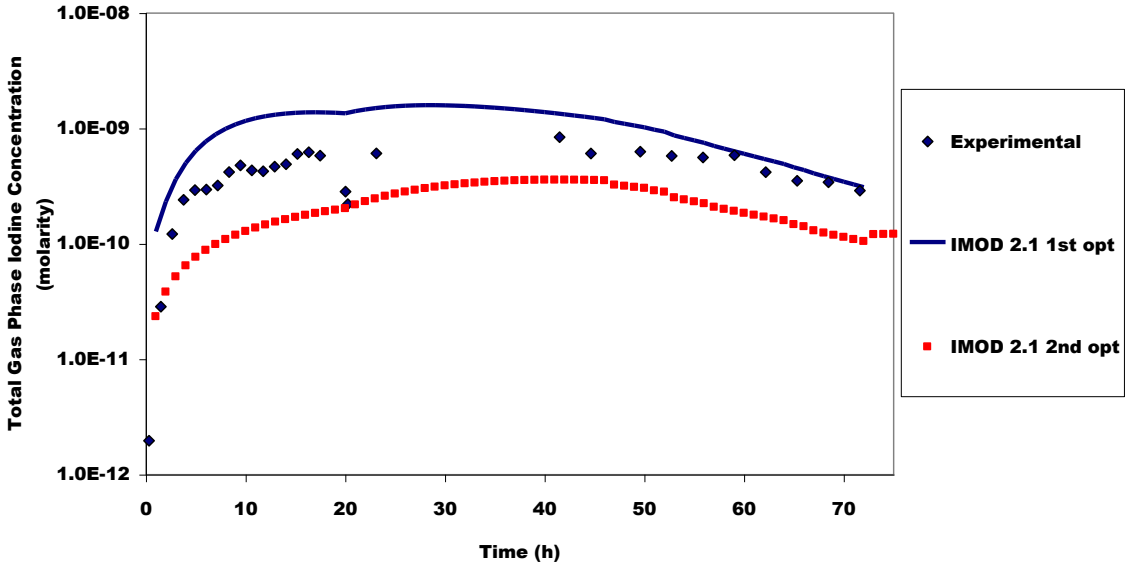

Figure A7: Total Gas Phase Iodine Concentration for CAIMAN 0101 as Compared to IMOD 2.1 Code Calculations (1st and 2nd optimization).

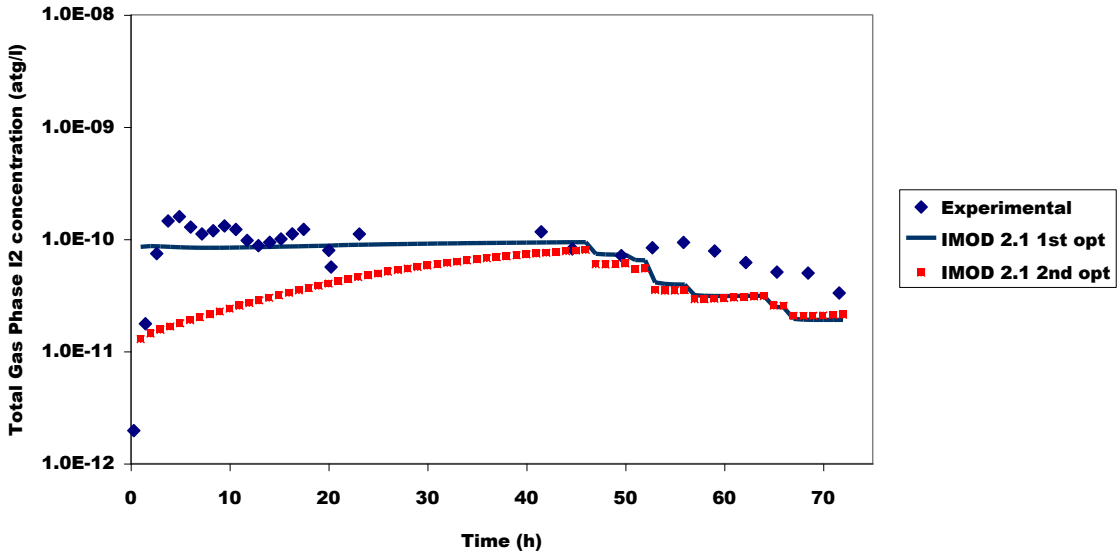

Figure A8: I_2 in the Gas Phase for CAIMAN 0101 as Compared to IMOD 2.1 Code Caculations (1st and 2nd optimization).

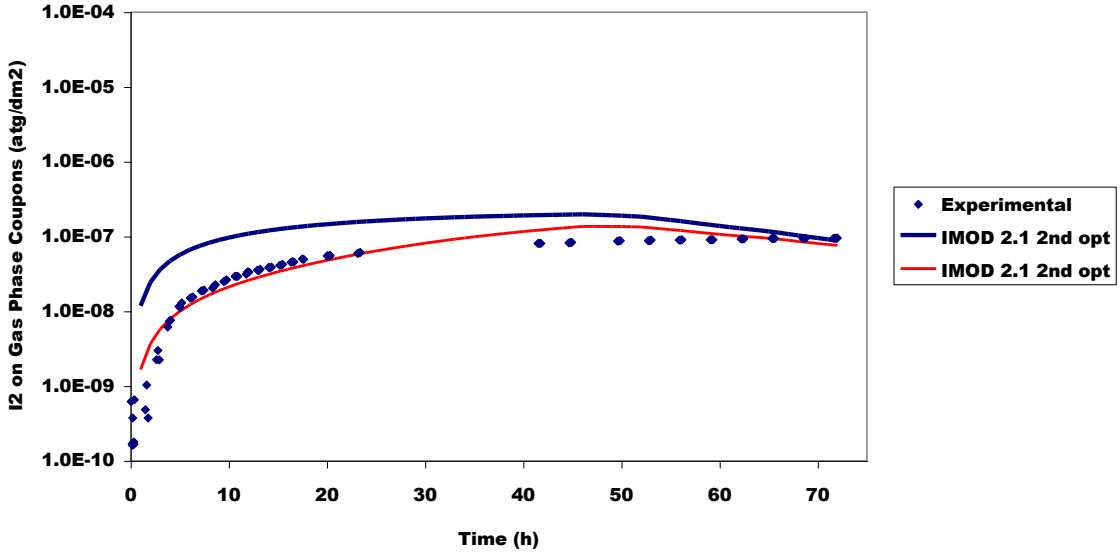

Figure A9: Total I_2 Adsorbed on Painted Coupon for CAIMAN 0101 as Compared to IMOD 2.1 Code Calculations (1st and 2nd optimization).

The results obtained in the 2nd optimization attempt are qualitatively similar to those in the first, and in general, agreement between experimental and calculated results are as good, or better using the 2nd optimization scheme. LIRIC 3.3 calculations using the same impurity model also give results that are in good agreement with experimental data, and qualitatively similar to those obtained in the first LIRIC 3.3 optimization exercise. These results are not shown here in the interests of brevity.

In conclusion, good agreement between experimental data and IMOD 2.1 and LIRIC 3.3 code calculations can be obtained using a consistent set of adsorption/desorption rate constants and activating a sub-model in the codes to account for complex formation between I_2 and organic impurities.

A2: IODE 5.1 (Laurent Cantrell and Carole Marchand)

Following the analysis of the ISP41 follow-up phase 2 results, some additional calculations were performed by IRSN concerning:

- the destruction of I_2 by radiolytic process (reaction $I_2 \rightarrow I^-$) in the liquid phase,
- the adsorption rate constant of I_2 on the stainless steel in the aqueous phase (only for PHEBUS/RTF1 experiment, linked to the 30% of iodine missing in the mass balance),
- the relative importance of the different ICH_3 production models (homogeneous in the liquid phase, heterogeneous in the gas phase).

Destruction of I_2 by radiolytic process :

After the analysis of the calculations, it was shown that the $[I_2]$ in the liquid phase was always underestimated (for the recommended mass transfer coefficient).This can be explained by a too high destruction process of I_2.
It is the reason why the activation energy of the reaction $I_2 \rightarrow I^-$ has been modified. The original activation energy value is 55 kJ/mol corresponding to the upper limit with regards to the uncertainty range. Now, if the mean value is retained, 40 kJ/mol, the results are in much better agreement than the previous ones for the three tests as shown by the following figures.
This modification has an influence on the gas molecular iodine and the gas organic iodide concentrations because the formation processes involve $[I_2]_{aq}$.

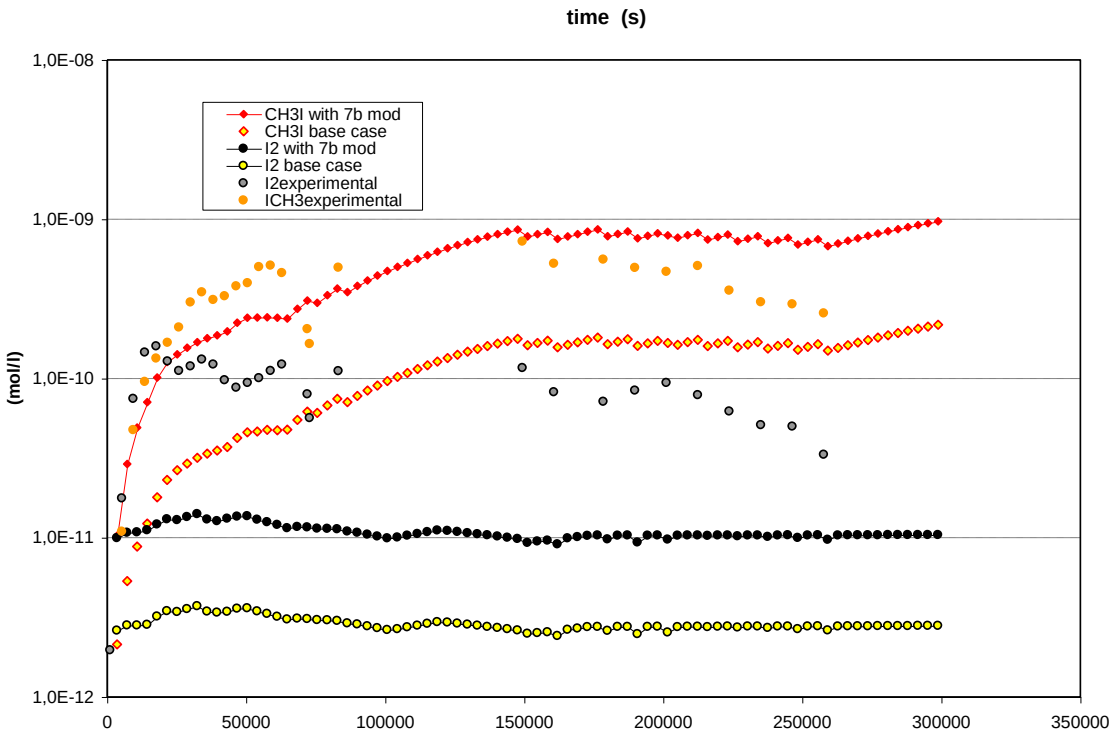

Figure A11: CAIMAN 2001/01, concentrations in the gas phase:

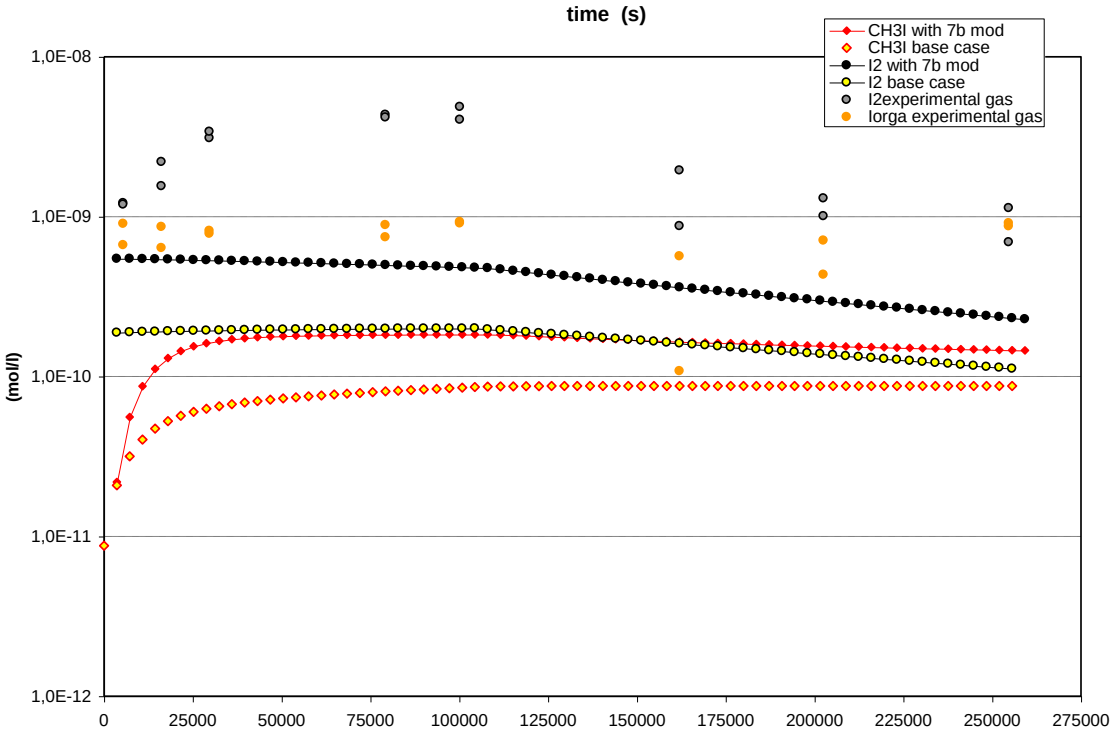

Figure A12: PHEBUS/RTF1, concentrations in the gas phase :

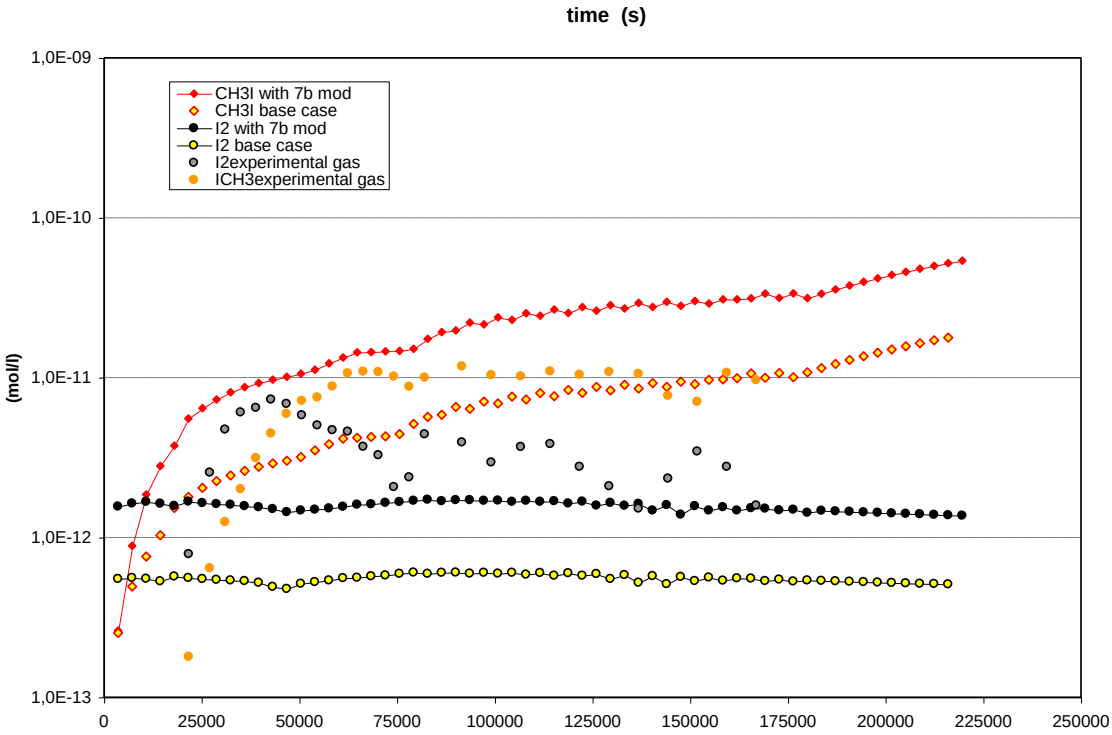

Figure A13: CAIMAN 97/02, concentrations in the gas phase:

Adsorption rate constant of I_2 on the stainless steel in the aqueous phase :

The PHEBUS/RTF1 mass balance is not closed. About 30% of the iodine is missing and this iodine is probably trapped onto the surfaces. With IODE 5.1 code, total iodine in the aqueous phase is overestimated using usual value for the steel adsorption rate constant. Thus it cannot take into account a higher adsorption due to the presence of surface defects. The rate constant has to be reviewed if there is more corrosion and adsorption in this test than in the others.

This point may explain the underestimation of iodine on the surfaces and especially on the immersed stainless steel one in PHEBUS/RTF1. The new calculations are made with a higher adsorption rate constant. But the point is to check that a change of adsorption rate constant of I_2 on the stainless steel in the aqueous phase can explain the difference between total experimental iodine and calculated one in the sump without changing any of the iodine concentrations in the gas phase. If it is the case, the result of total iodine in the liquid phase will be totally linked to the chosen k_{ads} without any significant effect on the other concentrations except on the iodine adsorbed on the immersed stainless steel.

The new calculation shows that an increase of the rate constant ($1.5.10^{-4}$ m/s instead of 2.10^{-6} m/s) leads to a good agreement in the aqueous phase and doesn't change so much the concentrations in the gas phase. So the conclusion is for IODE 5.1 calculations, in the PHEBUS/RTF 1 conditions, is that repartition of iodine in the aqueous phase is not an important parameter to validate the code because it directly depends on the chosen adsorption rate constant of I_2 on stainless steel.

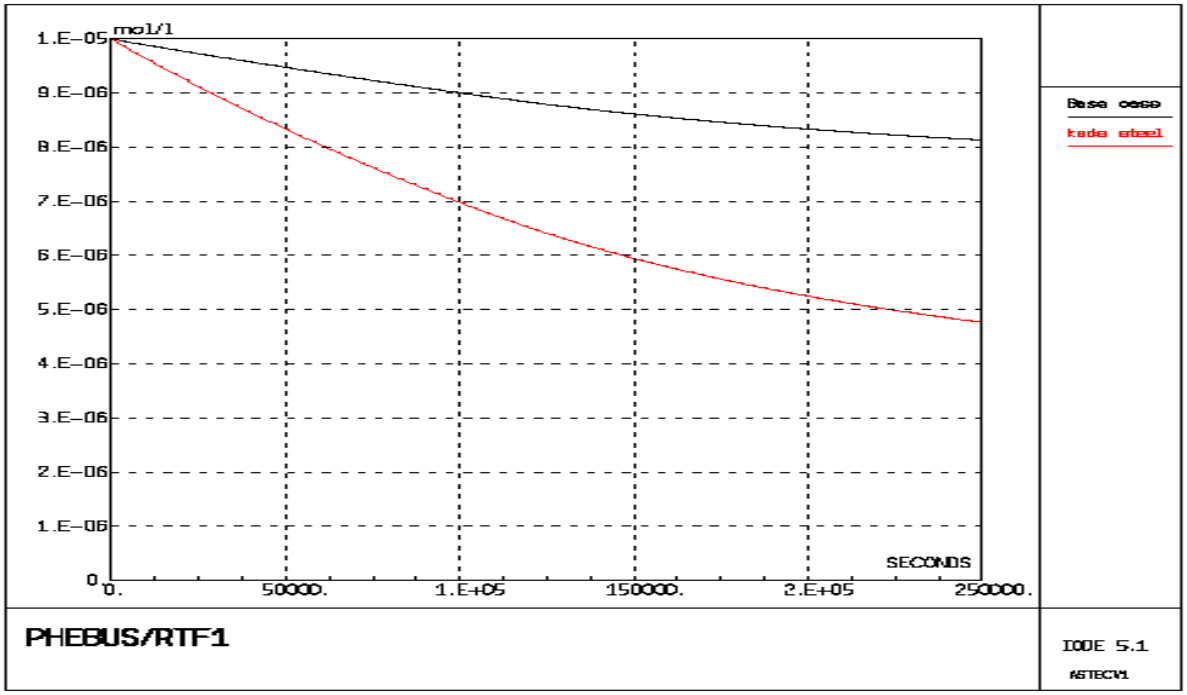

Figure A14: Phebus RTF1 Aqueous Concentrations

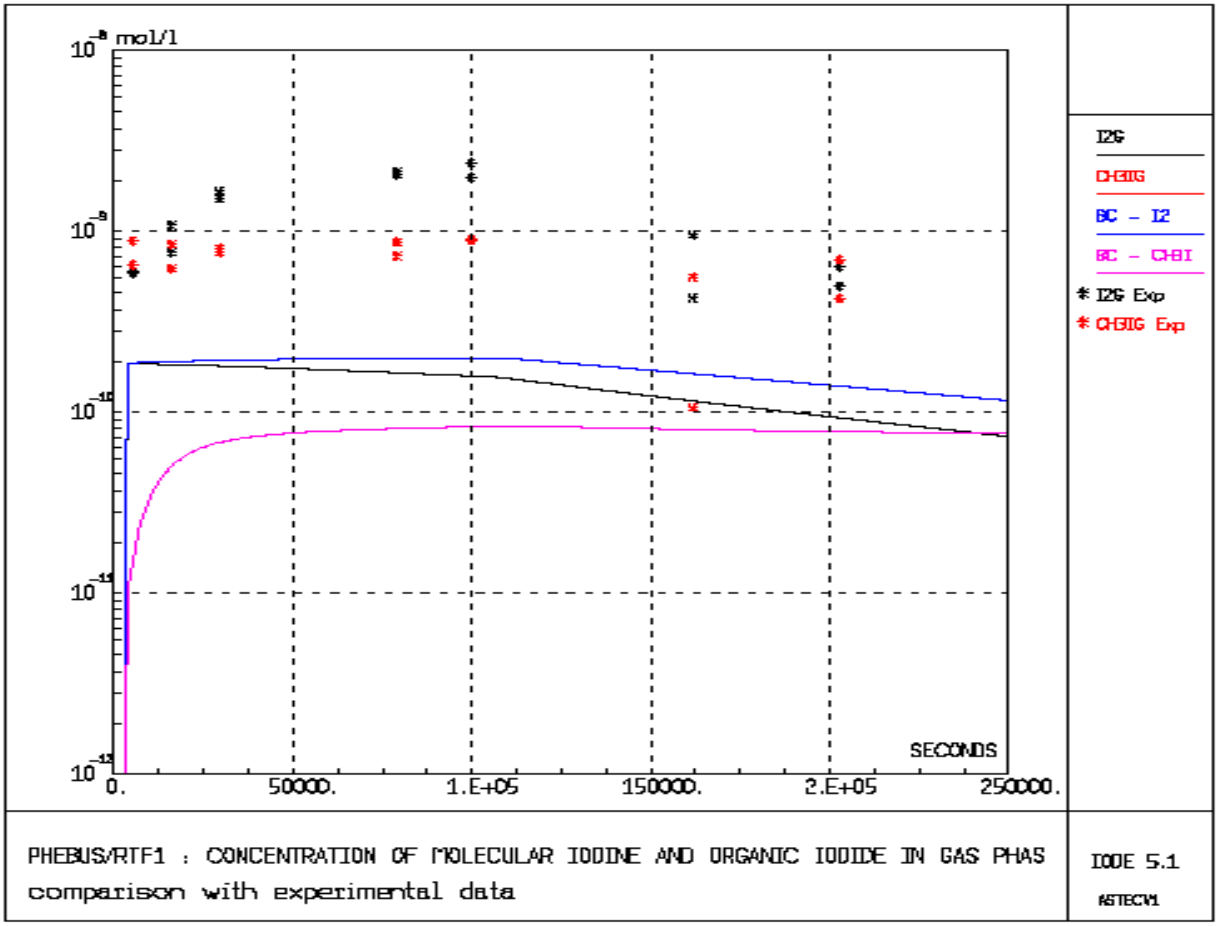

Figure A15: Phebus RTF1 Gas Concentrations

Relative importance of the different ICH_3 production models:

The relative importance of the ICH_3 production models was examined for CAIMAN 97/02 and PHEBUS/RTF1 tests. For CAIMAN 97/02, the principal source of ICH_3 comes from the sump because the dose rate in the gas phase is relatively low compared to the dose rate in the sump. For PHEBUS/RTF1, the dose rate is about the same in the gas phase and in the liquid phase so the formation of ICH_3 in the gas is enhanced. The following curves show the different contributions of the models. At the beginning of the test, the sump is the source of ICH_3 and after few hours, the main source is the gas phase. The adsorbed iodine in the gas painted coupons grows up with time so the formation of ICH_3 from the gas phase increases too.

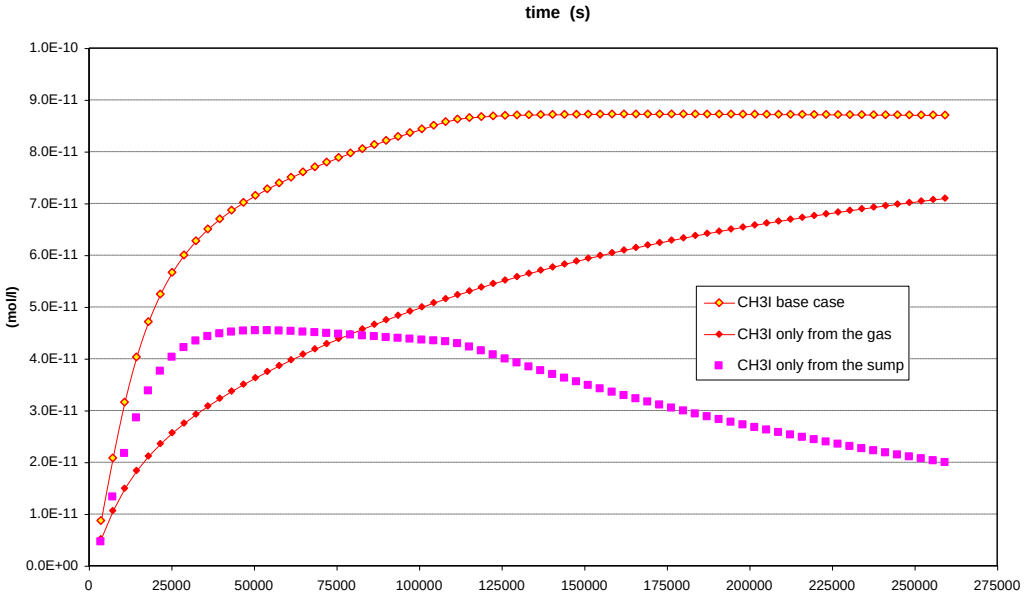

Figure A16: PHEBUS/RTF1, [ICH_3] in the gas phase:

A3: GRS COCOSYS/AIM-F1 (Gunter Weber)

Abstract

Subject of the International Standard Problem ISP-41 Follow Up/Phase 2 is the iodine behaviour in the containment during a severe LWR accident. Predictions of iodine behaviour codes are compared to four experiments performed in approx. 300 l vessels. GRS participates with COCOSYS/AIM-F1. After blind and open calculations on two French CAIMAN tests and two Canadian RTF tests the so-called final optimized calculations were performed. In these the results of the Final ISP-41 Meeting in June 2003 were considered.

For the final optimized COCOSYS-calculations four modifications compared to the open calculations were made. Among other things the pH-dependence of the radiolytic oxidation of I^- and IO_3^- in the water phase was decreased. Also some recommended adsorption/desorption rate constants were modified within their uncertainty margins. These modifications are based on the inputs for the codes LIRIC and IMOD.
The final optimized calculations show a significantly better agreement with the measurement than the open and blind calculations. In a rating following criteria established by the ISP participants the blind COCOSYS results got 5 of 16 possible points and the final optimized results 10 of 16 points.

As consequence from the ISP three improvements on the iodine modelling will be realized directly in the new version AIM-F2. Another improvement which concerns a stronger coupling between thermal hydraulic and iodine behaviour is planned. Finally it is proposed to perform an uncertainty and sensitivity analysis on two selected iodine experiments.

A4: Brief summary of last changes to IMPAIR Code /PSI to simulate tests Caiman 2001 and RTF Phase 10 (ISP41F) (Robin Cripps)

Final calculations were performed using the existing models in IMPAIR code with corrections to provide a better simulation of the Caiman 2001/01 and RTF Phase 10 test results.

Correction to radiolytic I_2 formation model:

$$d([I_2])/dt = k_f \times [I^-] \times [H^+]^n \times \text{dose rate (kGy/h)} \quad k_r \times [I_2] \times 2.0 \times \text{dose rate}$$

Test:	RTF Phase 10	Caiman 2001/01
Forward rate constant k_f	2.0×10^{-3}	3.0×10^{-5}
Reverse rate constant k_f	1.0×10^{-4}	2.0×10^{-6}
Exponent, n	0.35	0.35

Based on several calculations, the exponent, n, was set to 0.35, since a degree of pH sensitivity was necessary to simulate both tests Caiman 2001/01 and RTF Phase 10 Test 1 with a pH range from 5 to 10. Lower values of n with different values of k_f would have obtained a correlation with measured data from a single test in which the pH did not change very much. But in the RTF Phase 10 Test, lower n values are clearly inadequate. To obtain a satisfactory correlation for both tests, different values of rate constants had to be used. It is hoped that future work at PSI will provide a new empirical model based on findings from a mechanistic code, such as PSIodine or LIRIC to predict iodide oxidation under a wide range of experimental conditions (pH, concentration etc.). The above constants appear also dependent on competition for iodide from other models, for example, the deposition rate for iodide deposition on immersed paint surfaces.

Organoiodine modelling

The model to predict the formation of low volatile organic iodides has been removed due to lack of data. Until a better model can be designed, organic iodide formation, destruction and mass transfer will be (conservatively) represented by methyl iodide. The formation is predicted by two models:

1. After I_2 deposited on paint in the gas phase, methyl iodide is formed by thermal and radiolytic reactions according to the "Funke" model.

2. Dissolved I_2 and HOI react with CH_3 radicals. The concentration of the latter is given by the code user (typically $1.0\ 10^{-7}$). To reduce the change of $[CH_3\cdot]$, the partitioning of these radicals between the phases has been disabled. By comparison with measured concentrations, fitted rate constants are derived from the RTF Phase 10 test:

Homogeneous reactions	Rate constant

in water	(prev.optimised)
$CH_3\cdot + I_2$	6.0×10^{1} Ea = 0
$CH_3\cdot + HOI$	5.0×10^{1} Ea = 0
$[CH_3]$ RTF Phase 10	1×10^{-7} mol.dm^{-3}
$[CH_3]$ Caiman 2001/01	5×10^{-7} mol.dm^{-3}

Again, although the same rate constants was finally used for both tests, the initial $[CH_3]$ has to be provided by the user. In addition, this radical concentration is also dependent on the RI formation rate from the Funke model in the gas phase., since RI partitions into the water phase and undergoes hydrolysis to iodide and CH_3 in the IMPAIR code. Good correlations were obtained for the two tests, but therate constants for the RI formation (Funke) model in the gas phase had to be increased 10X. In the test RTF Phase 10 Test 1, the [MeI] concentration in the gas phase decreases as the pH increases back to pH10. The current models have predicted little change of concentration, although the initial pH reduction for pH10 to pH7 was partly predicted. These results have shown the necessity for a revision of the organic iodide modelling.

Deposition and Revolatilisation or dissolution rates

The tables below show the changes made to the constants for the IMPAIR code. Last changes are highlighted.

Adsorption Rate Constants Used in Phase 10 Test 1**.**

	Recommended [a]	IODE 5.1	COCOSYS	LIRIC	IMOD 2.1	CIEMAT BE	IMPAIR	NRIR
$K_{ads}I_2aq$ (m·s^{-1})	$8\ 10^{-4}$	$2\ 10^{-4}$	$2\ 10^{-4}$	$4\ 10^{-4}$	$6\ 10^{-4}$	$8\ 10^{-4}$	$4\ 10^{-4}$	$4\ 10^{-4}$
$K_{des}I_2aq$ (s^{-1})	$5\ 10^{-7}$	$5\ 10^{-7}$	$2\ 10^{-6}$	$2.5\ 10^{-7}$	$2.5\ 10^{-7}$	0	$1\ 10^{-6}$	$2.5\ 10^{-7}$
$K_{ads}I^-aq$ (m·s^{-1})	$4\ 10^{-8}$	0	$4\ 10^{-8}$	$2\ 10^{-8}$	$2\ 10^{-8}$	0	$2.0\ 10^{-8}$	$2\ 10^{-8}$
$K_{des}I^-aq$ (s^{-1})	$5\ 10^{-7}$	0	$4\ 10^{-5}$	$2\ 10^{-6}$	$1\ 10^{-6}$	0	$2.0\ 10^{-6}$	$2\ 10^{-6}$
$K_{ads}I_2gp$ (m·s^{-1})	$6\ 10^{-4}$	$6\ 10^{-4}$	$6\ 10^{-4}$	$6\ 10^{-4}$	$6\ 10^{-4}$	$6\ 10^{-4}$	$4\ 10^{-4}$	$6\ 10^{-4}$
$K_{des}I_2gp$ (s^{-1})	0	0	0	0	0	0	0	0
$K_{L\text{-}G}\ I_2$ (m·s^{-1})							$7.15\ 10^{-5}$	
$K_{L\text{-}G}\ CH_3I$ (m·s^{-1})							$7.15\ 10^{-5}$	

Adsorption Rate Constants Used in CAIMAN 2001/01

	Recommended [a]	IODE 5.1	COCOSYS	LIRIC	IMOD 2.1	CIEMAT BE	IMPAIR	NRIR
$K_{ads}I_2aqss$ (m·s^{-1})	negligible	1.10^{-8}	?	5.10^{-4}	2.10^{-3}	0	n/a	?
$K_{des}I_2aqss$ (s^{-1})	negligible	0	?	4.10^{-1}	4.10^{-1}	0	n/a	?
$I_2 \rightarrow I^-$ (ss ads aq) (m·s^{-1})	-	-	$7.9.10^{-7}$	?	?	-	$3.2\ 10^{-6}$	-
$K_{ads}I^-aqss$ (m·s^{-1})	-	-	?	0	0	-	0	-
$K_{des}I^-aqss$ (s^{-1})	-	-	?	0	0	-	0	-
$K_{ads}I_2gp$ (m·s^{-1})	4.10^{-3}	2.10^{-3}	2.10^{-3}	$4.5.10^{-3}$	$4.5.10^{-3}$	2.10^{-3}	$2.2\ 10^{-3}$	$1.3.10^{-3}$
$K_{des}I_2gp$ (s^{-1})	-	0	1.10^{-6}	2.10^{-5}	1.10^{-4}	0	1.10^{-4}	0
$K_{ads}I_2gss$ (m·s^{-1})	negligible	1.10^{-5}	1.10^{-4}	2.10^{-4}	2.10^{-4}	0	$2\ 10^{-4}$	?
$K_{des}I_2gss$ (s^{-1})	negligible	1.10^{-6}	$1.06.10^{-4}$	$7.3.10^{-4}$	$3.7.10^{-4}$	0	$2\ 10^{-6}$	?
$K_{L\text{-}G}\ I_2$ (m·s^{-1})	1.10^{-5}	1.10^{-5}	$8.3.10^{-6}$	$7.2.10^{-6}$	$7.2.10^{-6}$	$1.8.10^{-5}$	$1\ 10^{-5}$	5.10^{-5}
$K_{L\text{-}G}\ ICH_3$ (m·s^{-1})	1.510^{-5}	1.510^{-5}	?	?	?	$1.65.10^{-5}$	$1.5.10^{-5}$	5.10^{-5}

R. Cripps /28. 07. 2003

APPENDIX B: UNCERTAINTIES IN CAIMAN AND RTF MEASUREMENTS

Concentration uncertainties in CAIMAN facility

Introduction

The concentrations in CAIMAN tests are measured by gamma spectrometry associated with a theoretical modelling of the measurement efficiency. The code used for this modelling is MERCURE 5.
The uncertainties of these concentrations are linked to:

- The uncertainty of the initial iodine concentration introduced in the vessel (activity of label iodine and total mass of iodine),
- The uncertainty of the activity measurements made by spectrogammametry (detector and modelling uncertainties).

Mass uncertainty

There are two components of this uncertainty :

- The quantity of iodine introduced in the solution as CsI
- The ^{131}I source.

Both are presented here after.

Mass of iodine

The iodine is introduced as CsI in the vessel. The specific injector used for it is not very precise because it was studied especially for high pressure injections.
So ICP-MS analysis is made after the injection to determine the Cs^+ concentration and then to know the initial iodine concentration introduced in the vessel.
Its uncertainty is 5% with a confidence interval of 2σ.
This uncertainty is also dependent on a representative sample of the solution. So, the sample is taken half an hour after the introduction of iodine in the vessel to allow the homogenisation of the aqueous phase.

^{131}I source

To label the CsI, a standard liquid source is used. This source is supplied with a calibration certificate which gives its activity. Measured activities are corrected radioactive decrease. The activity of the dissolved tracer is checked by samples and gamma-counting (outside the facility). The uncertainty of this counting is 0.2% with confidence interval of 1σ.

So the uncertainty of the activity/concentration correlation coefficient is therefore 2.5% with confidence interval of 1σ.

Spectrometry measurement uncertainty

Caiman test loop surface activities or activity concentrations are determined by conventional gamma spectrometry associated with theoretical efficiency calculations using a straight line attenuation code – MERCURE 5.
The uncertainties of these measurements are due to the uncertainty of the efficiency of the detector itself and the uncertainty of the geometry efficiency (transfer factor FT).

Efficiency of the detector

The efficiency of the detector is a characteristic value of the detector itself. It is determined experimentally, using standard sources. Usually, we apply a conservative uncertainty margin of 10% for this factor with a confidence interval of 2σ.

Transfer factor – geometry

This factor is used to correlate the activity of the source and the activity seen by the detector. It depends on :

- The solid angle,
- The different photon absorptions occurring along photon paths.

The transfer factor is computed by the code MERCURE 5.
This transfer factor is independent of the detector and can be used for different detectors.
A conservative uncertainty margin of 10% is applied for this factor with a confidence interval of 2σ.

Total uncertainty

The absolute overall uncertainty associated with deposited iodine masses is 7.2% with a confidence interval of 1σ or 14.4% with a confidence interval of 2σ. It is calculated with the following formula:

$$\frac{\sigma M}{M}=\sqrt{\left(\frac{\sigma A}{A}\right)^2+\left(\frac{\sigma AI_{131}}{AI_{131}}\right)^2+\left(\frac{\sigma C_I}{C_I}\right)^2}$$

But we can consider the uncertainty of the absolute detector efficiency is reproducible and then the relative overall uncertainty is 6% with a confidence interval of 2σ.
This uncertainty concerns only the total mass on the may-pack or on the surfaces but not the calculated gas phase concentrations which is $\Delta[M]/\Delta V$.

Uncertainty linked to the efficiency of the May-pack filter

This uncertainty is added to the total uncertainty. The May-pack filter are made as following :

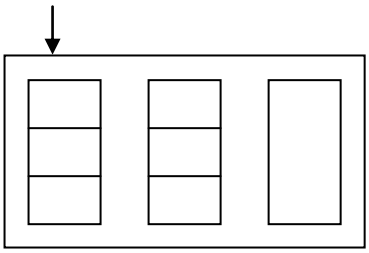

The first compartment is composed on 3 knitmesh pots (Ag as I_2 trap), the second one, on 3 charcoal pots and the third one is only one charcoal pot to be sure that all iodine is trapped in the two previous compartments of the May-pack.
The modeling of the transfer factor depends on the distribution of iodine in the May-pack. This distribution was supposed to be the same for all the tests and is shown here after for the two first compartments and is equal to 0% for the last one:

75%
25%
0%

In some experiments, the efficiency of the filters was not as good as envisaged and after the last control of the May-pack some other distributions have to be considered. The impact on iodine concentration could be relatively important. One example has been chosen : I_2 in the gas phase collected on the knitmesh filter for CAIMAN 2001/01 with a real (70/20/10) distribution compared to the imposed (75/25/0) distribution modelling.

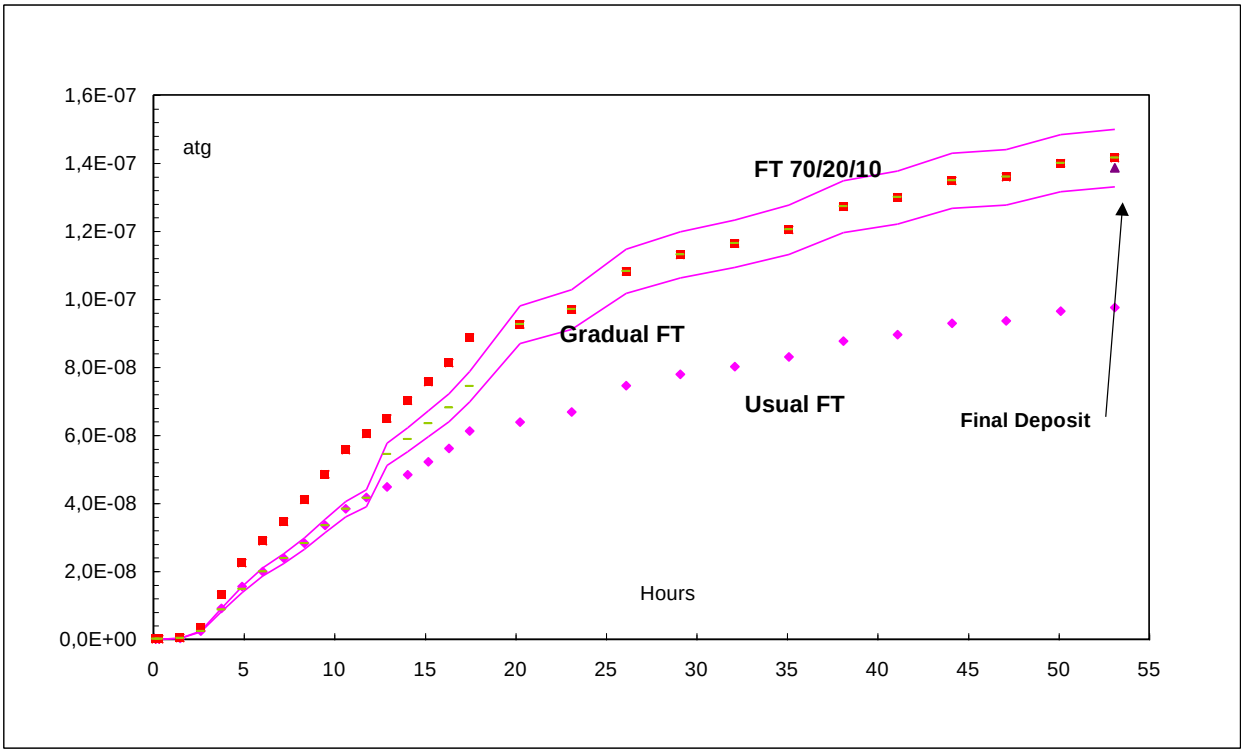

Figure B-1 : I_2 in the gas phase collected on the knitmesh filter for CAIMAN 2001/01 with a real (70/20/10) distribution compared to the imposed (75/25/0) distribution modelling.

The final quantity collected by the knitmesh filter is estimated to be about 9.10^{-8} gram·atoms with the usual distribution (75/25/0) and $1.4.10^{-7}$ gram·atoms with the real distribution (70/20/10). It is therefore necessary to take into account precisely this distribution to obtain a good estimation of iodine concentration in the gas phase.[6]

Sources and Estimates of RTF Experimental Uncertainty

Specific Activity (± 5%)

This is the value by which all activity measurements are converted to iodine quantities. It is based upon the average of several diluted samples of the tracer solution. Although the tracer solutions are diluted, the samples contains high activity, and counted decay rates are subject to detector "dead time" loss (saturated detector) for which the computer compensates. This compensation leads to some error in the measurement, estimated to be about 5% on the basis of comparison of several samples. Solutions of CsI for use in RTF experiments were prepared by accurately weighing, and dissolving CsI solid in distilled, deionised water. After addition of the tracer, 150 cm^3 of this solution was added to the 25 to 30 dm^3 solution in the RTF main vessel be addition via the aqueous sampling loop.

Aqueous Phase Iodine (± 5-10%)

To perform aqueous phase iodine measurements 5 cm^3 samples of the RTF aqueous solution were removed and γ-counted in a NaI well detector. Error in the measurement originates from variations in sampling size, as well as the conversion of the activity value to a concentration using the specific activity. This error is estimated to be about 5%. A further uncertainty associated with counting very active samples (at the beginning of a test when the aqueous phase iodine concentration and specific activity are at its highest, and therefore has higher dead time loss), is possible.

Aqueous Phase Iodine Speciation (Qualitative only)

Due to the high possibility of carryover between extractions, the results of this speciation are considered to be qualitative only. However, the sum total of all of the components of each extraction generally agrees well with the concentration derived by counting the aqueous grab samples (± 5 - 10%).

Speciation of the tracer usually shows that a small portion (0.1%) of the iodine is initially in the form of organic iodide. However this measurement should be considered

[6] Reference : P. SCHINDLER CEA/DEC/S3C/LTC

carefully. Because of the qualitative nature of this extraction, it is unknown whether or not this number reflects the true organic iodide percentage. This has repercussions in the assessment of the gas phase iodine speciation results, because it is unknown whether the organic iodide found in the gas phase originate from the tracer, or whether they originate from processes within the vessel.

Iodine Determinations by Gamma Spectrometry (± 10% error)

The instrument is calibrated relative to several aqueous sample geometries. Any deviation from this geometry results in increased uncertainty in the measurement. However various irregular sample geometries are used during the course of a test (paint scrapings, coupons, speciation tubes, silver wool, etc.), for which the error can only be estimated (10%). Highly active samples, such as specific activity measurement, early aqueous grab samples, and coupons with high loading sometimes force the detector system to do a dead time correction, which may be a further source of uncertainty.

Gas Phase Iodine Concentration (AAIS) (± 5 - 10% under ideal conditions)

Calculation of the gas phase iodine concentration by the automated airborne iodine sampler relied upon the measurement of flow rate during the "trapping" portion of the measurement. Errors in the flow rate, counting errors in the sample, and errors in defining the original specific activity, account for most of the error in this measurement. The flow rate detector generally provided reliable data except during some high temperature tests where condensation appeared to affect either the flow rate or the flow sensor. An erroneously low flow rate leads to an erroneously high gas phase concentrations, which is generally obvious when observing the plotted data. It also appears that fluctuations in the vessel temperature while the heaters cycle on and off to maintain temperature cause fluctuations in the pressure, which seem to affect flow rate through the sampling loop.

The detection limit for iodine in the gas phase varies from experiment to experiment because the background and specific activity of the initial tracer solution was different for each test. It also varies during the test as the tracer decays. Generally a reliable detection limit is approximately 1×10^{-13} mol·dm^{-3}. Care must be taken while assessing data in the detection limit range.

The results are given in mol·dm^{-3} iodine atoms, since the total gas phase iodine is a mixture of organic iodides and I_2. Scatter in the data tends to increase during periods of high molecular iodine concentration (at low pH), which is unavoidable due to the intrinsic problems with iodine experiments.

Gas Phase Iodine Speciation (± 15% on the total)

Gas phase iodine speciation works on the theory that various species of volatile iodine will be selectively trapped on species selective adsorbents while passing through a speciation tube. Sections of the tube are separated and gamma counted in the well detector relative to the 5 ml aqueous sample geometry, which is the primary source of error. Because of the adsorbing nature of molecular iodine, the sampling syringe assemble is also counted in various pieces to be added to the I_2 total.

Separation between the I_2 and the organic iodides is thought to be efficient, but separation between the high and low molecular weight organic iodide fractions is dependent on the species itself. Low molecular weight organic iodides such as iodomethane and iodoethane are trapped exclusively on the TEDA impregnated charcoal, but slightly heavier compounds such as iodobutane are trapped on both the iodophenol and TEDA impregnated charcoal traps. Thus, interpreting the organic iodide results is difficult.

During low temperature test, the total iodine derived from the iodine speciation is generally in reasonable agreement with the AAIS data. However, factors of ~2 difference have been observed during PHEBUS RTF test, which have been attributed to difficulties relating to high temperature.

Hydrogen Peroxide (± 1uM under ideal conditions)

This analysis for H_2O_2 is based upon a colorimetric method, which has inherent difficulties. Precipitation of metal hydroxides in the sump results in the aqueous solution having a slightly yellowish colour, and this colour can interfere with the method. Metal ion impurities are commonly detected in aqueous phase samples taken from the RTF and are thought to originate either from the vessel or aqueous loop surfaces. The release of metal impurities is facilitated by low pH. The colorimetric method is based on monitoring the absorbance of I_3^- produced when H_2O_2 from the sample is reacted with a KI solution. Obviously, any I_3^- in solution previous to the sampling can interfere with these results. Calculations indicate that aqueous phase I_2 concentrations of about 10^{-6} mol·dm^{-3} will interfere with the peroxide determinations. These concentrations can be attained at pH 5 from irradiated solutions. Therefore care must be taken when interpreting H_2O_2 results at low pH.

Aqueous anions (± 10%)

Samples were analyzed by Ion chromatography. The analyst quotes a 10% relative precision in the measurement.

Aqueous metal ions (± 10%)

Samples were analyzed by ICP without acidification. The analyst quotes a 10% relative precision in the measurement, based on spike and control recoveries.

Organic Compounds (± 15% on the total)

Aqueous carbonyls were analyzed by HPLC using a dinitrophenylhydrazine (DNPH) derivitization method. The gas phase species are quantified by direct injection GC. These techniques have been calibrated for the species measured by standard solutions. A solid phase micro extraction technique (SPME) has been utilized during some test to facilitate identification of aqueous and gas phase organic species, but the results are qualitative only. For detection in the gas phase the uncertainty in measurements has been estimated to be 12%. For the liquid phase, either by direct detection or DNPH derivatization, the measurement uncertainty is estimated to be 5%. For the SPME method the estimated uncertainty is 10%.

TABLE-B1: MINIMUM DETECTION LIMITS FOR ORGANICS IN THE AQUEOUS PHASE BY HPLC

Organic	Detection limit $\mu mol \cdot dm^{-3}$	Method
toluene, xylene (ortho and meta)	150	direct
benzaldehyde, cresol (meta and para)	10	direct
methyl,ethyl iodide	30	direct
dimethylphenol (2,4 and 2,6)	8	direct
formaldehyde	1.7	DNPH
acetaldehyde	2.0	DNPH
acetone	3.3	DNPH
MIBK	3.0	DNPH
MEK	4.5	DNPH
m-tolualdehyde	1.6	DNPH
2-heptanone	4.8	DNPH

TABLE-B2: MINIMUM DETECTION LIMITS FOR ORGANICS IN THE GAS PHASE BY GAS CHROMATOGRAPHY (GC)

Organic Compound	Detection limit $nmol \cdot dm^{-3}$	Detector
Methyl iodide	0.06	ECD
Methylene chloride	8	ECD
Ethyl iodide	0.12	ECD
Chloroform	0.40	ECD
Propyl & butyl iodide	0.20	ECD
1,1,1-trochloroethane	0.20	ECD
Acetone, MEK, MIBK	10	PID
Toluene	15	PID
Ethylbenzene, xylenes	20	PID

TABLE-B3: MINIMUM DETECTABLE LIMITS OF ORGANICS IN THE AQUEOUS PHASE BY SPME

Organic Compound	Detection limit $\mu mol \cdot dm^{-3}$	Fibre
ethylbenzene	0.06	PDMS
xylene (ortho and meta)	0.04	PDMS
toluene	0.30	PDMS
heptanone	1.0	PDMS
acetophenone	0.06	PA
methylbenzaldehyde	0.035	PA

Table B3 results are for a polydimethylsiloxane fibre (PDMS) with a 100 μm film and a polyacrylate (PA) with an 85 μm film. These detection limits are dependent on the condition of the fibre.

Mass Balance

The mass balance is based upon the amount of iodine that was injected into the vessel at the start of the test (in this case, 2.5×10^{-4} moles iodine), even though it appears as though the targeted *initial concentration* was sometimes not met. A low initial concentration may be due to initial rapid adsorption onto walls (very likely at low pH), slightly higher or lower volume than expected, or problems associated with high specific activity at beginning of a test. Because the initial solution is simply a diluted version of the tracer solution (prepared by weighing out CsI), it is unlikely that the quantity of iodine added (in moles) would be low. The quantity of iodine remaining in the aqueous phase is the final grab sample multiplied by the initial volume (± 5%, sampling is ignored) for a combined error of ~ 10%.

The total amount of iodine retained on gas phase and aqueous phase surfaces was derived from the loading on small coupons suspended in the vessel gas phase or placed in the vessel sump. Sometimes coupons were placed in the gas phase recirculation loop, and periodically removed and counted to estimate the kinetics of surface loading. For painted containment surfaces, paint scrape samples were often taken to determine the iodine retention. Mass balance determinations assume that loading on the coupons is homogeneous and that the loading on the small coupons is representative of that on the entire vessel surface. The error in the measurements is estimated to be 15%, but the assumption of homogeneous adsorption often led to larger uncertainties in the mass balance determination.

Loading on the stainless steel surfaces is very difficult to estimate if corrosion on the surfaces occurs, because "hot spots" develop on corroded areas, creating to a very non-homogeneous loading pattern impossible to accurately define. Furthermore, corrosion sediment, which settles throughout loops, pumps, vessels and joints etc., retains iodine.

There is generally a gradient in the loading on the gas phase surfaces (i.e., the highest loading is found at the surface just above the aqueous phase). For the purposes of the mass balance calculation, however, it is assumed to be homogeneous. The loading

estimated from measurements taken using the hand held detector are used if it is thought to give a more representative loading of the entire surface than that the coupon.

The determination of the amount of iodine released during the washes (± 10%) was often complicated by incomplete drainage of the sump after the charge was dumped, and after each wash. Corrections were applied to compensate. The washes were generally only a small component of the mass balance.

In many experiments, small samples of the gas and aqueous phase sampling and recirculation loops were removed and gamma counted to estimate loop loading. It must be assumed that the sample represents the loading throughout the entire loop, however under corrosion conditions, this assumption is suspect.

Sump pH (± 0.3 pH units)

The two pH probes were calibrated prior to each test with commercial pH standardization solutions. Typically the probes read within 0.3 pH units. An error message is printed if the probes differ by more than a set parameter (e.g., pH unit), the system is disabled, and operator action is required to correct the situation. If the values from each of the probes diverged significantly, one of the probes was replaced. The faulty probe was identified by its erroneous drift relative to acid or base addition by the pH control system. Probe failure has been observed to occur more frequently during higher temperature tests.

Temperature

Resistance temperature detectors (RTD's) were calibrated by the Instrument technicians prior to each test against standards traceable to National Bureau of Standards. The uncertainty in these probes is ± 0.2ºC.

The temperature was measured in various locations within the system and was slightly different depending upon the location (i.e., aqueous temperature, gas temperature, wall temperature, circulation loop temperature) of the RTD. The operating temperature of a test (given in Table 1) refers to the intended temperature of the sump. However, because of the heating cycles of the main sump heater and ambient temperature changes, most parts of the system could be maintained to within 3 degrees of the intended temperature (i.e., 25 ± 3ºC).

Dissolved Oxygen (± 1ppm)

Dissolved oxygen measurements were only possible for the low temperature tests (< 60ºC). A Beckman probe is located on the aqueous sample loop. Because this probe is not temperature compensated, it responds to changes in temperature, which is thought to be the reason for the daily oscillations observed during some tests. The other is a Rosemount probe, which is located on the aqueous recirculation loop and is temperature compensated. This probe is located on the pressure side of the pump, which may be a reason for the difference in readings between the probes. Another explanation is that both readings are correct and that the concentration of dissolved oxygen at the probe is affected by the time taken for the sump water to reach the probe.
The aqueous recirculation loop has a much faster flow rate.

Both dissolved oxygen probes were calibrated using air prior to the start of the test.

APPENDIX C: Information for Participants

INTRODUCTION

The following note is to provide a record of the information sent to ISP participants regarding the experiments chosen for the ISP-41F Phase 2 exercises on iodine behaviour codes. AECL is the lead organization for this International Standard Problem (ISP), and is responsible for documenting both the preparatory information as well as the results. The conditions and experimental events for two tests from the CEA/IRSN CAIMAN facility program, and two tests from AECL's RTF experimental program are described in this report. Diagrams describing the geometry of the two facilities are also provided. The note includes a recommendation for the rate constants to use for modelling adsorption of iodine species on surfaces, and for interfacial mass transfer of volatile species. Finally, it contains a list of specifications regarding the calculations to be performed, and the way in which they are to be provided for analysis by AECL and IPSN.

The first set of calculations is to be "blind" calculations, performed using only the information in these notes, and copies of the PowerPoint presentations from the preparatory workshop held on January 30th and 31st at IPSN in Fontenay-aux-Roses (these were e-mailed to participants in March 2002). Calculation results for the CAIMAN facility experiments are to be submitted to L. Cantrel (e-mail laurent.cantrel@irsn.fr), and those for the RTF facility experiments to J. Ball (e-mail ballj@aecl.ca). Calculation results are to be sent by June 30th, 2002.

THE CAIMAN FACILITY AND DESCRIPTION OF EXPERIMENTS

DIAGRAM OF CAIMAN FACILITY

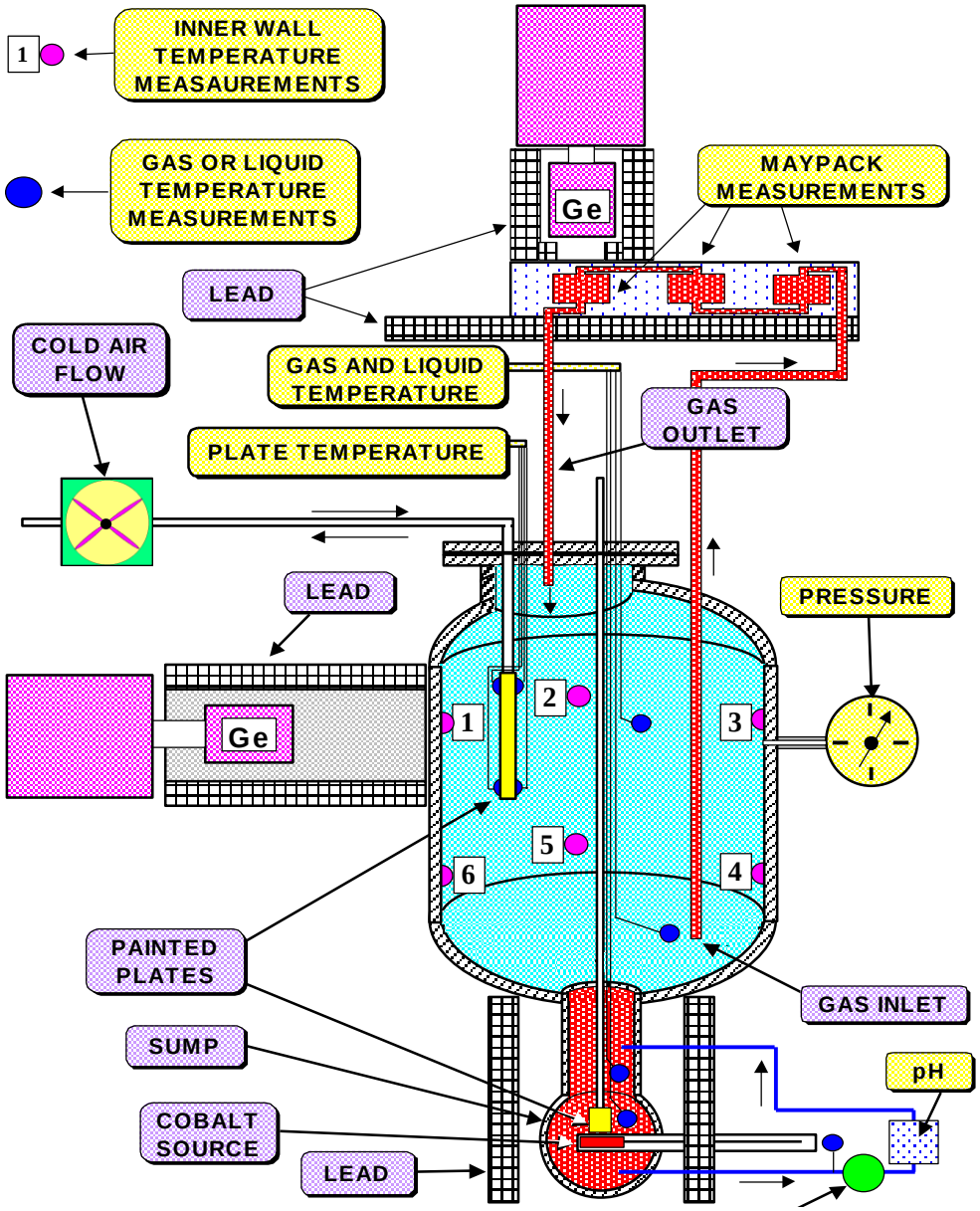

Figure C1: Features of the CAIMAN Facility

GEOMETRY OF CAIMAN FACILITY

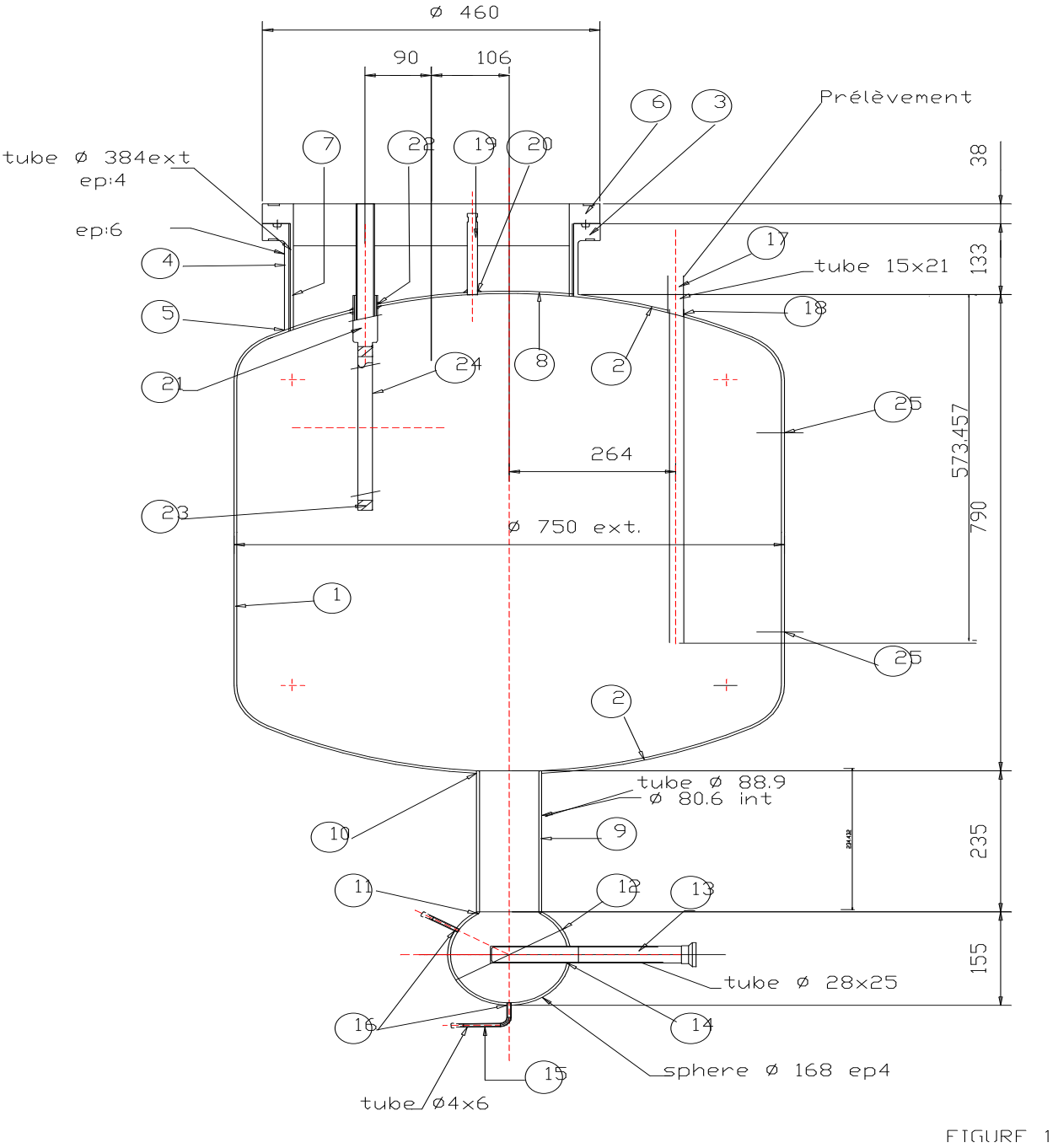

Figure C1: Geometry of the CAIMAN Facility (measurements are in millimetres)

CAIMAN TEST 01/01

Test Conditions for CAIMAN Test 01/01

Surface areas	
Sump walls - Electropolished stainless steel	13 dm^2
Liquid loop - Electropolished stainless steel	3 dm^2
Gas walls - Electropolished stainless steel	190 dm^2
Sump-gas interfacial area	0.51 dm^2
Volumes	
Sump (at the time of iodine injection)	3.32 dm^3
Liquid loop	negligible
Gaseous phase	300 dm^3
Flow rates	
Liquid loop	20 $dm^3 \cdot h^{-1}$
Gas phase (during the measurement period)	150 $dm^3 \cdot h^{-1}$
Irradiation cycle	45 min on, 15 min off, for the first 20 hours 165 min on, 15 min off, for the remaining hours
Measurement cycle	15 min every 1 h for the first 20 hours 15 min every 2 h for the remaining hour
Temperature	
Sump + Painted coupons in aqueous phase	110°C
Liquid loop	110°C/90°C
Gas walls	110°C
Painted coupons in gaseous phase	78°C
Dose rate	
Aqueous phase	3.2 $kGy \cdot h^{-1}$
Gas phase	2.0 $Gy \cdot h^{-1}$
[a]Starting pH (buffered with boric acid and controlled)	5.2
Starting concentration of iodide	4×10^{-5} $mol \cdot dm^3$
Painted coupons in gas Type: epoxy polyamide paint (from Ripolin company) 3 constituents:, paint hardener, solvent (mixture)	18.4 dm^2
Painted coupons in sump Type: epoxy polyamide paint (from Ripolin company) 3 constituents: paint base, paint hardener, solvent (mixture)	0.82 dm^2
Pressure relative to atmospheric ($P-P_{atm}$)	2.2 bar
Atmosphere composition	9% O_2 - 52% N_2 - 39% H_2O

[a] Note that boric acid is not an effective buffer at pH 5.2.

Test Events for CAIMAN Test 01/01

	Event
Pre-test	Wash of the vessel, calibration of the instrumentation
- 28.6	Filling of the sump with 3.52 dm^3 of purified water containing 0.1 mol/ dm^3 of H_3BO_3 - pH = 5.6 - 0A sampling
- 24.8	Filling of the vessel by compressed air
- 24.3	Heating up to 60°C
- 23.6	Heating up to 90°C and 1A sampling (-50 cm^3)
- 5.6	Heating up to 110°C (target thermal conditions)
0	Injection of labelled iodide solution (100 cm^3) - V_L = 3.32 dm^3
+0.7	Starting of the irradiation – pH = 5.2 (-14 cm^3)
+19.7	Injection of LiOH to keep the pH around 5, 2A sampling
23-42	No increase of the maypack activity (Compressor didn't work for this period of time?)
45.7	3A sampling for the total carbon determination (- 64 cm^3)
72.0	4A sampling for the total carbon determination (- 64 cm^3) End of the test

*Note: the designation #A samplings refer to aqueous phase sampling to determine the content of the total carbon dissolved in the solution

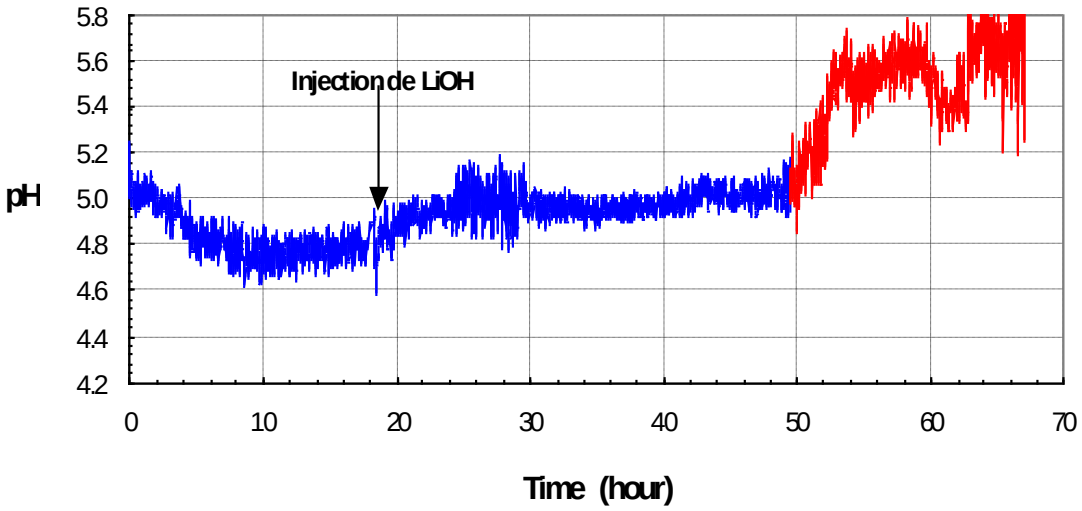

Figure C2: pH Evolution during Test 01/01

CAIMAN TEST 97/02

Conditions of CAIMAN Test 97/02

Surface areas	
Sump walls – Electropolished stainless steel	13 dm^2
Liquid loop - Electropolished stainless steel	3 dm^2
Gas walls – Electropolished stainless steel	190 dm^2
Sump-gas interfacial area	0.51 dm^2
Volumes	
Sump (at the time of iodine injection)	3.32 dm^3
Liquid loop	negligible
Gaseous phase	300 dm^3
Flowrates	
Liquid loop	30 $dm^3 \cdot h^{-1}$
Gas phase (during the measurement period)	200 $dm^3 \cdot h^{-1}$
Irradiation cycle	45 min on, 15 minutes off for the first 23 hours 105 min on, 15 minutes off for the remaining hours
Measurement cycle	15 min every 1 h for the first 23 hours 15 min every 2 h for the remaining hour
Temperature	
Sump + Painted coupons in aqueous phase	91°C
Liquid loop	90°C
Gas walls	108°C
Painted coupons in gaseous phase	110°C
Dose rate	
Aqueous phase	1.0 $kGy \cdot h^{-1}$
Gas phase	0.00
[a]Starting pH (buffered with boric acid and controlled)	5.0
Starting concentration of iodide	10^{-5} $mol \cdot dm^3$
Painted coupons in gas Type: epoxy polyamide paint (from Ripolin company) 3 constituents: paint base, paint hardener, solvent (mixture)	18.4 dm^2
Painted coupons in sump Type: epoxy polyamide paint (from Ripolin company) 3 constituents: paint base, paint hardener, solvent (mixture)	0.82 dm^2
Pressure relative to atmospheric ($P-P_{atm}$)	1.9 bar
Atmosphere composition	10% O_2 - 66% N_2 - 24% H_2O

[a] Note that boric acid is not an effective buffer at pH 5.0.

Test events for CAIMAN Test 97/02

Time (h)	Event
Pre-Test	Wash of the vessel, calibration of the instrumentation 0A sampling
- 4.3	Filling of the sump with 3.42 dm^2 of purified water containing 0.3 $mol \cdot dm^{-3}$ H_3BO_3
-3.5	Filling of the vessel by N_2 (0.6 bar)
- 3.2	Starting of the heating, up to 90°C and 1A sampling* (-47 cm^3)
0	Injection of iodide solution + tracer solution (+43 cm^3) V_L = 3.29 dm^3
1.0	Starting of the irradiation
23.5	2A sampling* (-43 cm^3)
46.8 h	3A sampling* (-43 cm^3)
61.5	End of the test
Post-Test	After cooling of the sump (20°C), 4A sampling*

Note: the designation #A sampling refers to aqueous phase sampling to determine the content of the total carbon dissolved in the solution

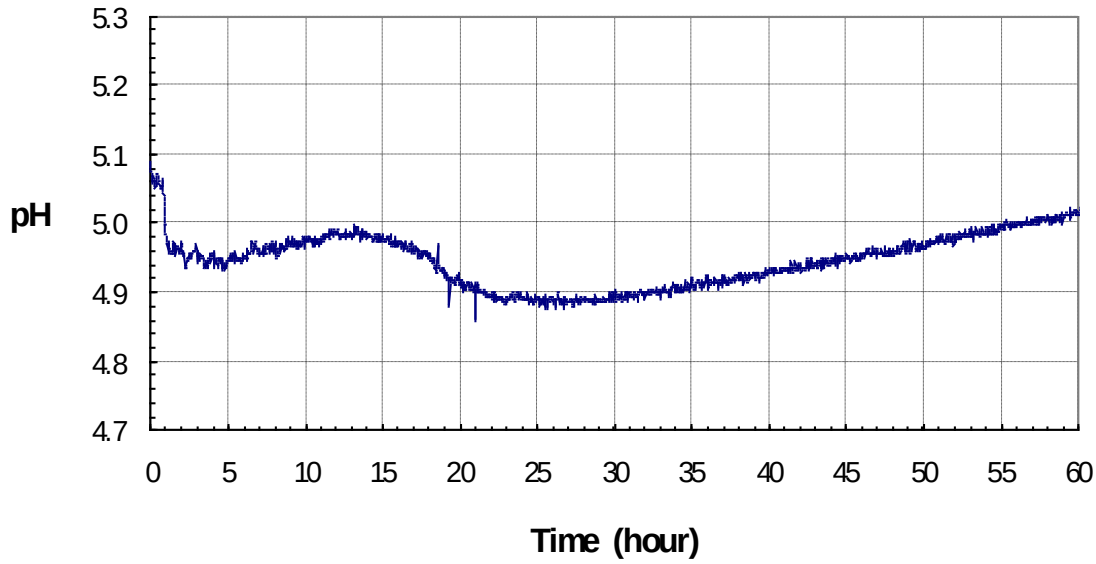

Figure C3: pH Evolution during Test 97/02

ADDITIONAL INFORMATION

Recommended Adsorption rate constants and mass-transfer values

CAIMAN 01/01 and CAIMAN 97/02:

- ***Adsorption coefficient of I_2 onto paints in gaseous phase (V_{AD})***
  $\nu_{AD} = 10^{-2}$ dm·s^{-1} (4×10^{-2} dm·s^{-1} in using the iodine adsorption formula on dry surfaces employed in ISP-41 phase 1)
- ***Adsorption coefficient of I_2 onto paints in aqueous phase (V_{AD})***
  ν_{AD} = ? (not measured but assumed to be much lower than in gaseous phase)

- ***Desorption coefficient of I_2 from paints in gaseous phase***
  $k_{DES} = 10^{-6}$ s^{-1} (no desorption considered in ISP-41 phase 1)

- **Interfacial Mass transfer coefficient (k_{MT})**
  K_{MT} = ? (not measured, a value of 5×10^{-5} dm·s^{-1} has been determined for a homogeneous temperature of 130°C)

Note that adsorption onto electropolished surfaces exposed to the gas and aqueous phases is assumed to be negligible.

THE RTF AND DESCRIPTION OF EXPERIMENTS

DIAGRAM OF THE RTF

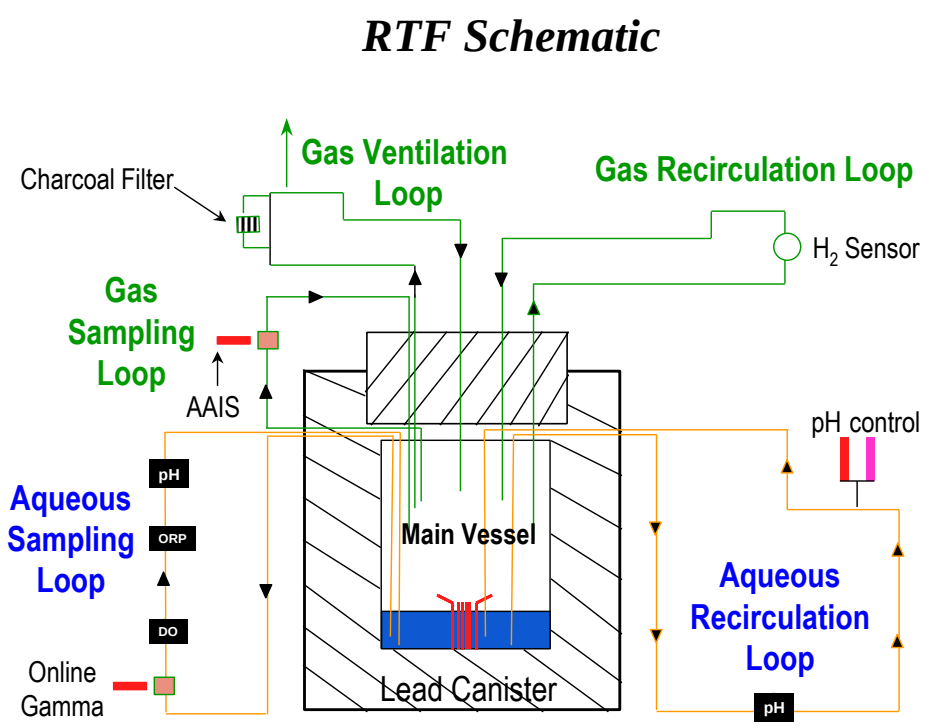

Figure C4: Features of the RTF

GEOMETRY OF THE RTF

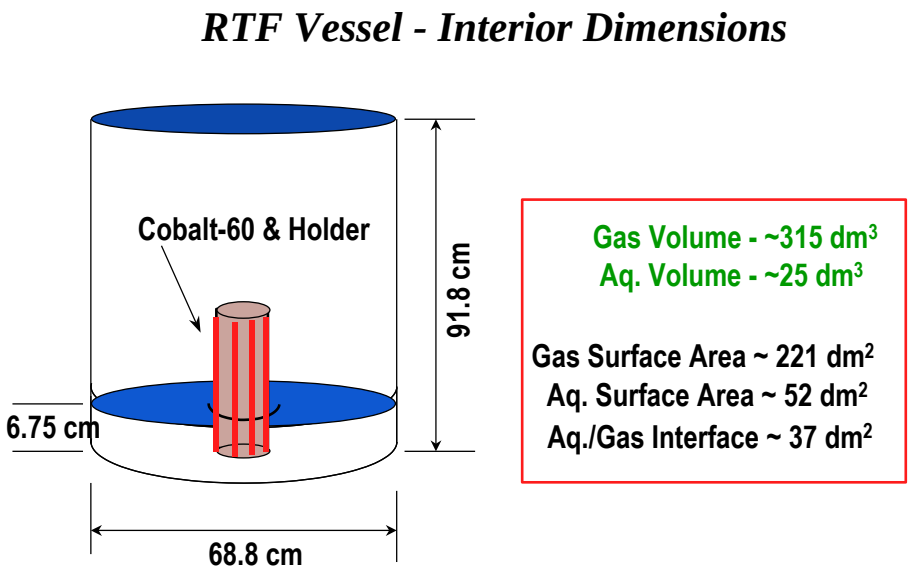

Figure C5: Geometry of the RTF

PHASE 10 TEST 1

Test Conditions for Phase 10 Test 1

Vessel Surface	Ameron Amerlock 400 epoxy paint (xylene based), aged about 3 months prior to test
Dose Rate (gas and aqueous phase)	0.67 $kGy \cdot h^{-1}$
Temperature	60ºC
Atmosphere	Normal air
Pressure	atmospheric
Starting Concentration of I^-	8.6×10^{-6} $mol \cdot dm^3$
Inorganic Additives	None
Vessel Shape and Size	Cylindrical Interior Diameter – 6.86 dm Interior Height – 9.18 dm
Aqueous Volume	25 dm^3
Gas phase Volume	315 dm^3
Aqueous/Gas Surface Area	37 dm^2
Starting pH	Initially controlled at 10 for 72 hours
Aqueous Surface Area (Vessel)	52 dm^2
Gas phase Surface Area (Vessel)	221 dm^2

Amercoat #65 thinner (mainly xylene and ethyl benzene) was used during the preparation of the paint. Manufacturers data sheet can be supplied upon request.

Loop Conditions for Phase 10 Test 1

Loop	**Material**	**Flow Rate**	**Surface Area**
Aqueous Sampling Loop	Glass-lined SS	1 dm^3/min	14.6 dm^2
Aqueous Recirculation Loop	SS	10 dm^3/min	27.9 dm^2
Gas Sampling Loop	Glass-lined SS	1.2 dm^3/min	16.0 dm^2
Gas Recirculation Loop	SS	20 dm^3/min	34.5 dm^2
Gas Vent Loop	SS	10 dm^3/min	33.5 dm^2

SS = Stainless Steel

Experimental Events for Phase 10 Test 1

Time (h)	Event
-46	Pre-test charge (25 dm^3 of distilled water) was added
-46 to -3	Pre-test sampling of organic species in both aqueous and gas phase
-3	Pre-test charge was dumped
-2	Fresh charge (25 dm^3 of distilled water) was added
0	Tracer addition
72	pH control was removed
285	pH raised and controlled at 10
335	Test was terminated (vessel drained)
431	^{60}Co was removed
433	Coupons were removed

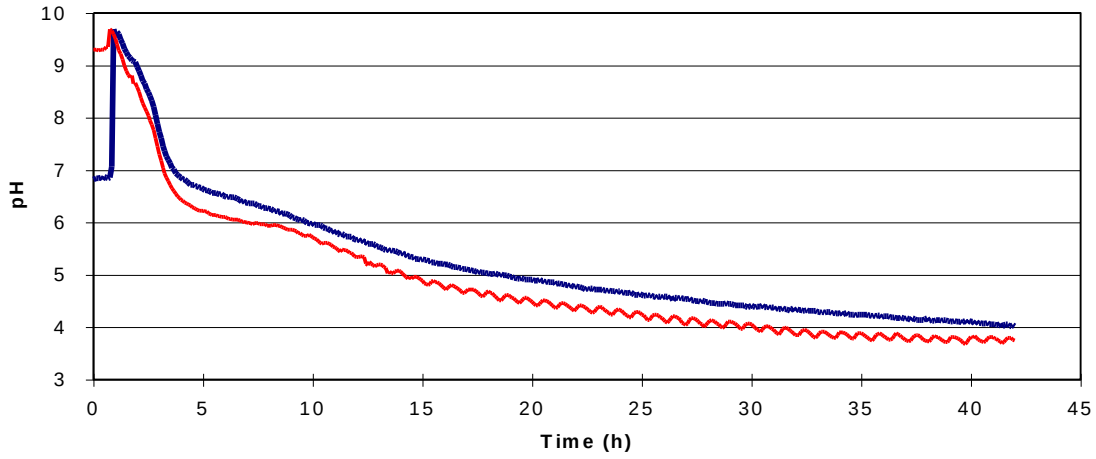

Figure C6: pH Evolution during the Pre-Test Stage of Phase 10 Test 1

Note that the pH during the test is a variable to be calculated, or estimated by other means by each participant.

PHEBUS RTF1

Test Conditions

Vessel Surface	**Electropolished Stainless Steel**
Dose Rate	1.06 $kGy \cdot h^{-1}$
Temperature	Sump 90ºC, Walls 110ºC
Atmosphere	5 % O_2, 95 % N_2
Pressure	atmospheric
Starting Concentration of I^-	1×10^{-5} $mol \cdot dm^{-3}$
Inorganic Additives	0.3 $mol \cdot dm^{-3}$ boric acid
Vessel Shape and Size	Shape - Cylindrical Interior Diameter - 6.86 dm Interior Height - 9.18 dm
Aqueous Volume	30 dm^3
Gas phase Volume	310 dm^3
Aqueous/Gas Surface Area	37 dm^2
Starting pH	Initially controlled at ~5
Aqueous Surface Area (vessel)	52.3 dm^2
Gas Phase Surface Area (vessel)	220.7 dm^2
Aqueous Surface Area (coupons)	8 coupons, 0.187 dm^2 each
Gas Phase Surface Area (coupons)	3 coupons, 2.40 dm^2 each

Coupons were painted with Centrepox N Ripolin primer and Hydrocentrifugon 901 Ripolin white finishing coating. Aged for approximately 6 -12 months. Contains ketones and aromatics.

Loop Conditions

Loop	**Material**	**Flow Rate**	**Surface Area**
Aqueous Sampling Loop	EP SS	1 dm^3/min	14.6 dm^2
Aqueous Recirculation Loop	EP SS	10 dm^3/min	27.9 dm^2
Gas Sampling Loop	EP SS	4 dm^3/min	16.0 dm^2
Gas Recirculation Loop	N.A.	0 dm^3/min	none
Gas Vent Loop	N.A.	0 dm^3/min	none

EP SS = Electropolished stainless steel

Experimental Events

Time (h)	Event
-168	Cobalt source installed
-96	Vessel connected, 30 dm^3 of 90ºC water added
-3.5	Fresh 30 dm^3 90ºC water added 5% O_2 purge begins
0	Trace labelled CsI added
36	pH controller disabled
51	Aqueous pump failed and was restarted
58	Aqueous pump failed and was restarted
68	Aqueous pump failed and was restarted
72	Test terminated

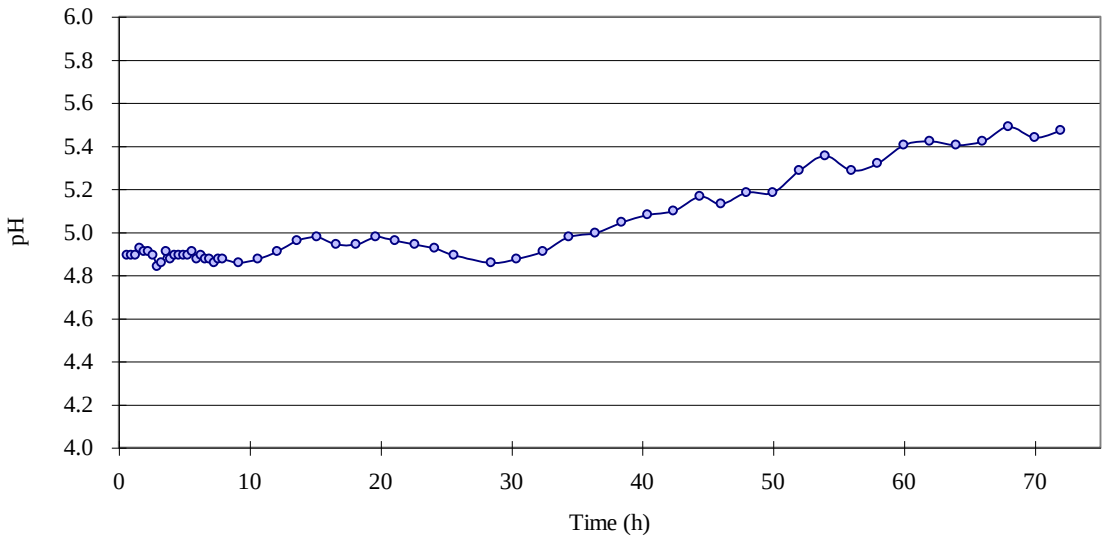

Figure C7: pH during PHEBUS RTF 1

ADDITIONAL INFORMATION

Recommended adsorption rate constants and mass-transfer values

FOR BOTH RTF TESTS:

- ***Adsorption coefficient of I_2 onto surfaces in gaseous phase***

  - **electropolished stainless steel**

    υ_{AD} (dm·s^{-1}) = 0.001
    k_{DES} (s^{-1}) = $RO_2 \times 9 \times 10^{-7} \times \exp(8973 \times (1/298 - 1/T)$

  - **paint**
    υ_{AD} (dm·s^{-1}) = $0.001 \times \exp(5100 \times (1/298 - 1/T))$
    k_{DES} (s^{-1}) = 0

RO_2 is the fraction of oxygen in the gas phase relative to that in normal air.

- ***Adsorption coefficient of iodine species onto paints in aqueous phase***

  Γ^- υ_{AD} (dm·s^{-1}) = 4×10^{-7}, k_{DES} (s^{-1}) = 1×10^{-6}
  I_2 υ_{AD} (dm·s^{-1}) = 2×10^{-3}, k_{DES} (s^{-1}) = 5×10^{-7}

PHASE 10 TEST 1

- **Mass transfer coefficients:**

  k_{maq} (dm·s^{-1}) = $7 \times 10^{-4} \times (T/298)^{1.5}$
  k_{mg} (dm·s^{-1}) = $0.1 \times (T/298)$
  $1/k_{MT} = 1/k_{maq} + H_X/k_{mg}$

PHEBUS RTF 1

- **Mass transfer coefficients:**

  k_{maq} (dm·s^{-1}) = $7 \times 10^{-4} \times (T/298)^{1.5}$
  k_{mg} (dm·s^{-1}) = $0.01 \times (T/298)$
  $1/k_{MT} = 1/k_{maq} + H_X/k_{mg}$

k_{maq} and k_{mg} are the mass transfer coefficients representing resistance to diffusion (dm·s^{-1}) through boundary layers in the aqueous and gas phase respectively, and k_{MT} is the interfacial mass transfer coefficient.
H_X is the dimensionless partition coefficient for a species X defined as concentration in the aqueous phase at equilibrium/concentration in the gas phase at equilibrium [X(aq)]/[X(g)], T is temperature in Kelvin.

Requirements for Reporting of Calculation Results

The following outlines the information that should be provided by each of the participants when submitting calculation results. It also specifies the format in which the results should be submitted. It is important to follow these guidelines to ensure consistency in comparison of results from various organizations, and the correct interpretation of the calculations.

1. **Name of organization**

2. **Code used (with version # specified)**

3. **List assumptions used, with relevant rate equations for:**

   a) The formation and depletion of organic iodides
      - Describe mechanisms (e.g., organic iodide formation only by processes in the aqueous phase).
      - Describe assumptions (if any) regarding the concentration of organic compounds in the gas and aqueous phase.
      - Provide equations and rate constants.

   b) The adsorption and desorption of iodine on surfaces
      - Describe mechanisms for processes occurring on submerged surfaces and surfaces exposed to the gas phase (e.g., I_2 and I^- adsorbed onto and desorbed from painted surfaces exposed to the aqueous phase, I_2 adsorbed onto and desorbed from painted and stainless steel surfaces exposed to the gas phase).
      - Provide adsorption and desorption rate constants for each species and process.

   c) The conversion of I^- to I_2
      - IODE and IMPAIR code users should provide the values for the rate constant for conversion of I^- to I_2, and the factor n used to determine pH dependence.

   d) Initial iodine speciation (i.e., does the calculation assume some fraction of the initial iodine is in the form of organic iodides?)

   e) Partitioning of iodine species
      - List the iodine species that are assumed to be volatile, and report the temperature dependent partition coefficient for each species.

4. Variables to be provided/calculated

The calculation results should be provided in Excel spreadsheet format. The time should be shown in intervals of 1 hr, and the spreadsheet should contain a column each for the variables:

a) Time (h),
b) Aqueous pH,
c) Total concentration of iodine ($g \cdot atoms \cdot dm^{-3}$) in the aqueous phase,
   - e.g., (1×10^{-9} $mol \cdot dm^{-3}$ I_2 and 1×10^{-9} $mol \cdot dm^{-3}$ CH_3I = 3×10^{-9} $g \cdot atom \cdot dm^{-3}$ total iodine)
d) Total concentration of iodine ($g \cdot atoms \cdot dm^{-3}$) in the gas phase,
   - Ensure that a list of each species assumed to be volatile has been provided as part of the list of assumptions.
e) Total concentration organic iodides ($mol \cdot dm^{-3}$) in the gas phase,
f) Iodine adsorbed ($mol \cdot dm^{-2}$) on surfaces exposed to the aqueous phase,
g) Iodine adsorbed ($mol \cdot dm^{-2}$) on electropolished surfaces exposed to the gas phase and
h) Iodine adsorbed ($mol \cdot dm^{-2}$) on painted surfaces exposed to the gas phase.

Please provide the information in the order outlined above. The columns should be labelled appropriately. Additional information regarding the speciation of iodine in the gas phase is required if species other than I_2 and organic iodides are assumed to be present in the gas phase (e.g., iodine atom, iodate). This information should be provided in a series of additional columns in the spreadsheet. Other information of interest (e.g., speciation in the aqueous phase) can be provided as well.

Format

All calculation results must be provided in a Microsoft Excel Spreadsheet format (Microsoft Excel 2000 or earlier release). It is not necessary to provide information in graphical form. Assumptions, relevant rate equations and any discussion or explanatory text must be provided as a Microsoft Word (Microsoft Word 2000 or earlier release) document.

Additional Information Provided for Optimized Calculations

The above 5 sections were provided to participants prior to the blind calculations. Subsequently, the results of each experiment were made available to the participants. These included, for CAIMAN facility experiments:

- on-line measurements of gas phase I_2 and organic iodine concentrations as measured by MAYPACK filters,
- on-line measurements of the iodine adsorption on painted coupons as determined by gamma counting

- temperature measurements throughout the experimental vessel.
- Total Carbon (TC) analysis was also provided.
- Mass balance at test end

For RTF experiments, the following information was supplied

- On-line measurements of total iodine in the gas phase (obtained using automated airborne iodine sampling)
- Speciation measurements of iodine in the gas phase (giving I2, high molecular weight organic iodides and low molecular weight organic iodides
- Measurements of total iodine in the aqueous phase (grab samples)
- Measurements of total iodine in the aqueous phase (speciation samples)
- Mass balance at test end.

As well, for RTF experiment Phase 10 Test 1, the aqueous pH as a function of time was provided (this was an optional parameter for the participants to calculate). The pH measured during the test is shown in Figure C8. Participants were also informed that additional information such as, analysis for organic compounds in the gas phase by gas chromatography, and HPLC analysis of organic compounds in the aqueous phase, anion analysis of species in the aqueous phase, and analysis for metals in the aqueous phase were available on request.

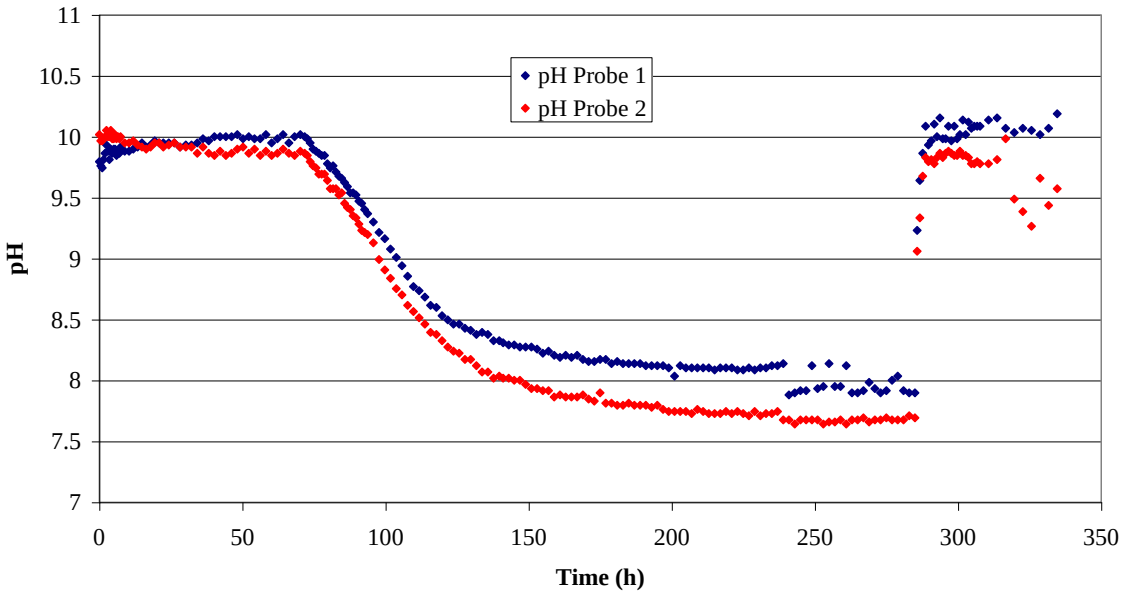

Figure C8: pH during RTF P10T1

APPENDIX D: RECORD OF OTTAWA MEETING

SUMMARY RECORD OF AN INTERIM MEETING ON PRELIMINARY RESULTS OF THE SECOND PHASE OF THE FOLLOW-UP TO THE ISP-41 EXERCISE [7]
(Ottawa, Canada, 17-18 September 2002)

I. General - Opening remarks

1. A list of participants is given in Annex I.

2. Dr. Ball and Dr. Cantrel, who were jointly chairing the meeting, and the Secretary welcomed the participants. Dr. Royen thanked AECL and IRSN for their strong support to the organisation and performance of the ISP-41 exercise. He also thanked AECL, in particular Dr. Ball, Dr. Wren and Mr. Glowa, for hosting the meeting and taking care of all the necessary arrangements in Ottawa and Chalk River.

3. An apology for absence had been received from Mr. J. Rydl (UJV, Czech Republic).

4. The Rules of Procedure of the OECD clearly specify that meetings of the Committees of the Organisation as well as their working parties, expert groups, etc. only require the drawing up of a summary record of the decisions and conclusions reached by the Committees.

II. Adoption of the agenda

5. The agenda was adopted as proposed in document NEA/SEN/SIN/AMA(2002)20, with the addition of a brief presentation by Dr. Allelein on the outcome of a meeting of experts to develop a Containment Code Validation Matrix, which had been held at the end of August 2002..

III. Approval of the summary record of the previous meeting

6. The summary record of the ISP-41 Follow-up Phase-2 Preparatory Workshop, held on 30-31 January 2002 [NEA/SEN/SIN/AMA(2002)6] was approved without any change.

IV. Objectives and scope of the ISP-41 exercise

7. The objective of the exercise was to demonstrate iodine code capabilities over a large range of experimental conditions, and to support development and maintenance of expertise to respond to licensing issues and ensure emergency preparedness. The scope of Phase 2 of the ISP-41 follow-up exercise was the comparison of predictions of the iodine behaviour codes to four intermediate-scale experiments on iodine behaviour; *Caiman 1997/02, PHEBUS RTF1, CAIMAN 2001/01, RTF P10T1 (Phase 10 Test 1).* The experiments covered a large range of experimental conditions (see below for a brief description of these tests). The first part of the exercise was a blind exercise, i.e., the code users had been given experimental conditions and boundary conditions for each experiment, and asked to predict various output parameters (iodine inventory and speciation in gas and aqueous phases and on surfaces exposed to the gas

[7] Including comments made by the participants on an earlier version.

and aqueous phases). After the blind exercise results had been submitted (by 30 June 2002), and the output parameters from each of the experiments had been distributed (15 July 2002). The code users would now be able to optimize their codes in order to provide a best fit of all of the available data.

8. The four experiments chosen for this exercise could be divided into two categories:

CAIMAN 97/02 & PHEBUS RTF1: These experiments had been performed with sump temperatures of 90 °C, a sump pH of 5, and painted coupons in both the gas and aqueous phase. The differences between the two tests were scale (CAIMAN facility: gas phase volume, 300 l, sump volume, 3 l, RTF: gas phase volume 315 l, sump volume 25 l), sump dose-rate (CAIMAN facility: dose-rate ≈ 1 kGy/h in the liquid phase, 0.7 Gy/h in the gas phase, RTF dose-rate ≈1 kGy/hr), interfacial mass transfer rate (CAIMAN facility: interfacial surface area 51 cm^2, sump phase volume circulated but gas phase volume not circulated, RTF: interfacial surface area 3700 cm^2, sump and gas phase volumes circulated); moreover, the surface areas of the painted coupons are somewhat different. Comparison of code predictions against results from these two experiments will assess the ability of the codes to predict the influence of these parameters on iodine volatility.

CAIMAN 2001/01 & RTF P10T1: These two tests differed primarily in the amount of painted surfaces present (CAIMAN facility: painted surface area from coupons in gas phase 1800 cm^2; there is no coupon in the aqueous phase in CAIMAN 2001/01; RTF: painted surface area from vessel walls contacting gas phase 22000 cm^2, painted surface area from vessel walls contacting aqueous phase 5200 cm^2), temperature (CAIMAN facility: sump temperature 110°C, gas phase coupon temperature around 100°C, RTF: sump temperature 60°C, wall temperature 60°C), sump dose-rate (CAIMAN facility: dose-rate: ≈ 3.2 kGy/hr, RTF dose-rate ≈ 0.6 kGy/hr) and pH (CAIMAN facility: pH ≈ 5, remaining unchanged, RTF experiment, pH initially maintained at 10, then uncontrolled, pH 10-7.8, then controlled at 10 again). Comparison of code predictions for these two experiments focused on the organic iodide models in each of the codes, and in evaluating the effects of these parameters on organic iodide production.

V. Overview of blind calculation results

9. Dr. Cantrel presented a summary of the results obtained by AECL, CIEMAT, GRS, IRSN, PSI and UJV (NRI). The following parameters had been calculated for CAIMAN tests 1997/02 and 2001/01 (Dr. Cantrel reminded the participants of the main conditions of the tests and the mass transfer coefficients used):

- total aqueous iodine,
- total gaseous iodine,
- organic iodide concentration in the gas phase,
- deposited iodine on the painting coupon in the gas phase,
- deposited iodine on the wall in the gas phase,
- deposited iodine on the painting coupon in the liquid phase,
- mass balance at the end of the test.

Dr. Cantrel pointed the differences between the code predictions and the experimental data and proposed possible explanations for the discrepancies.

10. The main topic of the discussion was the experimental uncertainty that should be attached to the results. Dr. Cantrel and Dr. Ball stressed that experimental uncertainty was difficult to evaluate, for the following reasons:

- measurements had to be made in the presence of radiation ;
- measurements were made at the end of the test .

Ms. Schindler said she would elaborate on these points later in the meeting. It was recognised, however, that experimental uncertainty bands should be taken into account in the comparisons of the code predictions with the experimental values.

11. Dr. Ball presented a summary of the results obtained for the tests PHEBUS RTF1 and RTF P10T1. For the first test, general observations were that most codes overestimated iodine adsorption by surfaces and underestimated the amount of iodine remaining in the aqueous phase, most codes overestimated iodine volatility, and most codes underestimated organic iodide formation. For the second test, general observations were that most codes underestimated iodine volatility at pH 10 during the initial stages of the test, and most codes underestimated organic iodide formation during the initial stages of the test, most codes did not predict the aqueous pH (and assumed that it dropped to pH 5), and most codes overestimated the loss of iodine from the aqueous phase (due to assumed lower pH). A general observation valid for the two tests was that the mass balance at the end of the tests was incorrect (different from 100 %) in some calculations; this should be carefully checked by the participants. Dr. Ball also presented specific observations related to each calculation submitted.

VI. Estimates of experimental uncertainties

12. Mr. Glowa made a presentation about the sources and estimates of RTF experimental uncertainty, making the following observations:

- total aqueous phase : ± 10 % :
  - this is the most reliable RTF measurement ;
  - measured twice (grab sample, speciation method) ;
  - there is also an online detector on the aqueous sampling loop ;
  - the starting concentration is rarely exactly the planned value.
- pH : ± 0.3 pH unit :
  - generally there are two pH probes ; they generally agree to within 0.5 pH units ;
  - there are several sources of error in pH measurement (e.g., calibration error, temperature fluctuations, flow rate, probe failure) .
- temperature : ± 5 °C when trying to maintain a high temperature.
- total gas phase : factor of 3 :
  - there are two different measurements made.
- gas phase speciation :
  - total concentration is reliable, usually close to the concentration measured by the online iodine sampler ;
  - the concentration of low-molecular weight organic iodides compares well to GC measurements of methyl iodide ;
  - we do not know exactly what chemical components are trapped on the iodophenol portion of the speciation tube.
- gas phase iodine speciation :

  - a gas sample of known volume is drawn through a tube packed with a series of selective adsorbents ; each portion is then gamma counted separately.
- mass balance :
  - the iodine that has been lost from the aqueous phase gives a good indication of the total amount that has been deposited onto surfaces within the RTF ;
  - the amount of iodine in the gas phase is negligible ;
  - unfortunately, much of the iodine inventory is lost to various surfaces in the RTF, which is difficult to quantify ;
  - there is uncertainty in surface adsorption measurements.
- There are questions about the purity of water :
  - Organic material (paints, other contamination) ;
  - Chloride (probes), sulfate and lithium (pH control) ;
  - Metal ions (lines, vessel) ;
  - Nitrate/nitrite (air radiolysis) ;
  - Others ?

13. During the discussion, Dr. Ball pointed out that as far as iodine concentration and related experimental uncertainties were concerned, one should worry about the total, rather about than individual elements. Dr. Allelein disagreed with this point of view, stressing that individual element concentrations were important for reactor applications. He also pointed that that uncertainties about deposition onto electropolished surfaces, important in RTF, did not matter in real plants where most surfaces are painted and where cables may play an important role (there was no general agreement on this last point). Dr. Allelein emphasised the need to look at realistic reactor conditions, keeping in mind that initial conditions are not known and that severe accident temperature conditions are high (chemical data cannot be extrapolated to much higher temperatures). Sensitive parameters should be identified, and examined carefully.

14. Ms. Schindler presented a paper on estimates of experimental uncertainties for the CAIMAN facility, which she had prepared with Dr. Cantrel. She described in detail all possible sources of uncertainty related to γ measurements including for the boundary conditions such as sump volume, temperature and pH. The uncertainties can be summarised as follows:

- iodine concentration: $\pm$ 6 %; iodine mass deposited: $\pm$ 8 %;
- uncertainties linked to absolute efficiency of the γ detector and to the transfer function were considered; these values correspond to a 2σ range interval;
- temperature: $\pm$ 3° C;
- pH: $\pm$ 0.3 pH unity;
- sump volume: $\pm$ 3 %;

To illustrate the range of uncertainties affecting iodine determination, the errors associated to activity measurements were shown for both CAIMAN tests.

VII. Blind calculation results

GRS COCOSYS/AIM Results :

15. Dr. Weber described the main features of COCOSYS/AIM (the iodine model in the COCOSYS code), the general nodalisation used, calculations made on the CAIMAN tests, and calculations made on the RTF tests. The current phase of the ISP-41 follow-up exercise was offering an excellent opportunity to validate the current version of the code. Dr. Weber proposed the following conclusions for his work:

- The results of the blind COCOSYS/AIM calculations were not in good agreement with the CAIMAN and RTF measurements made for the iodine species of radiological interest: the I_2 concentration in the gas phase was significantly overestimated ; the CH_3I concentration in the gas phase was significantly underestimated for two tests.
- Several recommended reaction coefficients had been used in the calculations instead of the AIM default values. These modifications in the iodine chemistry model and the measurement uncertainties had to be taken into account when discussing the COCOSYS/AIM results.
- The following steps would be to recalculate RTF P10T1 with the measured pH history, and to review the I_2 and organic iodide reaction models in AIM.

PSI IMPAIR3 Results :

16. Mr. Cripps described the IMPAIR3 models and presented the results that had been obtained for the CAIMAN and RTF tests. Preliminary conclusions had been drawn from this work :

- CAIMAN 2001/01 :
  - Calculated dominant species in gas space: I_2 deposited on paint, trend consistent with experiment, but calculated is eight times the measured fraction.
  - $[I_2]$ (gas) compares well with the measured values.
  - [RI] (gas) is predicted about ten times lower than measured, despite unrealistic low partition coefficient for high molecular weight organic iodides - HMRI).
  - Comparable fractions remaining in water.
- CAIMAN 1997/02 :
  - I_2 deposited on paint coupon in sump is twice the measured value - dominant fraction outside H_2O.
  - $[I_2]$ (gas) compares well with measured value.
  - [RI] (gas) predicted concentration slope is lower than measured ; calculated and experimental values converge.
  - Fraction remaining in water is half the experimental value.
- RTF P10T1 :
  - I_2 deposited on paint coupon in the sump is half the measured value; underprediction of fraction remaining in water increasing after about 100 hours to approximately 3 times less than measured fraction.
  - $[I_2]$ (gas) is underpredicted (by a factor 10) ; final values coincide.
  - [HMRI] (gas) is predicted correctly from 100-150 hours but not the slope.
  - $[CH_3I]$ is underpredicted, but < 10 times; calculated and experimental values converge.
  - Predicted and measured total iodine species remaining in sump coincide to 100 hours then there is underprediction.
  - Fraction remaining in water is 3.5 times the experimental value.
- PHEBUS RTF1 :
  - I_2 deposited on paint coupons strongly overpredicted for gas and sump coupons (both seven times).
  - $[I_2]$ (gas) prediction satisfactory.
  - [HMRI] and $[CH_3I]$ (gas) are both about ten times underpredicted.
  - Fraction remaining in water is correctly predicted until about 20 hours, then overpredicted 2-3 times.

CIEMAT IODE Results :

17. Dr. Herranz's presentation was divided into two main parts:

- Generic modelling.
- Results for the four sets of calculations and discussion.

He had reached the following conclusions :

- RTF P10T1 :
  - The comparison of the experimental data to the base case predictions and the default case predictions led to the conclusion that increasing the radiolytic I_2 oxidation rate in basic solutions could improve IODE predictive capability.
  - The search for a better fit of the calculations to the data led to the conclusion that the formation rate of CH_3I from wet painted surfaces via radiolysis should be decreased in the IODE code.
  - It seemed that IODE code modelling is capable of simulating a scenario similar to that tested in the first 72 hours of RTF Phase 10 Test 1, with no other requirement than tuning some radiolytic reaction rates (in other words, no major chemical or physical process is missing).
- PHEBUS RTF1 :
  - The comparison of the experimental data to the base case predictions and the default case predictions led to the conclusion that decreasing the radiolytic I_2 oxidation rate in acid solutions could improve IODE predictive capability.
  - The consistency observed in gas phase predictions seemed to indicate that the overall IODE modelling of I_2 under the scenario conditions is rather complete and accurate enough.
  - It seemed that IODE code modelling was capable of simulating a scenario such as the one of PHEBUS RTF without no other changes than tuning of some radiolytic reaction rates.
- CAIMAN 1997/02 :
  - The comparison of the experimental data to the base case predictions and the default case predictions led to the conclusion that decreasing the radiolytic I_2 oxidation rate in acid solutions could improve IODE predictive capability.
  - Several factors should be considered in the explanation of the discrepancies found in the fit of gas phase predictions to experimental data (a delay in reaching the dose rate level experimentally prescribed, a speed up of radiolytic processes, IODE modelling weaknesses in the area of CH_3I formation from wet surfaces).
  - It seemed that IODE code modelling was unable to simulate a scenario such as CAIMAN 1997/02 without substantial modifications.
- CAIMAN 2001/01 :
  - The comparison of the experimental data to the base case predictions and the default case predictions led to the conclusion that decreasing the radiolytic I_2 oxidation rate in this scenario would reproduce the order of magnitude of I_2 (gas) but would miss the experimental trends of both I_2 (gas) and CH_3I (gas).
  - It seemed that IODE modelling could be fitted with no major changes to accomplish a better match of the iodine mass distribution. It was noteworthy, however, that CH_3I had been substantially overpredicted.
  - It seemed that IODE code modelling is capable of simulating a scenario such as CAIMAN 2001/01 within an order of magnitude. Predictions did not show the I_2-CH_3I coupling shown by the experimental data .

IRSN IODE 5.0 and 5.1 Results :

18. Dr. Cantrel's presentation started with a description of the differences between versions 5.0 and 5.1 of IODE. He then presented the calculations made for the four tests and discussed the results, and also discussed possible improvements. The main tendencies are:

- CAIMAN 1997/02 :
  - The organic iodide concentration is well predicted by IODE5.1; on the other hand, IODE 5.0 overestimates it.
  - The experimental gaseous molecular iodine values lie between the values calculated by IODE 5.0 and those calculated by IODE 5.1.
  - The total aqueous concentration calculated is more satisfactory in IODE 5.1 than in IODE 5.0
  - The amount adsorbed onto the painted coupons is very well predicted in both phases by IODE 5.1
- CAIMAN 2001/01 :
  - The ICH_3 and I_2 concentrations are well predicted by IODE 5.0 but the values obtained with IODE 5.1 are somewhat less satisfactory. IODE 5.1 predicts better the evolution of these concentrations.
  - The amount deposited on the painted coupon is well predicted by IODE 5.1 and overestimated by IODE 5.0.
- PHEBUS RTF1 :
  - IODE 5.0 predicts better the total gas concentration than IODE 5.1 but the trend is more consistent with the experimental data. Nevertheless, the discrepancy is less than an order of magnitude for both versions.
  - IODE 5.0 underestimates the total aqueous iodine concentrations whereas IODE 5.1 overestimates it.
  - the amount adsorbed onto painted aqueous coupons is well predicts by IODE 5.1 but strongly overpredicted by IODE 5.0.
- RTF P10T1 :
  - There is no module to predict pH evolution in IODE, and so the pH values are not reproduced. As iodine chemistry depends a lot on pH, it is not possible to draw conclusions from this test modelling excepted for the first hours where the pH was controlled.
  - For the first seventy hours where the pH is maintained constant at 10, IODE 5.1 gives good agreement between experimental data and the calculated $[I_2]$ and $[ICH_3]$ gas concentrations.

From a general point of view, IODE 5.1 is able to reproduce rather well the experimental data; the discrepancy is less than an order of magnitude. The results obtained with IODE 5.0 are also acceptable but for some calculated parameters the discrepancy can be higher (2 orders of magnitude).

AECL IMOD-2.0 Results :

19. Mr. Glowa said that the IMOD Default parameters had been used. The interfacial mass transfer had been decreased by a factor of ten from the PHEBUS RTF tests, and the measurement cycles had been modelled. He then presented the results obtained for the four tests:

- CAIMAN 1997/02 :
  - IMOD predicts the gas phase I_2 well.
  - It predicts the amount of iodine lost from the sump.
  - It predicts the amount adsorbed onto painted aqueous coupons.
  - It does not predict the 'delay' seen in the gas phase.
  - The initial organic concentration is too large and too fast.
- CAIMAN 2001/01 :
  - pH was modelled as 5.2.

  - IMOD underestimates the amount of I_2 and therefore the amount adsorbed onto surfaces.
  - It underestimates the amount of organic iodide.
  - A better way to predict the amount of organic compounds reaching the aqueous phase is needed. (Where does the carbon come from ?)
- RTF P10T1 :
  - pH and total aqueous iodine concentration are modelled well.
  - The amount of organic iodide is overpredicted (organic material was thought to be evaporating from the surfaces in contact with the gas phase as well as the surfaces in contact with the sump.
- PHEBUS RTF1 :
  - IMOD models total gas and total aqueous iodine concentrations well.
  - There is a problem with the rate of organic addition.
  - Organic material must be dissolving in throughout the test.
  - Loading onto painted gas coupons is overestimated by IMOD-2.0.
  - IMOD-2.0 underestimates loading onto electropolished stainless steel gas walls.

20. The general conclusions were that:

- In general, IMOD-2.0 predicts the major iodine sinks.
- Organic material source term is difficult to define and has a major impact on the total gas phase concentration.
- A slower, steadier rate of introduction of organic material seems to be needed.
- Adsorption, desorption and saturation capacities are difficult to define for some surfaces. These parameters have a major impact on iodine behaviour.
- IMOD-2.0 cannot properly model the portion of the tests when there is no dose.

21. Finally, Mr. Glowa discussed briefly changes to IMOD-2.0 that may improve the simulations (new version IMOD-2.1).

AECL LIRIC-3.2 Results :

22. Dr. Ball said that no attempt had been made to optimize calculations even with the RTF test; standard default values (except mass transfer for CAIMAN experiments) had been used. Desorption from painted surfaces had been assumed to be zero. Dissolution of solvents from immersed paint had been assumed to occur. The default paint age had been assumed to be 0.5 years, the default paint thickness 0.25 cm. Solvent had been assumed to be released by evaporation from coupons in the gas phase.

23. The following general observations could be made. Default values (no desorption from gas phase painted surfaces) overestimate the amount adsorbed on gas phase surfaces. Default adsorption/desorption values underestimate iodine remaining in the sump. Default values for paint thickness and age result in underestimation of organic iodide formation.

24. Dr. Ball presented the calculation results obtained for the four tests. This led her to discuss a general approach to model optimization:

- Increase paint thickness so that total carbon concentrations from CAIMAN 2001/01 and CAIMAN 1997/02 are reasonably reproduced.
- Use a desorption rate constant for painted surfaces in the gas phase (= 1/20 desorption rate constant for stainless steel in the gas phase).

25. The general conclusions were that:

- The LIRIC-3.2 model performs well if dissolution from painted surfaces is reasonably modelled, and if adsorption/desorption rate constants are known.
- PHEBUS RTF1, CAIMAN 2001/01 and CAIMAN 1997/02 can be reasonably represented with the same input parameters.

26. Many specific issues were discussed during the presentation of the results. It was pointed out that all organisations participating in the ISP-47 exercise use different codes or different versions of the same code. Two general remarks were made:

- There is no code giving good results, or at least acceptable results, for all parameters. All models need further improvements.
- Many results are sensitive to assumptions made for paint thickness. In real life, paint thickness varies with time and is generally not known accurately.

VIII. Strategies for model optimization

27. Dr. Herranz opened the discussion, saying that the comparison between the calculated results and the experimental data, in his opinion, led to two major considerations:

- Regarding the kinetics of radiolytic oxidation of I^- :

Radiolytic reactions seemed to play a major role in organic iodine chemistry. At least, this was supported by IODE calculations (version used by CIEMAT). All cases analysed led to the conclusion that IODE modelling of aqueous I_2 production from I^- via radiation could be susceptible to some changes resulting in:

  - an increase in I_2 formation under alkaline conditions,
  - a decrease in I_2 formation under acid conditions.

As a short-term action, Dr. Herranz suggested to analyse the evolution of iodine species as a function of pH in RTF tests. As a long-term action, he suggested to compare predictions with representative data, that is, to set up an experimental matrix against which to validate further code development.

- Regarding the kinetics of organic iodide formation :

Under basic conditions, IODE modelling of heterogeneous Org I generation from wet painted surfaces seemed to require a lower reaction rate. However, no clear trends had been observed with acid pHs. As a short-term action, Dr. Herranz suggested to analyse in more detail model performance in CAIMAN calculations (e.g., the delay in gas concentration rise in test 1997/02 should be clarified). As a long-term action, he recommended to set up a matrix of experiments in which organics play a role.

28. Dr. Herranz also made recommendations regarding 'acceptability' criteria for code predictions:

- based on measurement capability :
  - 20 % in total aqueous iodine
  - 300 % in total gaseous iodine
  - 20 % in total iodine deposited
  - right fraction of gaseous species
  - right fraction of deposited iodine between gas-wet surfaces
- based on safety assessments and accident management needs :
  - aqueous iodine concentration and speciation (e.g., spray recirculation)
  - gaseous iodine concentration and speciation (e.g., spray recirculation)

He also emphasised the need to assess uncertainties on the main iodine input parameters at times at which iodine chemistry dominates the 'potential source term'.

29. On the last point, Dr. Allelein said that the parameters that have major influence on source terms are well known, in particular from previous ISP exercises. He mentioned:

- the rate constants : a sum-up of the current experience in defining them and the known applicability ranges would be a useful output of the ISP exercise ;
- pH evolution : this is a key factor 'forgotten' in present formulations ;
- the dose rates : is a module to calculate these variables inside chemistry codes necessary ?

The other participants agreed that these parameters were indeed most important but stressed that they were very hard to quantify. They also stressed that, although it was clear that codes should be validated over the range of temperatures one would expect in an accident, this was a formidable task, which was maybe not completely possible, and maybe not fully necessary. Moreover, accident management considerations played an important role in this. Other important considerations were related to uncertainty evaluation and combinations of uncertainties, and how to evaluate the overall uncertainty.

30. Dr. Allelein wondered who was able to define a representative accident sequence for a given type of reactor.

31. It was agreed that there was a need to make sure that available models can model all tests without making changes to the main parameters (except if really justified). Otherwise, one would need to conclude that improvements are necessary. The discussion showed that there were interrogations concerning currently used mass transfer coefficients and wet paint coefficients.

32. Dr. Allelein presented a number of preliminary considerations on the behaviour of iodine (completing some of the points made earlier by Dr. Herranz):

Point A. *What are the main parameters - and their margins - that are of major importance to assess the quality of a calculation?*

- absolutely necessary :
  - total amount in the aqueous phase : ± 20 %
  - total amount in the gaseous phase : factor 3
- of direct or indirect radiological importance :
  - organic iodine (RI) in the gaseous phase (partition between RI and total I : ± 20 %)
  - iodine adsorbed on:
    - painted surface in both phases : each a factor of 10
    - steel surface in gaseous phase : factor 10
  - total gas and aqueous phase : ± 20 %

Furthermore, the general trend over time should be calculated, not only the situation at a fixed point in time.

Point B. *How can one decide that an experiment gives acceptable results for values mentioned under point A?* [An example of possible criterion could be, e.g., that aqueous phase measurements are reliable within 5 % (CAIMAN) or 10 % (RTF)]. This question is even more difficult to answer if the experimental mass balance is not closed. Assuming that the missing iodine is deposited on the surfaces leads to a more general question: *How does the uncertainty on the surface concentration in the gaseous phase influence the gaseous phase itself, especially*

the organic iodine? As a result of the discussion, it was agreed to perform a number of calculations in order to try to answer this question, especially the possible impact of the gap in the mass balances. Dr. Ball said she would perform such work before the final meeting of the group; participants having models allowing calculations to study this effect intended to add further investigations into this direction.

Dr. Allelein made a few more remarks:

- Aqueous phase measurement accuracy has only a slight influence.
- The value becomes high in tests with low gaseous concentrations, and high gap in mass balance.
- The uncertainty on the total gas management influences the criteria directly, e.g. a factor 3 for the RTF tests.

Point C. *What should be expected from future work?*

- a clarification of the uncertainty issue,
- a general harmonisation of relevant input values.

Point D. *How to transfer ISP exercise results to plant applications?*

- Using different models based on detailed expert discussions will help iodine source term calculations go onto the direction of better reliability ; this approach is currently hampered because of reasons related to availability of time and resources, and confidentiality of data.
- Dr. Allelein doubted that a specialist with a normal chemistry background , who is not a code developer, is able today to perform reliable source term calculations.

33. Finally, Dr. Allelein mentioned a few areas where iodine behaviour has an impact on reactor safety:

- early containment failure,
- long-term aspects, e.g. :
    - increasing leakage caused by containment overpressurisation,
    - filtered venting
- influence of spray elements,
- cable burns,
- hydrogen recombiners

34. There was consensus during the following discussion on the need to adopt 'hard' numbers to be used in calculations on the four tests selected for the ISP-41 exercise. The adopted numbers are:

CAIMAN : interfacial mass transfer rate constant :

I_2 : 1.0×10^{-5} m/s (uncertainty ~ factor 2)

CH_3I (90 °C) : 1.5×10^{-5} m/s (uncertainty ~ factor 2)

overall adsorption rate constant k_{ads} (paint, liquid) ~ $(2.5 \pm 1.5) \times 10^{-4}$ m/s

k_{ads} (paint, gas) = 4×10^{-3} m/s (uncertainty ~ factor 2) (same value for 97/02 and 2001/1 because the painted coupons are at about the same temperatures, respectively 110 °C and 100 °C)

k_{des} : options :

- use the given k_{ads} values without desorption

- use k_{des} but the overall adsorption rate constant should be the given k_{ads}

RTF : use the values given earlier:

RTF 1 : k_{ads} (paint/gas) ~ 4.5 x 10^{-3} m/s at 90 °C (uncertainty ~ factor 2)

Phase 10 : k_{ads} (paint/gas) ~ 6.0 x 10^{-4} m/s at 60 °C (uncertainty ~ factor 2)

Stainless steel / electropolished surfaces (based on bench-scale studies) :

k_{ads} (SS/gas) ~ 1.0 x 10^{-4} m/s at 90 °C (uncertainty ~ factor 2)

k_{des} (SS/gas) : use the values given earlier (uncertainty ~ factor 2)

I_2 on wet stainless steel: $k_{ads} < 2.0 \times 10^{-6}$ m/s

Wet paint:

- I_2 on paint :
  - k_{ads} ~ 8.0 x 10^{-4} m/s (uncertainty ~ factor 2)
  - k_{des} ~ 5.0 x 10^{-7} s^{-1} (uncertainty ~ factor 2)

- I^- on paint :
  - k_{ads} ~ 4.0 x 10^{-8} m/s (uncertainty ~ factor 2)
  - k_{des} ~ 1.0 x 10^{-6} s^{-1} (uncertainty ~ factor 2)

pH :

- use the pH as measured
- AECL will provide nitrate/nitrite analysis results [8]
- IRSN will provide other chemical analysis.

35. As a general principle, it was decided that for future calculations in the ISP-41 exercise, participants would not be allowed to make random changes on model parameters. The same consistent model should be used for the four tests. Allowable changes will be restricted to some boundary conditions or input parameters that are not well defined or not provided. Even these values must be defensible from the point of view of physics with respect to other experimental information. Error bars will be put on gaseous and aqueous result computations. Where experimental results fall into the shaded area, the rating of the calculations will be 1; outside the error band, the rating of the calculation will be 0. The following parameters will be calculated:

At the end	**Experiment**	**Ratings: within**	**Ratings: outside**
Total aqueous iodine	10 %	1	0
Total gas iodine	Factor 3	1	0
Gas organic iodine fraction	20 %	1	0

Trend	
Total aqueous iodine	
Total gas iodine	
Gaseous organic iodine	

[8] Note of the Secretary: this was done on 20 November 2002.

Gaseous iodine	

It was recognised that quantifying the ratings of different calculations would be a difficult task. In a first step, it would be left to the qualitative judgement of the authors of the Comparison and Interpretation Report. A collective discussion would take place in a second step. The need to check the mass balance at the end of the calculations was stressed. Dr. Allelein suggested performing parametric calculations to see if the surface of the gas phase has a major impact or not. Some participants said they would look into the possibility of performing such calculations.

36. Broadening the discussion, Dr. Ball asked whether the iodine models would be validated at the end of the exercise. Dr. Allelein said that the answer would probably be different in Canada and France and in the other countries. Canada and France had accumulated and were still accumulating a large number of experimental data that should be most useful in their validation programme. Other countries in need of validating their models did not have the same information.

37. Dr. Allelein suggested that a useful future international activity would be to perform a iodine code comparison exercise on a real plant, perhaps on a decommissioned plant as plant data might be easier to obtain in such a case. Such an exercise should make use only of data that would normally be available in a real reactor application. The objective would be to demonstrate what current codes really could do in a realistic situation. Several participants expressed interest in the suggestion.

38. Finally, Dr. Allelein presented a brief report on the main results of a meeting of experts on the development of a phenomena-based validation matrix for ex-vessel (containment) models and codes that had been held at the end of August. Iodine behaviour data would be collected, in due course (in a first step, the work was concentrating on thermal-hydraulics and hydrogen combustion).

IX. Remaining tasks - Timetable for exercise completion

38. The schedule and milestones for the remaining tasks were discussed. The following timetable was adopted:

Resubmission of results after model optimisation	15 December 2002 (instead of 15 October 2002)
Draft Comparison & Interpretation Report	1 May 2003 (instead of 15 January 2003)
Comments on the draft Comparison & Interpretation Report	15 May 2003 (instead of 30 January 2003)
Meeting to finalise the Comparison & Interpretation Report	June 2003 (instead of 28 February 2003)
Transmission of the Final draft Comparison & Interpretation Report to the Secretariat and GAMA	15 August 2003 (instead of 30 April 2003)

X. Other matters

39. None was mentioned.

XI. Date and place of the next meeting

40. The next meeting will be held at the Paul Scherrer Institute, Villigen, Switzerland on 26 and 27 June 2003.

XII. Close of the meeting

41. On behalf of the participants and the OECD, the Secretary thanked the organisers of the ISP-41 exercise, AECL and IRSN. He also thanked AECL for their kind hospitality.

XIII. Visit to CRL

42. A visit to the AECL Chalk River Laboratories (CRL) was organised on 19 September.

Annex 1:

LIST OF PARTICIPANTS

Delegates :

CANADA	
Dr. Joanne M. Ball Containment Chemistry Section Fuel Safety Branch AECL Chalk River Laboratories Chalk River, Ontario K0J 1J0	Telephone: +1 613 584 8811 ext. 3874 Fax: +1 613 584 1220 E-mail: 'ballj@aecl.ca'
Mr. Glenn A. Glowa Fuel Safety Branch AECL Chalk River Laboratories Chalk River, Ontario K0J 1J0	Telephone: +1 613 584 3311 ext. 6052 Fax: +1 613 584 1220 E-mail: 'glowag@aecl.ca'
Dr. J. Clara Wren Section Head, Containment Chemistry Fuel Safety Branch AECL Chalk River Laboratories Chalk River, Ontario K0J 1J0	Telephone: +1 613 584 8811 ext. 3065 Fax: +1 613 584 2550 E-mail: 'wrenc@aecl.ca'
FRANCE	
Dr. Laurent Cantrel Service d'Etudes et de Modélisation d'Accidents de Réacteurs (SEMAR) Département de Recherches en Sécurité (DRS) Institut de Radiorotection et de Sûreté Nucléaire (IRSN) Bâtiment 702 Centre d'Etudes Nucléaires de Cadarache F-13115 Saint-Paul-lez-Durance CEDEX	Telephone: +33 4 42 25 49 06 Fax: +33 4 42 25 63 99 E-mail: 'laurent.cantrel@irsn.fr'
Dr. Carole Marchand DPEA/SEAC Institut de Radioprotection et de Sûreté Nucléaire (IRSN) Centre d'Etudes Nucléaires de Fontenay-aux-Roses B.P. 6 F-92265 Fontenay-aux-Roses	Telephone: +33 1 58 35 90 57 Fax: +33 1 46 54 32 64 E-mail: 'carole.marchand@irsn.fr'
Ms. Patricia Schindler DEN/DEC/S3C Commissariat à l'Energie Atomique (CEA) Bâtiment 224	Telephone: +33 4 42 25 73 62 Fax: +33 4 42 25 47 77 E-mail: 'schindler@drncad.cea.fr'

F-13108 Saint-Paul-lez-Durance CEDEX	
GERMANY	
Dr. Hans-Josef Allelein Gesellschaft für Anlagen- und Reaktorsicherheit GRS) mbH Schwertnergasse 1 Postfach 10 16 50 D-50667 Köln 1	Telephone: +49 221 2068 668 Fax: +49 221 2068 834 E-mail: 'all@grs.de'
Dr. Günter Weber Gesellschaft für Anlagen- und Reaktorsicherheit (GRS) mbH Forschungsgelände D-85748 Garching	Telephone: +49 89 32004 506 Fax: +49 89 32004 491 E-mail: 'weg@grs.de'
SPAIN	
Dr. Luis E. Herranz Group Leader, Research on Nuclear Safety Technology Department of Nuclear Fission CIEMAT Avda. Complutense, 22 28040 Madrid	Telephone: + 34 91 346 62 19 Fax: + 34 91 346 62 33 E-mail: 'luisen.herranz@ciemat.es'
SWITZERLAND	
Dr. Robin C. Cripps Paul Scherrer Institute Laboratory for Thermohydraulics OVGA/310 CH-5232 Villigen-PSI	Telephone: + 41 56 310 27 09 Fax: + 41 56 310 21 99 E-mail: 'robin.cripps@psi.ch'

An apology for absence had been received from :

CZECH REPUBLIC	
Mr. Adolf Rydl Department of Reactor Technology NRI (Nuclear Research Institute) Řež (UJV) 250 68 Řež	Telephone: +420 2 6617 2471 Fax: +420 (2) 688 2029 E-mail: 'ryd@ujv.cz'

OECD Nuclear Energy Agency:

Dr. Jacques Royen Deputy Head Nuclear Safety Division OECD Nuclear Energy Agency Le Seine – Saint Germain 12 Boulevard des Iles F-92130 Issy-les-Moulineaux France	Telephone: +33 1 45 24 10 52 Fax: +33 1 45 25 11 29 or 11 10 E-mail: 'jacques.royen@oecd.org' 'royen@nea.fr'